High-Affinity Alkynyl Bisubstrate Inhibitors of NicotinamideN-Methyltransferase (NNMT)

High-Affinity Alkynyl Bisubstrate Inhibitors of Nicotinamide N-Methyltransferase (NNMT)

Supporting Information Part 1: Supplementary Figures & Tables, Synthetic Schemes, and Experimental Protocols

Rocco L. Policarpo*, Ludovic Decultot*, Elizabeth May†, Petr Kuzmič§, Samuel Carlson†, Danny Huang*, Vincent Chu*, Brandon Wright*, Saravanakumar Dhakshinamoorthy‡, Aimo Kannt⋆, Shilpa Rani‡, Sreekanth Dittakavi‡, Joseph Panarese*, Rachelle Gaudet†, and Matthew D. Shair*

*Department of Chemistry & Chemical Biology, Harvard University, Cambridge MA 02138, USA
†Department of Molecular & Cellular Biology, Harvard University, Cambridge MA 02138, USA
§BioKin Ltd., Watertown MA 02472, USA
‡Jubilant Biosys Ltd., Yeshwantpur Bangalore - 560 022, Karnataka, India
⋆Sanofi Research and Development, Industriepark Hoechst, H823, D-65926, Frankfurt am Main, Germany

Table of Contents

1 Supplementary Figures & Tables

List of Figures

List of Tables

Table S1: Catalyst/solvent pairs screened in this work. All metathesis catalysts below were purchased from Strem, with the exception of Grubbs Catalyst C571, which was purchased from Millipore Sigma.

Catalyst/Solvent Pair in Figure S1	Catalyst	Solvent	Catalyst CAS #	Catalyst Structure
1	nitro-Grela	MTBE	502964-52-5	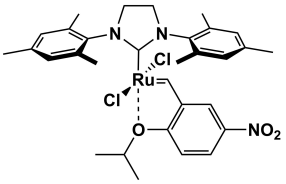
2	Grubbs Catalyst C571	CH_2Cl_2	927429-61-6	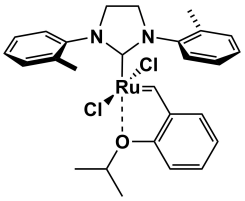
3	StickyCat Cl	CH_2Cl_2	1452227-72-3	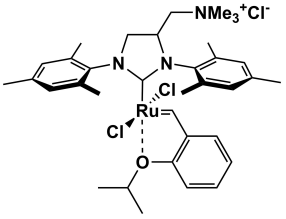
4	GreenCat	CH_2Cl_2	1448663-06-6	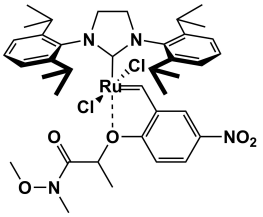
5	M71-S1Pr	CH_2Cl_2	1212008-99-5	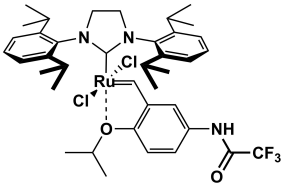
6	nitro-Grela	fluorobenzene	502964-52-5	see entry 1
7	nitro-Grela	CH_2Cl_2	502964-52-5	see entry 1

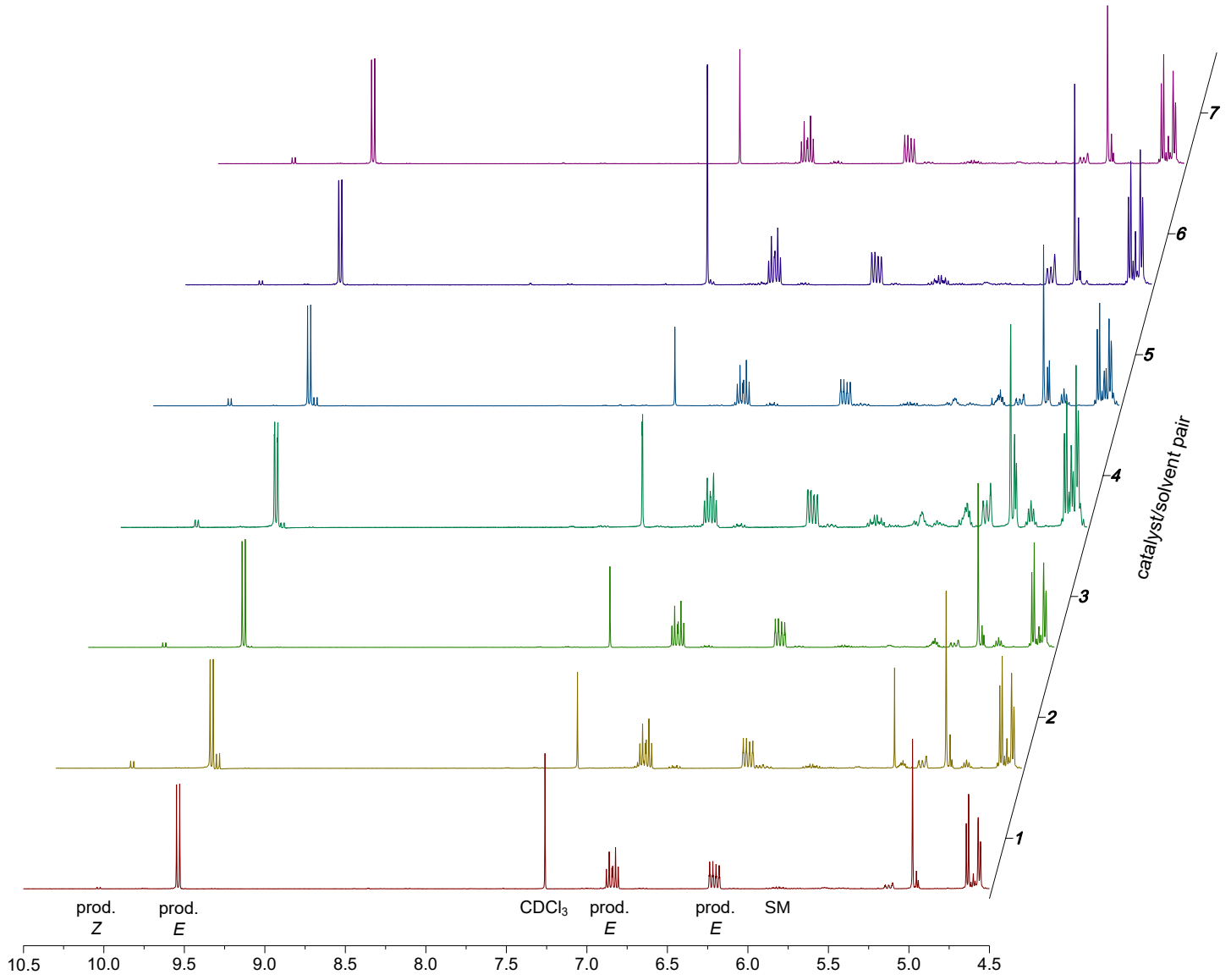

Figure S1: Crude ^{1}H NMR traces of alkene/aldehyde regions for solvent/catalyst pairs screened and shown in Table S1. All reactions were performed on 1 mmol of alkene **3** with 1 mol % catalyst loading and 5 mmol of crotonaldehyde (5 equiv.). Crotonaldehyde (predominantly *trans*) was used as received from Millipore Sigma (catalog #: 262668, CAS: 123-73-9).

Table S2: Data collection and refinement statistics.

Wavelength (Å)	0.97910
Resolution range (Å)	42.6–2.25 (2.33–2.25)
Space group	P 1
Unit cell (a, b, c (Å); α, β, γ (°))	46.07 62.20 108.20 82.52 81.84 68.35
Total reflections	80875 (8176)
Unique reflections	46037 (4664)
Multiplicity	1.8 (1.8)
Completeness (%)	87.23 (86.28)
Mean I/σ(I)	3.15 (1.34)
Wilson B-factor	28.87
R_{merge}	0.1752 (1.151)
R_{meas}	0.2478 (1.628)
R_{pim}	0.1752 (1.151)
$CC_{1/2}$	0.919 (0.182)
CC*	0.979 (0.555)
Reflections used in refinement	45689 (4534)
Reflections used for R_{free}	2293 (220)
R_{work}	0.2220 (0.3070)
R_{free}	0.2631 (0.3378)
CC(work)	0.925 (0.673)
CC(free)	0.876 (0.669)
Number of non-hydrogen atoms	8600
macromolecules	8243
ligands	178
solvent	179
Protein residues	1058
RMS(bonds) (Å)	0.002
RMS(angles) (°)	0.48
Ramachandran favored (%)	99.14
Ramachandran allowed (%)	0.86
Ramachandran outliers (%)	0.00
Rotamer outliers (%)	0.88
Clashscore	3.40
Average B-factor	36.33
macromolecules	36.48
ligands	28.70
solvent	36.80
Number of TLS groups	24

Statistics for the highest-resolution shell are shown in parentheses.

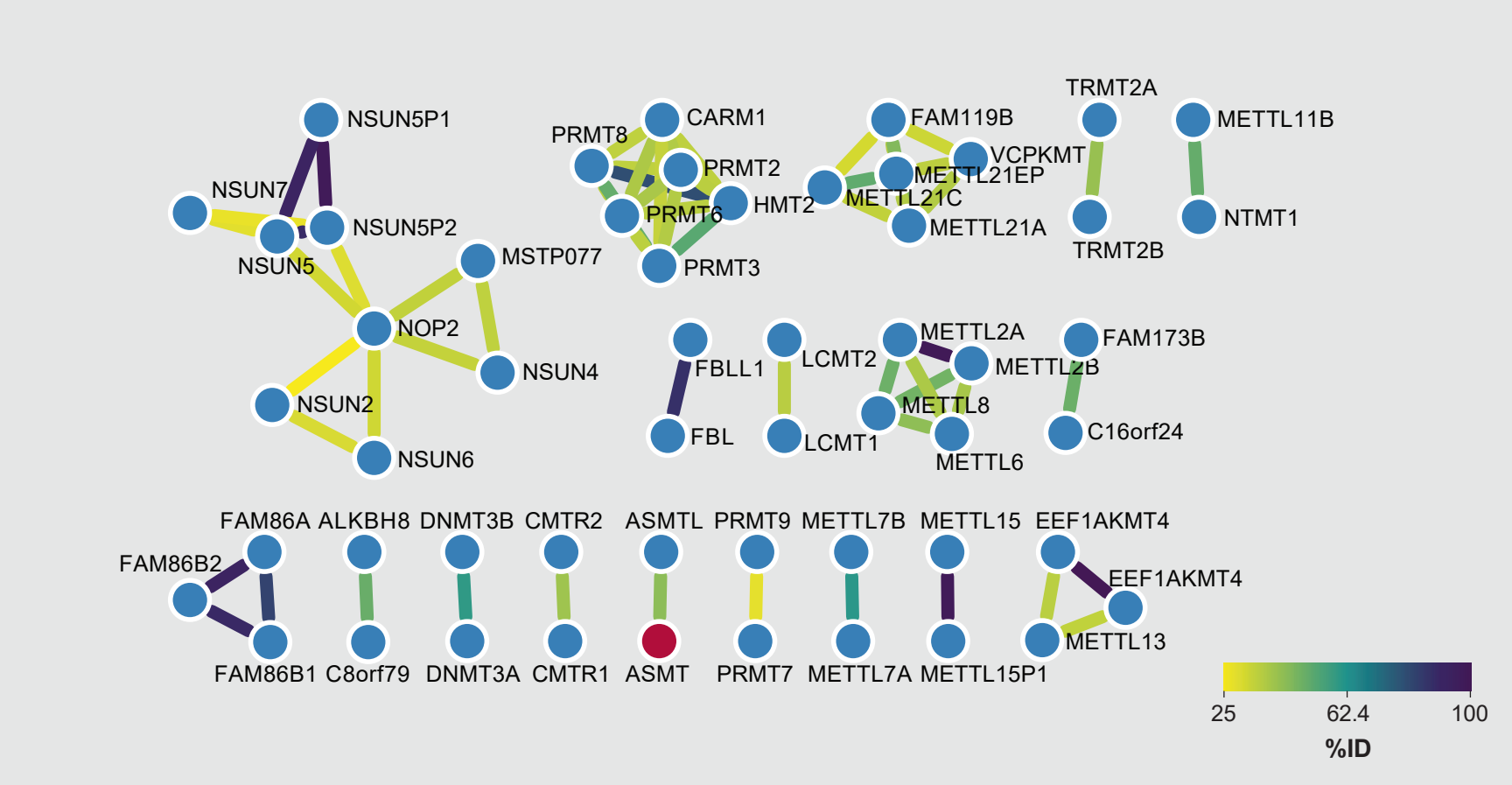

Figure S2: Sequence similarity network (SSN) of human methyltransferases. Node labels correspond to UniProt IDs and Protein Names found in Table S3. Red nodes correspond to small-molecule methyltransferases. Edges are color coded according to sequence similarity (%ID, legend at bottom right). A description of the SSN generation work flow is detailed in Section 6.3.

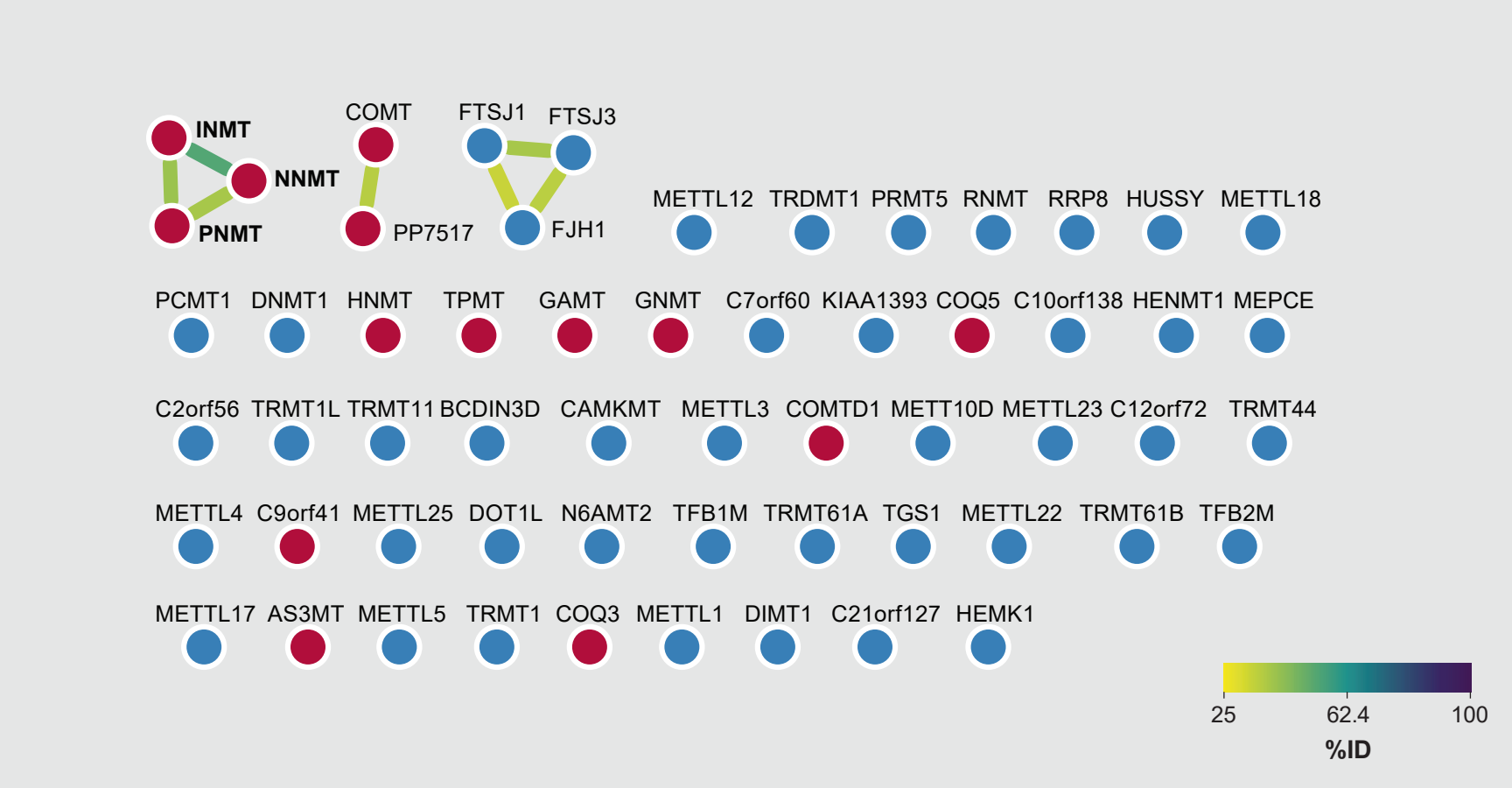

Figure S2 (Cont.): Sequence similarity network (SSN) of human methyltransferases. **The NNMT, INMT, PNMT cluster appears at top left**. Node labels correspond to UniProt IDs and Protein Names found in Table S3. Red nodes correspond to small-molecule methyltransferases. Edges are color coded according to sequence similarity (%ID, legend at bottom right). A description of the SSN generation workflow is detailed in Section 6.3.

Table S3: Human methyltransferases used to construct a sequence similarity network (SSN). A description of the SSN generation workflow is provided in Section 6.3.

SSN Node Label	UniProt Entry ID	UniProt Entry Name	Gene Names	Protein Name
ALKBH8	Q96BT7	ALKB8_HUMAN	ALKBH8 ABH8	Alkylated DNA repair protein alkB homolog 8
AS3MT	Q9HBK9	AS3MT_HUMAN	AS3MT CYT19	Arsenite methyltransferase
ASMT	P46597	ASMT_HUMAN	ASMT	Acetylserotonin O-methyltransferase
ASMTL	O95671	ASML_HUMAN	ASMTL	N-acetylserotonin O-methyltransferase-like protein Short-ASMTL
BCDIN3D	Q7Z5W3	BN3D2_HUMAN	BCDIN3D	Pre-miRNA 5'-monophosphate methyltransferase
C10orf138	Q5JPI9	EFMT2_HUMAN	EEF1AKMT2 C10orf138 METTL10	EEF1A lysine methyltransferase 2
C12orf72	Q8IXQ9	ETKMT_HUMAN	ETFBKMT C12orf72 METTL20	Electron transfer flavoprotein beta subunit lysine methyltransferase
C16orf24	Q9BQD7	F173A_HUMAN	FAM173A C16orf24 RJD7	Protein N-lysine methyltransferase FAM173A
C21orf127	Q9Y5N5	N6MT1_HUMAN	N6AMT1 C21orf127 HEMK2 PRED28	Methyltransferase N6AMT1
C2orf56	Q7L592	NDUF7_HUMAN	NDUFAF7 C2orf56 PRO1853	Protein arginine methyltransferase NDUFAF7, mitochondrial
C7orf60	Q1RMZ1	SAMTR_HUMAN	BMT2 C7orf60 SAMTOR	S-adenosylmethionine sensor upstream of mTORC1
C8orf79	Q9P272	TRM9B_HUMAN	TRMT9B C8orf79 KIAA1456 TRM9L	Probable tRNA methyltransferase 9B
C9orf41	Q8N4J0	CARME_HUMAN	CARNMT1 C9orf41	Carnosine N-methyltransferase
CAMKMT	Q7Z624	CMKMT_HUMAN	CAMKMT C2orf34 CLNMT	Calmodulin-lysine N-methyltransferase ShortCLNMT ShortCaM KMT
CARM1	Q86X55	CARM1_HUMAN	CARM1 PRMT4	Histone-arginine methyltransferase CARM1
CMTR1	Q8N1G2	CMTR1_HUMAN	CMTR1 FTSJD2 KIAA0082 MTR1	Cap-specific mRNA (nucleoside-2'-O-)-methyltransferase 1
CMTR2	Q8IYT2	CMTR2_HUMAN	CMTR2 AFT FTSJD1	Cap-specific mRNA (nucleoside-2'-O-)-methyltransferase 2
COMT	P21964	COMT_HUMAN	COMT	Catechol O-methyltransferase
COMTD1	Q86VU5	CMTD1_HUMAN	COMTD1 UNQ766/PRO1558	Catechol O-methyltransferase domain-containing protein 1
COQ3	Q9NZJ6	COQ3_HUMAN	COQ3 UG0215E05	Ubiquinone biosynthesis O-methyltransferase, mitochondrial
COQ5	Q5HYK3	COQ5_HUMAN	COQ5	2-methoxy-6-polyprenyl-1,4-benzoquinol methylase, mitochondrial
DIMT1	Q9UNQ2	DIM1_HUMAN	DIMT1 DIMT1L HUSSY-05	Probable dimethyladenosine transferase
DNMT1	P26358	DNMT1_HUMAN	DNMT1 AIM CXXC9 DNMT	DNA (cytosine-5)-methyltransferase 1 ShortDnmt1
DNMT3A	Q9Y6K1	DNM3A_HUMAN	DNMT3A	DNA (cytosine-5)-methyltransferase 3A ShortDnmt3a
DNMT3B	Q9UBC3	DNM3B_HUMAN	DNMT3B	DNA (cytosine-5)-methyltransferase 3B ShortDnmt3b
DOT1L	Q8TEK3	DOT1L_HUMAN	DOT1L KIAA1814 KMT4	Histone-lysine N-methyltransferase, H3 lysine-79 specific
EEF1AKMT4	P0DPD7	EFMT4_HUMAN	EEF1AKMT4	EEF1A lysine methyltransferase 4

Table S3 continued from previous page

EEF1AKMT4	P0DPD8	EFCE2_HUMAN	EEF1AKMT4-ECE2	EEF1AKMT4-ECE2 readthrough transcript protein
FAM119B	Q96AZ1	EFMT3_HUMAN	EEF1AKMT3 FAM119B HCA557A METTL21B	EEF1A lysine methyltransferase 3
FAM173B	Q6P4H8	F173B_HUMAN	FAM173B	Protein N-lysine methyltransferase FAM173B
FAM86A	Q96G04	EF2KT_HUMAN	EEF2KMT FAM86A SB153	Protein-lysine N-methyltransferase EEF2KMT
FAM86B1	Q8N7N1	F86B1_HUMAN	FAM86B1	Putative protein N-methyltransferase FAM86B1
FAM86B2	P0C5J1	F86B2_HUMAN	FAM86B2	Putative protein N-methyltransferase FAM86B2
FBL	P22087	FBRL_HUMAN	FBL FIB1 FLRN	rRNA 2'-O-methyltransferase fibrillarin
FBLL1	A6NHQ2	FBLL1_HUMAN	FBLL1	rRNA/tRNA 2'-O-methyltransferase fibrillarin-like protein 1
FJH1	Q9UI43	MRM2_HUMAN	MRM2 FJH1 FTSJ2	rRNA methyltransferase 2, mitochondrial
FTSJ1	Q9UET6	TRM7_HUMAN	FTSJ1 JM23	Putative tRNA (cytidine(32)/guanosine(34)-2'-O)-methyltransferase
FTSJ3	Q8IY81	SPB1_HUMAN	FTSJ3 SB92	pre-rRNA processing protein FTSJ3
GAMT	Q14353	GAMT_HUMAN	GAMT	Guanidinoacetate N-methyltransferase
GNMT	Q14749	GNMT_HUMAN	GNMT	Glycine N-methyltransferase
HEMK1	Q9Y5R4	HEMK1_HUMAN	HEMK1 HEMK	HemK methyltransferase family member 1
HENMT1	Q5T8I9	HENMT_HUMAN	HENMT1 C1orf59	Small RNA 2'-O-methyltransferase
HMT2	Q99873	ANM1_HUMAN	PRMT1 HMT2 HRMT1L2 IR1B4	Protein arginine N-methyltransferase 1
HNMT	P50135	HNMT_HUMAN	HNMT	Histamine N-methyltransferase ShortHMT
HUSSY	O43709	BUD23_HUMAN	BUD23 MERM1 WBSCR22 HUSSY-03 PP3381	Probable 18S rRNA (guanine-N(7))-methyltransferase
INMT	O95050	INMT_HUMAN	INMT	Indolethylamine N-methyltransferase ShortIndolamine N-methyltransferase
KIAA1393	Q32P41	TRM5_HUMAN	TRMT5 KIAA1393 TRM5	tRNA (guanine(37)-N1)-methyltransferase
LCMT1	Q9UIC8	LCMT1_HUMAN	LCMT1 LCMT CGI-68	Leucine carboxyl methyltransferase 1
LCMT2	O60294	TYW4_HUMAN	LCMT2 KIAA0547 TYW4	tRNA wybutosine-synthesizing protein 4 ShorttRNA yW-synthesizing protein 4
MEPCE	Q7L2J0	MEPCE_HUMAN	MEPCE BCDIN3	7SK snRNA methylphosphate capping enzyme Short-MePCE
METT10D	Q86W50	MET16_HUMAN	METTL16 METT10D	RNA N6-adenosine-methyltransferase METTL16
METTL1	Q9UBP6	TRMB_HUMAN	METTL1 C12orf1	tRNA (guanine-N(7)-)-methyltransferase
METTL11B	Q5VVY1	NTM1B_HUMAN	METTL11B C1orf184 NRMT2	Alpha N-terminal protein methyltransferase 1B
METTL12	A8MUP2	CSKMT_HUMAN	CSKMT METTL12	Citrate synthase-lysine N-methyltransferase CSKMT, mitochondrial
METTL13	Q8N6R0	EFNMT_HUMAN	EEF1AKNMT KIAA0859 METTL13 CGI-01	Methyltransferase-like protein 13
METTL15	A6NJ78	MET15_HUMAN	METTL15 METT5D1	Probable methyltransferase-like protein 15

Table S3 continued from previous page

METTL15P1	P0C7V9	ME15P_HUMAN	METTL15P1 METT5D2	Putative methyltransferase-like protein 15P1
METTL17	Q9H7H0	MET17_HUMAN	METTL17 METT11D1	Methyltransferase-like protein 17, mitochondrial
METTL18	O95568	MET18_HUMAN	METTL18 ASTP2 C1orf156	Histidine protein methyltransferase 1 homolog
METTL21A	Q8WXB1	MT21A_HUMAN	METTL21A FAM119A HCA557B	Protein N-lysine methyltransferase METTL21A
METTL21C	Q5VZV1	MT21C_HUMAN	METTL21C C13orf39	Protein-lysine methyltransferase METTL21C
METTL21EP	A6NDL7	MT21E_HUMAN	METTL21EP METTL21CP1	Putative methyltransferase-like protein 21E pseudogene
METTL22	Q9BUU2	MET22_HUMAN	METTL22 C16orf68 LP8272	Methyltransferase-like protein 22
METTL23	Q86XA0	MET23_HUMAN	METTL23 C17orf95	Methyltransferase-like protein 23
METTL25	Q8N6Q8	MET25_HUMAN	METTL25 C12orf26	Methyltransferase-like protein 25
METTL2A	Q96IZ6	MET2A_HUMAN	METTL2A METTL2 HSPC266	Methyltransferase-like protein 2A
METTL2B	Q6P1Q9	MET2B_HUMAN	METTL2B	Methyltransferase-like protein 2B
METTL3	Q86U44	MTA70_HUMAN	METTL3 MTA70	N6-adenosine-methyltransferase catalytic subunit
METTL4	Q8N3J2	METL4_HUMAN	METTL4	Methyltransferase-like protein 4
METTL5	Q9NRN9	METL5_HUMAN	METTL5 DC3 HSPC133	Methyltransferase-like protein 5
METTL6	Q8TCB7	METL6_HUMAN	METTL6	Methyltransferase-like protein 6
METTL7A	Q9H8H3	MET7A_HUMAN	METTL7A PRO0066 UNQ1902/PRO4348	Methyltransferase-like protein 7A
METTL7B	Q6UX53	MET7B_HUMAN	METTL7B UNQ594/PRO1180	Methyltransferase-like protein 7B
METTL8	Q9H825	METL8_HUMAN	METTL8	Methyltransferase-like protein 8
MSTP077	Q9H649	NSUN3_HUMAN	NSUN3 MSTP077 UG0651E06	tRNA (cytosine(34)-C(5))-methyltransferase, mitochondrial
N6AMT2	Q8WVE0	EFMT1_HUMAN	EEF1AKMT1 N6AMT2	EEF1A lysine methyltransferase 1
NNMT	P40261	NNMT_HUMAN	NNMT	Nicotinamide N-methyltransferase
NOP2	P46087	NOP2_HUMAN	NOP2 NOL1 NSUN1	Probable 28S rRNA (cytosine(4447)-C(5))-methyltransferase
NSUN2	Q08J23	NSUN2_HUMAN	NSUN2 SAKI TRM4	tRNA (cytosine(34)-C(5))-methyltransferase
NSUN4	Q96CB9	NSUN4_HUMAN	NSUN4	5-methylcytosine rRNA methyltransferase NSUN4
NSUN5	Q96P11	NSUN5_HUMAN	NSUN5 NSUN5A WBSCR20 WBSCR20A	Probable 28S rRNA (cytosine-C(5))-methyltransferase
NSUN5P1	Q3KNT7	NSN5B_HUMAN	NSUN5P1 NSUN5B WBSCR20B	Putative NOL1/NOP2/Sun domain family member 5B
NSUN5P2	Q63ZY6	NSN5C_HUMAN	NSUN5P2 NSUN5C WBSCR20B WBSCR20C	Putative methyltransferase NSUN5C
NSUN6	Q8TEA1	NSUN6_HUMAN	NSUN6 NOPD1	Putative methyltransferase NSUN6
NSUN7	Q8NE18	NSUN7_HUMAN	NSUN7	Putative methyltransferase NSUN7
NTMT1	Q9BV86	NTM1A_HUMAN	NTMT1 C9orf32 METTL11A NRMT NRMT1 AD-003	N-terminal Xaa-Pro-Lys N-methyltransferase 1
PCMT1	P22061	PIMT_HUMAN	PCMT1	Protein-L-isoaspartate(D-aspartate) O-methyltransferase ShortPIMT
PNMT	P11086	PNMT_HUMAN	PNMT PENT	Phenylethanolamine N-methyltransferase ShortPNMTase
PP7517	Q8WZ04	TOMT_HUMAN	LRTOMT COMT2 TOMT PP7517	Transmembrane O-methyltransferase

Table S3 continued from previous page

PRMT2	P55345	ANM2_HUMAN	PRMT2 HMT1 HRMT1L1	Protein arginine N-methyltransferase 2
PRMT3	O60678	ANM3_HUMAN	PRMT3 HRMT1L3	Protein arginine N-methyltransferase 3
PRMT5	O14744	ANM5_HUMAN	PRMT5 HRMT1L5 IBP72 JBP1 SKB1	Protein arginine N-methyltransferase 5
PRMT6	Q96LA8	ANM6_HUMAN	PRMT6 HRMT1L6	Protein arginine N-methyltransferase 6
PRMT7	Q9NVM4	ANM7_HUMAN	PRMT7 KIAA1933	Protein arginine N-methyltransferase 7
PRMT8	Q9NR22	ANM8_HUMAN	PRMT8 HRMT1L3 HRMT1L4	Protein arginine N-methyltransferase 8
PRMT9	Q6P2P2	ANM9_HUMAN	PRMT9 PRMT10	Protein arginine N-methyltransferase 9
RNMT	O43148	MCES_HUMAN	RNMT KIAA0398	mRNA cap guanine-N7 methyltransferase
RRP8	O43159	RRP8_HUMAN	RRP8 KIAA0409 NML hucep-1	Ribosomal RNA-processing protein 8
TFB1M	Q8WVM0	TFB1M_HUMAN	TFB1M CGI-75	Dimethyladenosine transferase 1, mitochondrial
TFB2M	Q9H5Q4	TFB2M_HUMAN	TFB2M NS5ATP5	Dimethyladenosine transferase 2, mitochondrial
TGS1	Q96RS0	TGS1_HUMAN	TGS1 HCA137 NCOA6IP PIMT	Trimethylguanosine synthase
TPMT	P51580	TPMT_HUMAN	TPMT	Thiopurine S-methyltransferase
TRDMT1	O14717	TRDMT_HUMAN	TRDMT1 DNMT2	tRNA (cytosine(38)-C(5))-methyltransferase
TRMT1	Q9NXH9	TRM1_HUMAN	TRMT1	tRNA (guanine(26)-N(2))-dimethyltransferase
TRMT11	Q7Z4G4	TRM11_HUMAN	TRMT11 C6orf75 MDS024	tRNA (guanine(10)-N2)-methyltransferase homolog
TRMT1L	Q7Z2T5	TRM1L_HUMAN	TRMT1L C1orf25 TRM1L MSTP070	TRMT1-like protein
TRMT2A	Q8IZ69	TRM2A_HUMAN	TRMT2A HTF9C	tRNA (uracil-5-)-methyltransferase homolog A
TRMT2B	Q96GJ1	TRM2_HUMAN	TRMT2B CXorf34	tRNA (uracil(54)-C(5))-methyltransferase homolog
TRMT44	Q8IYL2	TRM44_HUMAN	TRMT44 C4orf23 METTL19	Probable tRNA (uracil-O(2)-)-methyltransferase
TRMT61A	Q96FX7	TRM61_HUMAN	TRMT61A C14orf172 TRM61	tRNA (adenine(58)-N(1))-methyltransferase catalytic subunit TRMT61A
TRMT61B	Q9BVS5	TR61B_HUMAN	TRMT61B	tRNA (adenine(58)-N(1))-methyltransferase, mitochondrial
VCPKMT	Q9H867	MT21D_HUMAN	VCPKMT C14orf138 METTL21D	Protein-lysine methyltransferase METTL21D

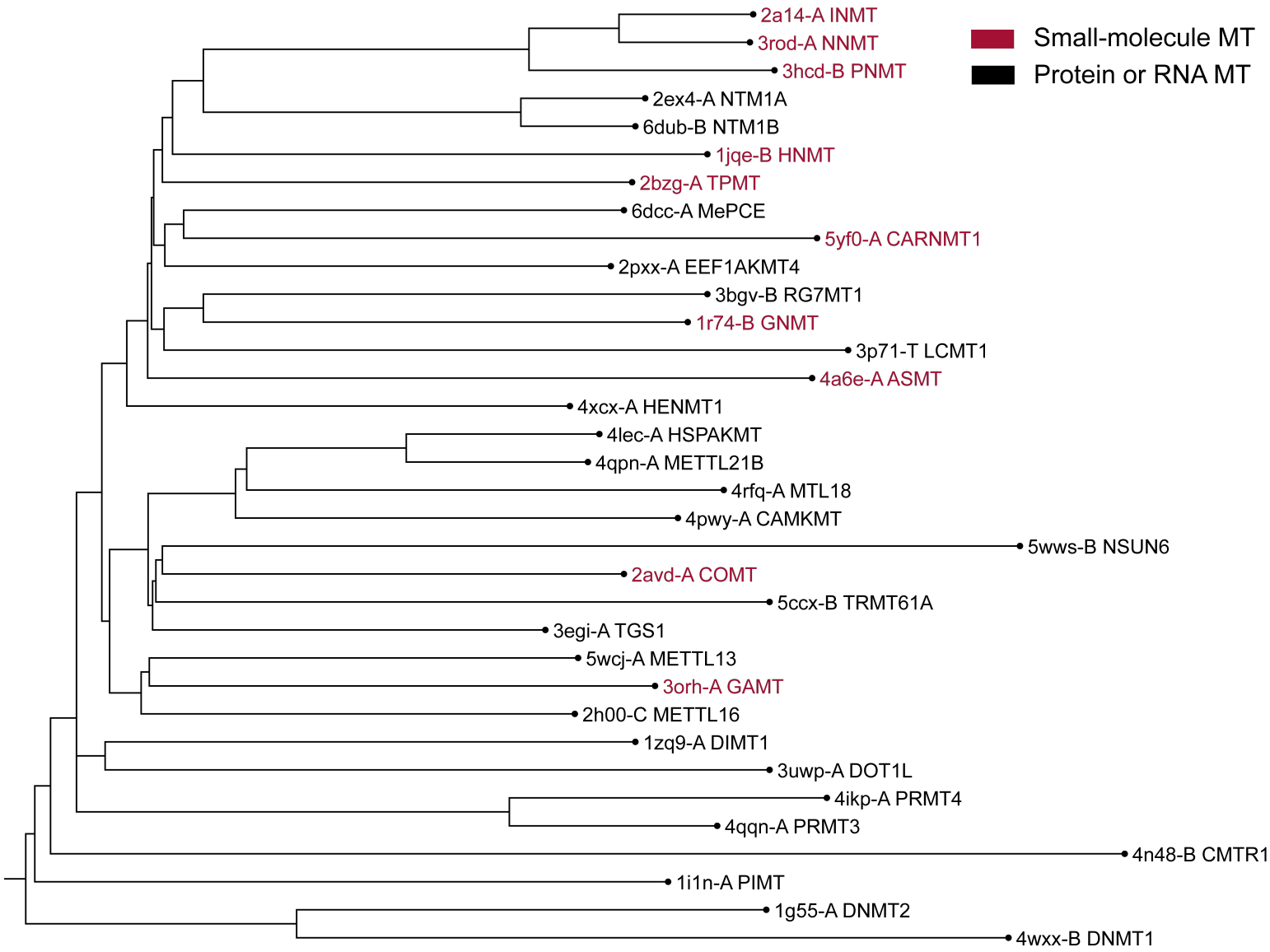

Figure S3: Structural similarity dendrogram. The dendrogram is derived by average linkage clustering of the structural similarity matrix (Dali Z-scores).

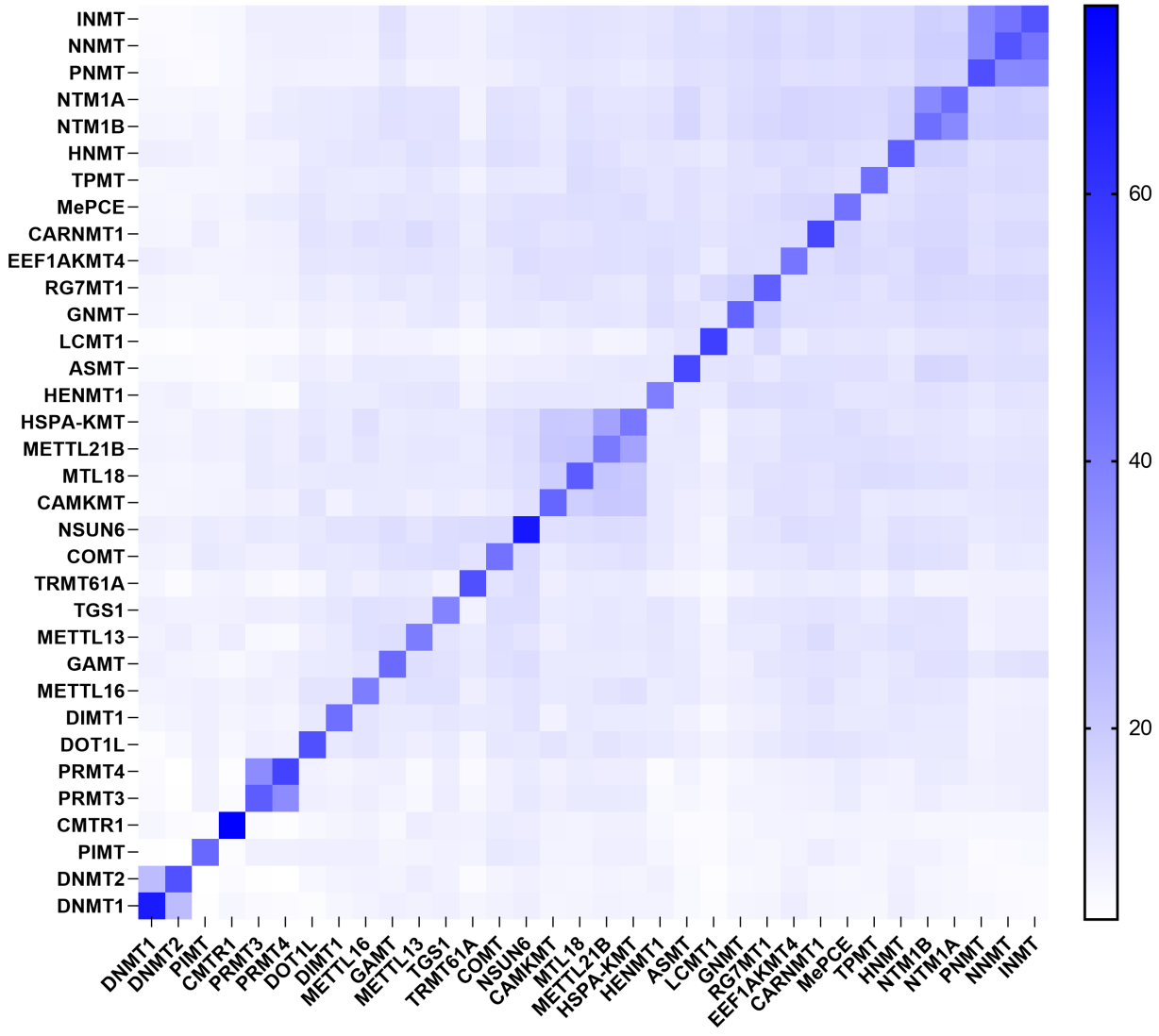

Figure S4: Heatmap of DALI Z-scores. Axes are labelled with protein abbreviations and correspond to those listed in Table S4. Note the NNMT/INMT/PNMT cluster (top right) indicating high structural similarity between these proteins.

Table S4: DALI output used to rank human methyltransferases by structural similarity (sorted by Z-score). A detailed description of the DALI structural alignment workflow is given in Section 6.4

Number	PDB ID	Z	rmsd	lali	nres	%id	Abbrev.	Full Name	Substrate	UniProt ID
1	3rod-A	51.2	0	260	260	100	NNMT	nicotinamide N-methyltransferase	SM	P40261
30	2a14-A	43.2	1.1	258	258	52	INMT	indolethylamine N-methyltransferase	SM	O95050
35	3hcd-B	37.6	1.5	252	269	39	PNMT	phenylethanolamine N-methyltransferase	SM	P11086
115	6dub-B	18.7	2.9	197	218	15	NTM1B	alpha N-terminal protein methyltransferase 1B	protein	Q5VVY1
117	2ex4-A	18.5	2.9	197	222	18	NTM1A	N-terminal Xaa-pro-lys N-methyltransferase 1	protein	Q9BV86
285	3bgv-B	15.9	3.2	192	271	13	RG7MT1	mRNA cap guanine-N7 methyltransferase	RNA	O43148
349	2bzg-A	15.5	2.8	190	230	12	TPMT	thiopurine S-methyltransferase	SM	P51580
385	5yf0-A	15.4	3.1	192	337	14	CARNMT1	carnosine N-methyltransferase	SM	Q8N4J0
422	1jqe-B	15.2	3.0	188	281	12	HNMT	histamine N-methyltransferase	SM	P50135
498	1r74-B	14.9	2.7	183	279	16	GNMT	glycine N-methyltransferase	SM	Q14749
517	2pxx-A	14.8	2.9	173	214	14	EEF1AKMT4	EEF1A lysine methyltransferase 4	Protein	P0DPD7
625	4a6e-A	14.4	3.1	188	346	14	ASMT	acetylserotonin O-methyltransferase	SM	P46597
633	6dcc-A	14.4	3.1	179	222	17	MePCE	7SK snRNA methylphosphate capping enzyme	RNA	Q7L2J0
666	3p71-T	14.2	3.5	205	315	8	LCMT1	leucine carboxyl methyltransferase 1	protein	Q9UIC8
886	4xcx-A	13.1	3.2	169	217	12	HENMT1	Small RNA 2'-O-methyltransferase	RNA	Q5T8I9
897	4rfq-A	13.0	3.5	182	269	17	MTL18	histidine protein methyltransferase 1 homolog	protein	O95568
–	3orh-A	13.0	3.3	192	231	17	GAMT	guanidinoacetate N-methyltransferase	SM	Q14353
977	4qpn-A	12.5	2.8	162	203	17	METTL21B	EEF1A lysine methyltransferase 3	protein	Q96AZ1
991	4pwy-A	12.4	3.3	174	251	15	CLNMT	calmodulin-lysine N-methyltransferase	Protein	Q7Z624
1078	4lec-A	12.0	3.1	163	203	13	HSPA-KMT	protein N-lysine methyltransferase METTL21A	protein	Q8WXB1
1090	5wws-B	12.0	3.6	166	458	14	NSUN6	putative methyltransferase NSUN6	RNA	Q8TEA1
1160	2avd-A	11.4	3.6	163	220	10	COMT	catechol O-methyltransferase domain-containing protein 1	SM	Q86VU5
1230	3egi-A	10.4	3.0	156	195	10	TGS1	trimethylguanosine synthase	RNA	Q96RS0
1233	5wcj-A	10.3	3.2	155	222	14	METTL13	methyltransferase-like protein 13	protein	Q8N6R0
1246	3uwp-A	10.1	3.2	166	341	11	DOT1L	histone-lysine N-methyltransferase, H3 lysine-79 specific	protein	Q8TEK3
1266	4ikp-A	10.0	2.9	157	335	13	PRMT4	histone-arginine methyltransferase CARM1	protein	Q86X55
1270	1zq9-A	9.9	2.8	156	279	13	DIMT1	probable dimethyladenosine transferase	RNA	Q9UNQ2
1315	2h00-C	9.7	3.3	161	204	14	METTL16	RNA N6-adenosine-methyltransferase METTL16	RNA	Q86W50
1342	4qqn-A	9.6	2.9	149	299	15	PRMT3	protein arginine N-methyltransferase 3	protein	O60678
1351	5ccx-B	9.5	3.4	155	371	11	TRMT61A	tRNA (adenine(58)-N(1))-methyltransferase catalytic subunit TRMT61A	RNA	Q96FX7
1558	4n48-B	7.7	4.0	164	406	6	CMTR1	cap-specific mRNA (nucleoside-2'-O-)-methyltransferase 1	RNA	Q8N1G2
1588	4wxx-B	7.3	3.5	142	1178	10	DNMT1	DNA (cytosine-5)-methyltransferase 1	DNA	P26358
1589	1i1n-A	7.2	3.3	137	225	15	PIMT	protein-L-isoaspartate(D-aspartate) O-methyltransferase	protein	P22061
1601	1g55-A	7.0	4.5	132	314	11	TRDMT1	tRNA (cytosine(38)-C(5))-methyltransferase	RNA	O14717

Table S5: Assays performed in the course of this work to evaluate selectivity for NNMT.

Enzyme/Assay	Source	Substrate/Stimulus Tracer	Incubation	Measured Component	Detection Method	Reference
thiopurine S-methyltransferase (TPMT)	HR (E. coli)	6-mercaptopurine (8 µM), SAM (1.5 µM)	30 min, 22°C	SAH	MS	Krijt et al.[a]
indoleethylamine N-methyltransferase (INMT)	HR (E. coli)	tryptamine (1 mM), SAM (10 µM)	30 min, 22°C	luminescence	plate reader	this work
catechol O-methyltransferase (COMT)	HR (E. coli)	pyrocatechol (15 µM), SAM (10 µM)	15 min, 37°C	SAH	MS	Krijt et al.[a]
phenylethanolamine N-methyltransferase (PNMT)	HR (E. coli)	DL-normetanephrine (35 µM), SAM (6 µM)	45 min, 22°C	SAH	MS	Krijt et al.[a]
glycine N-methyltransferase (GNMT)	HR (E. coli)	glycine (100 µM), SAM (20 µM)	30 min, 22°C	SAH	MS	Krijt et al.[a]
guanidinoacetate N-methyltransferase (GAMT)	HR (E. coli)	guanidineacetic acid (4 µM), SAM (7 µM)	30 min, 22°C	SAH	MS	Krijt et al.[a]
histamine N-methyltransferase (HNMT)	HR (E. coli)	histamine (4 µM), SAM (4 µM)	15 min, 22°C	SAH	MS	Krijt et al.[a]
DNMT3a	HR (Sf9 cells)	poly(dI-dC)-poly(dI-dC) (0.6 mU/ml), [3H] SAM (100 nM)	10 min, 37°C	methylated poly(dI-dC)-Poly(dI-dC)	scint. counting	Aoki et al.[b]
PRMT1	HR (E. coli)	histone H4 full length (50 nM), [3H]SAM (700 nM)	20 min, 22°C	methylated histone H4 full length	scint. counting	Cheng et al.[c]
ASH1L	HR (E. coli)	polynucleosome (1.5 µg/ml), [3H] SAM (150nM)	15 min, 22°C	methylated polynucleosome	scint. counting	An et al.[d]
DOT1L	HR (E. coli)	polynucleosome (2.5 µg/ml), [3H]SAM (100 nM)	15 min, 22°C	methylated polynucleosome	scint. counting	Yost et al.[e]
EHMT1	HR (E. coli)	histone H3 full length (10 nM), [3H]SAM (25 nM)	120 min, 22°C	methylated histone H3 full length	scint. counting	Yost et al.[e]
G9a	HR (E. coli)	histone H3 full length (5 nM), [3H]SAM (25 nM)	120 min, 22°C	methylated histone H3 full length	scint. counting	Yost et al.[e]
SETDB1	HR (cellules Sf9)	histone H3 full length (30 nM), [3H]SAM (250 nM)	30 min, 22°C	methylated histone H3 full length	scint. counting	Schultz et al.[f]

[a] Krijt, J.; Dutá, A.; Kožich, V. *J. Chromatogr., B* **2009**, *877*, 2061–2066.
[b] Aoki, A. *Nucleic Acids Res.* **2001**, *29*, 3506–3512.
[c] Cheng, D.; Yadav, N.; King, R. W.; Swanson, M. S.; Weinstein, E. J.; Bedford, M. T. *J. Biol. Chem.* **2004**, *279*, 23892–23899.
[d] An, S.; Yeo, K. J.; Jeon, Y. H.; Song, J.-J. *J. Biol. Chem.* **2011**, *286*, 8369–8374.
[e] Yost, J. M.; Korboukh, I.; Liu, F.; Gao, C.; Jin, J. *Curr. Chem. Genomics* **2011**, *5*, 72–84.
[f] Schultz, D. C.; Ayyanathan, K.; Negorev, D.; Maul, G. G.; Rauscher, F. J. *Genes & Dev.* **2002**, *16*, 919–932.

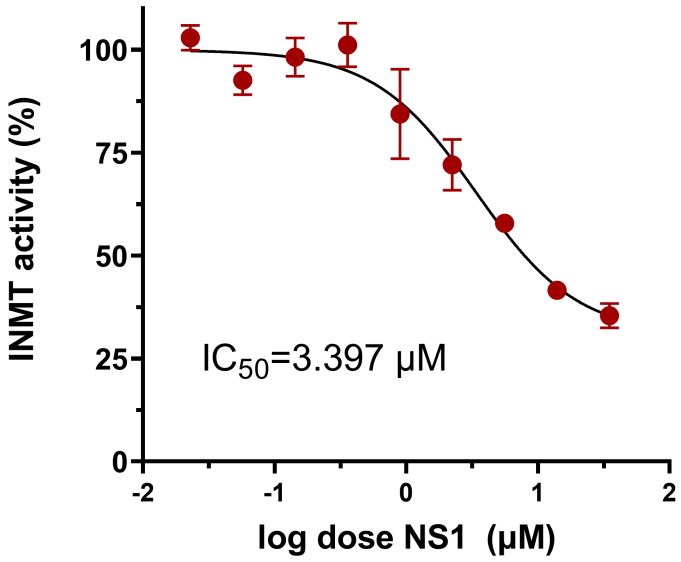

Figure S5: INMT IC_{50} assay performed using the Promega MTase-Glo™ assay. Full experimental details are reported in Section 6.6.2.

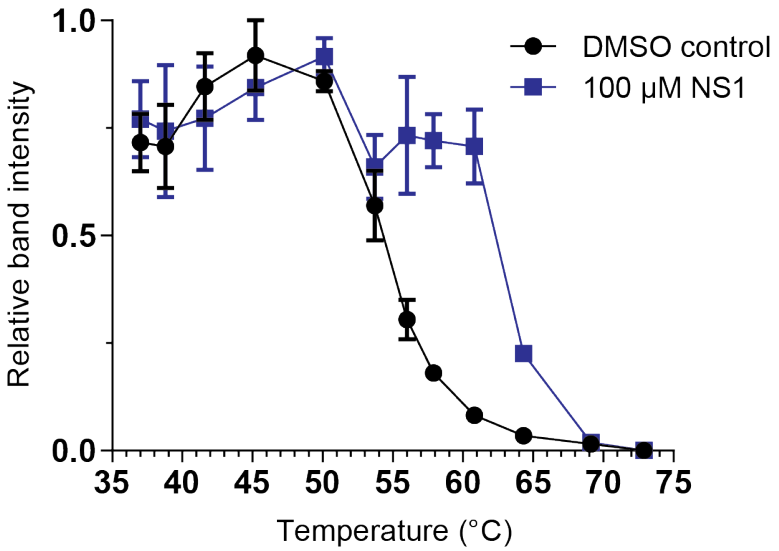

Figure S6: Cellular Thermal Shift Assay (CETSA) with NS1 (**10**), performed according to experimental protocols outlined in the manuscript Experimental section.

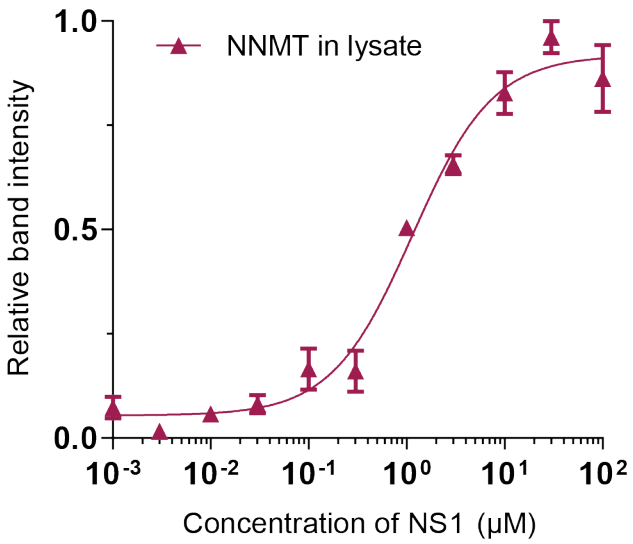

Figure S7: Isothermal Dose Reponse (ITDR) CETSA with with NS1 (**10**), performed according to experimental protocols outlined in the manuscript Experimental section.

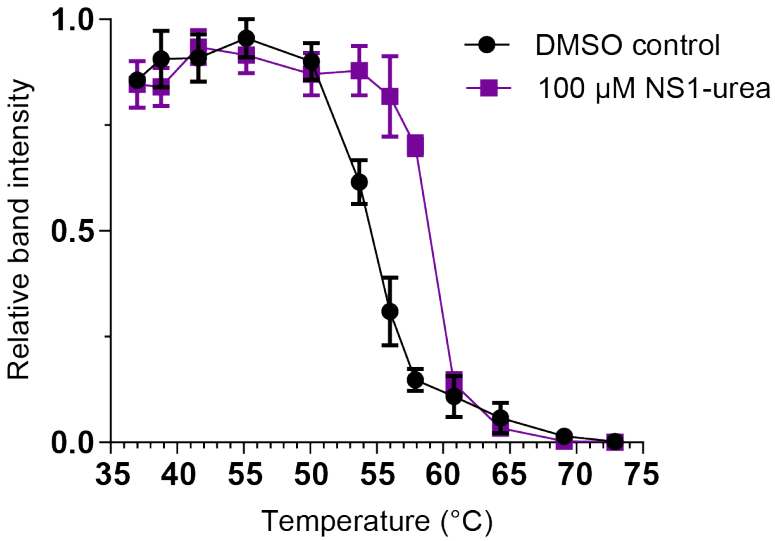

Figure S8: Cellular Thermal Shift Assay (CETSA) with **25** (NS1-Urea), performed according to experimental protocols outlined in the manuscript Experimental section.

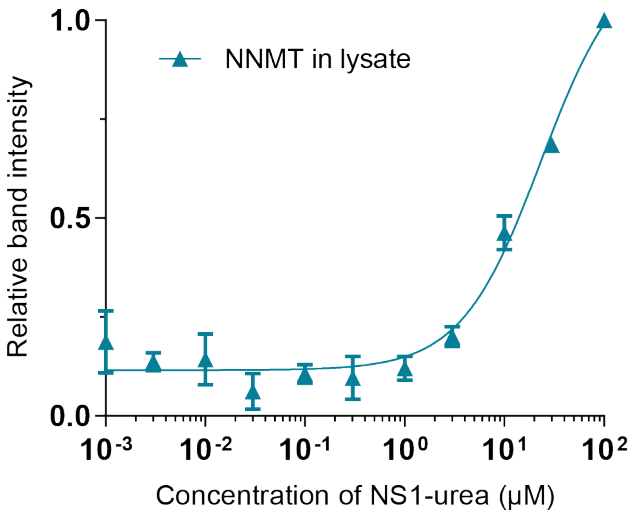

Figure S9: Isothermal Dose Reponse (ITDR) CETSA with **25** (NS1-Urea), performed according to experimental protocols outlined in the manuscript Experimental section.

Table S6: Average % viability in a CellTiter-Glo cytotoxicity assay (U2OS cells, **24 h timepoint**). Experimental details are reported in the manuscript Experimental section.

Compound Identifier	Trivial Name	0.032 µM	0.1 µM	0.32 µM	1 µM	3.2 µM	10 µM	31.6 µM	100 µM
10	NS1	103	105	104	105	106	111	104	106
21	NS1-Amine	102	100	98	99	105	104	97	102
23	NS1-MethylEster	102	104	103	104	106	109	105	106
24	NS1-AminoAmide	99	97	98	100	101	105	101	104
25	NS1-Urea	103	103	100	103	104	107	103	105
Doxorubicin (Positive control)		At 3 µM	At 5 µM	At 10 µM					
		66	39	33					

Table S7: Average % viability in a CellTiter-Glo cytotoxicity assay (U2OS cells, **48 h timepoint**). Experimental details are reported in the manuscript Experimental section.

Compound Identifier	Trivial Name	0.032 µM	0.1 µM	0.32 µM	1 µM	3.2 µM	10 µM	31.6 µM	100 µM
10	NS1	103	105	104	103	103	103	102	106
21	NS1-Amine	102	104	104	103	103	102	103	102
23	NS1-MethylEster	102	104	104	102	102	103	102	104
24	NS1-AminoAmide	101	103	104	102	102	101	102	103
25	NS1-Urea	103	104	103	104	104	102	104	105
Doxorubicin (Positive control)		At 3 µM	At 5 µM	At 10 µM					
		26	25	16					

Table S8: Cellular MNAM levels measured by LC-MS/MS after compound treatment. Compounds noted with [A] were ran on one plate and compounds noted with [B] were ran on a separate plate. ***N1*** and ***N2*** refer to independent experiments performed on different days. Each experiment was run with n=2 replicates. *JBSNF-0088 refers to 6-methoxynicotinamide, a known NNMT inhibitor, and was used a control inhibitor for assay validation.

		N1		***N2***	
Compound Identifier	**Compound Name**	**IC_{50} (µM)**	**% Inhibition at 31.6 µM**	**IC_{50} (µM)**	**% Inhibition at 31.6 µM**
P180810[A]	JBSNF-0088* (control)	1.24		1.03	
10[A]	NS1	>31.6	15	>31.6	21
23[A]	NS1-MethylEster	>31.6	31	>31.6	29
P180810[B]	JBSNF-0088* (control)	0.78		1.01	
21[B]	NS1-Amine	NA		NA	
24[B]	NS1-AminoAmide	>31.6	18	>31.6	17
25[B]	NS1-Urea	NA		NA	

Table S9: A-B permeability assay (Caco-2, pH 6.5/7.4). Incubation: 0 and 60 min, 37°C. Detection, HPLC-MS/MS.[1]

Compound Identifier	Trivial Name	Conc. µM	Perm., 1st 10^{-6} cm/s	2nd	Mean	% Recovery 1st	2nd	Mean	Flags
21	NS1-Amine	10	1.16	1.52	1.3	76	78	77	
23	NS1-MethylEster	10	0.07	0.06	0.1	74	83	78	
25	NS1-Urea	10	0.18	0.2	<0.2	70	65	68	BLQ[2]
10	NS1	10	0.75	0.75	<0.7	90	100	95	BLQ
24	NS1-AminoAmide	10	0.07	0.07	<0.1	92	92	92	BLQ

Table S10: Reference compounds used in the validation of the Caco-2 assay.

Reference Compound	Conc. µM	Perm. 1st 10^{-6} cm/s	2nd	Mean	% Recovery 1stst	2nd	Mean
colchicine	10	0.17	0.22	0.2	72	85	78
labetalol	10	8.53	9.16	8.8	85	87	86
propranolol	10	22.25	25.12	23.7	66	68	67
ranitidine	10	0.56	0.46	0.5	97	96	97

[1] Hidalgo, I. J.; Raub, T. J.; Borchardt, R. T. *Gastroenterology*, **1989**, *96*, 736–749.

[2] *BLQ*: Below the Limit of Quantitation. Test compound was well detected in donor samples but not detected in receiver samples. The concentration of test compound in receiver sample was below the limit of quantitation.

2 List of Abbreviations

Å	angstrom
E	*Ger.*, entgegen
Z	*Ger.*, zusammen
1MQ	1-methylquinolinium
Ac	acetate
Bn	benzyl
BPE	bis(phospholano)ethane
BSA	*N,O*-bis(trimethylsilyl)acetamide
Bz	benzoyl
Cbz	benzyloxycarbonyl
DMAP	4-(dimethylamino)pyridine
DMEAD	di-2-methoxyethyl azodicarboxylate
DMF	*N,N*-dimethylformamide
DMP	Dess-Martin periodinane
DMPU	*N,N'*-dimethylpropylene urea
DMSO	dimethyl sulfoxide
DTBMP-OTf	2,6-di-*tert*-butyl-4-methylpyridinium triflate
equiv.	equivalent
Fmoc	9-fluorenylmethoxycarbonyl
HMPA	hexamethylphosphoramide
HRMS	high-resolution mass spectrometry
LDA	lithium diisopropylamide
M.S.	molecular sieves
MTBE	methyl *tert*-butyl ether
NAM	nicotinamide
Ns	2-nitrobenzenesulfonyl

ODE	ordinary differential equation
PhH	benzene
PhMe	toluene
PMHS	(poly)methylhydrosiloxane
Pyr	pyridine
quant.	quantitative
rbf	round-bottom flask
rfu	relative fluorescence units
RT	room temperature
SAH	S-adenosylhomocysteine
SAM	S-adenosylmethionine
SAR	structure-activity relationship
TASF	tris(dimethylamino)sulfonium difluorotrimethylsilicate
TBAF	tetra-*n*-butylammonium fluoride
TBAI	tetra-*n*-butylammonium iodide
TBDPS	*tert*-butyldiphenylsilyl
TBS	*tert*-butyldimethylsilyl
Tf_2O	trifluoromethanesulfonic (triflic) anhydride
TFA	trifluoroacetic acid / trifluoroacetyl
Tf	trifluoromethanesulfonyl
THF	tetrahydrofuran
TIPS	triisopropylsilyl
TMS	trimethylsilyl
Ts	*p*-toluenesulfonyl

3 Positional Numbering System

The following figure features representative examples of the positional numbering system used in this work. Several compound names directly derive from it, such as NS1-Pyr12' for the analog where the carbon atom at the 12' position was replaced by a nitrogen atom or NS1-12'Cl for the analog where a chloro substituent was added at the 12' position.

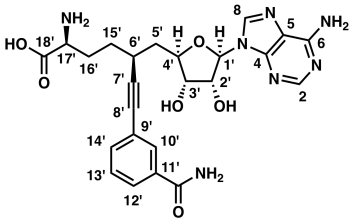

NS1 (**10**)

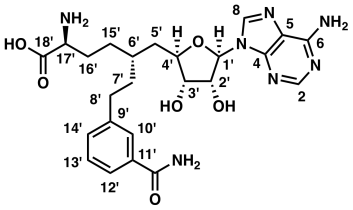

NS1-6'EpiAlkane (**16**)

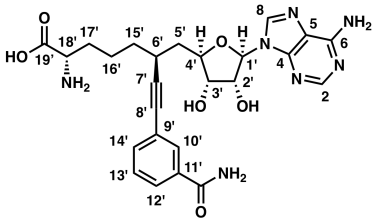

Homo-NS1 (**26**)

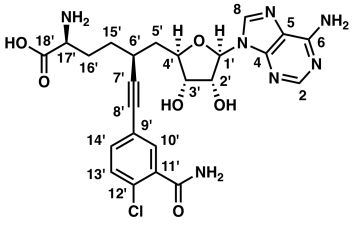

NS1-12'Cl (**33**)

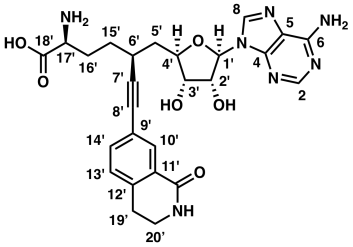

NS1-Benzolactam6 (**34**)

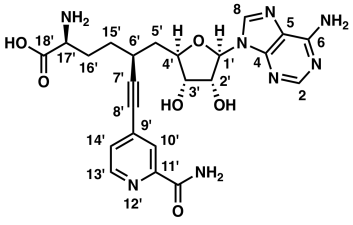

NS1-Pyr12' (**38**)

*(Intermediates that have not been assigned numbering in the main text are numbered sequentially in the experimental section starting with **S1**).*

4 Supplemental Schemes

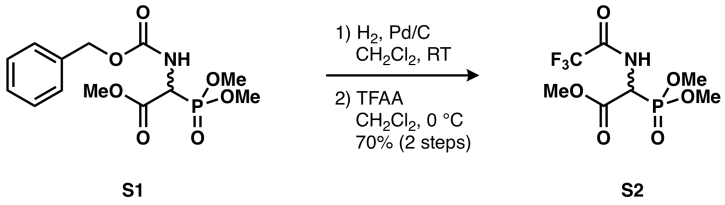

Scheme S1

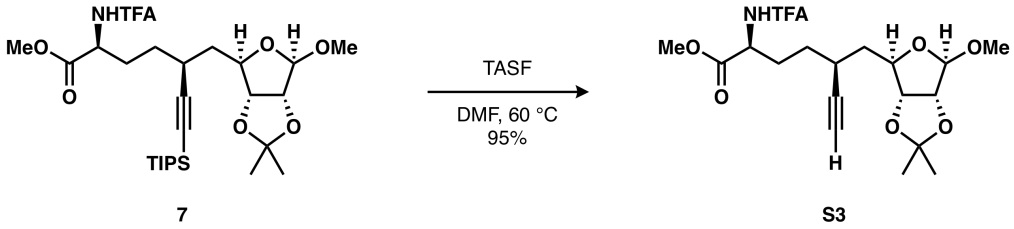

Scheme S2

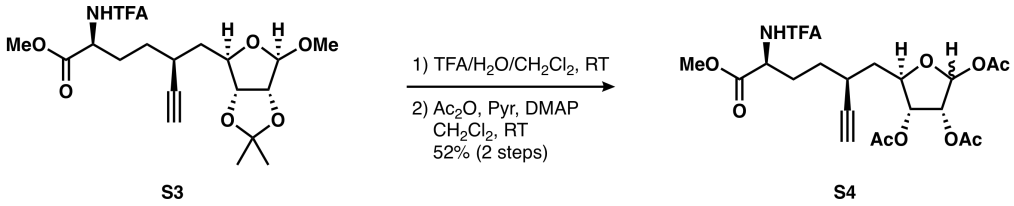

Scheme S3

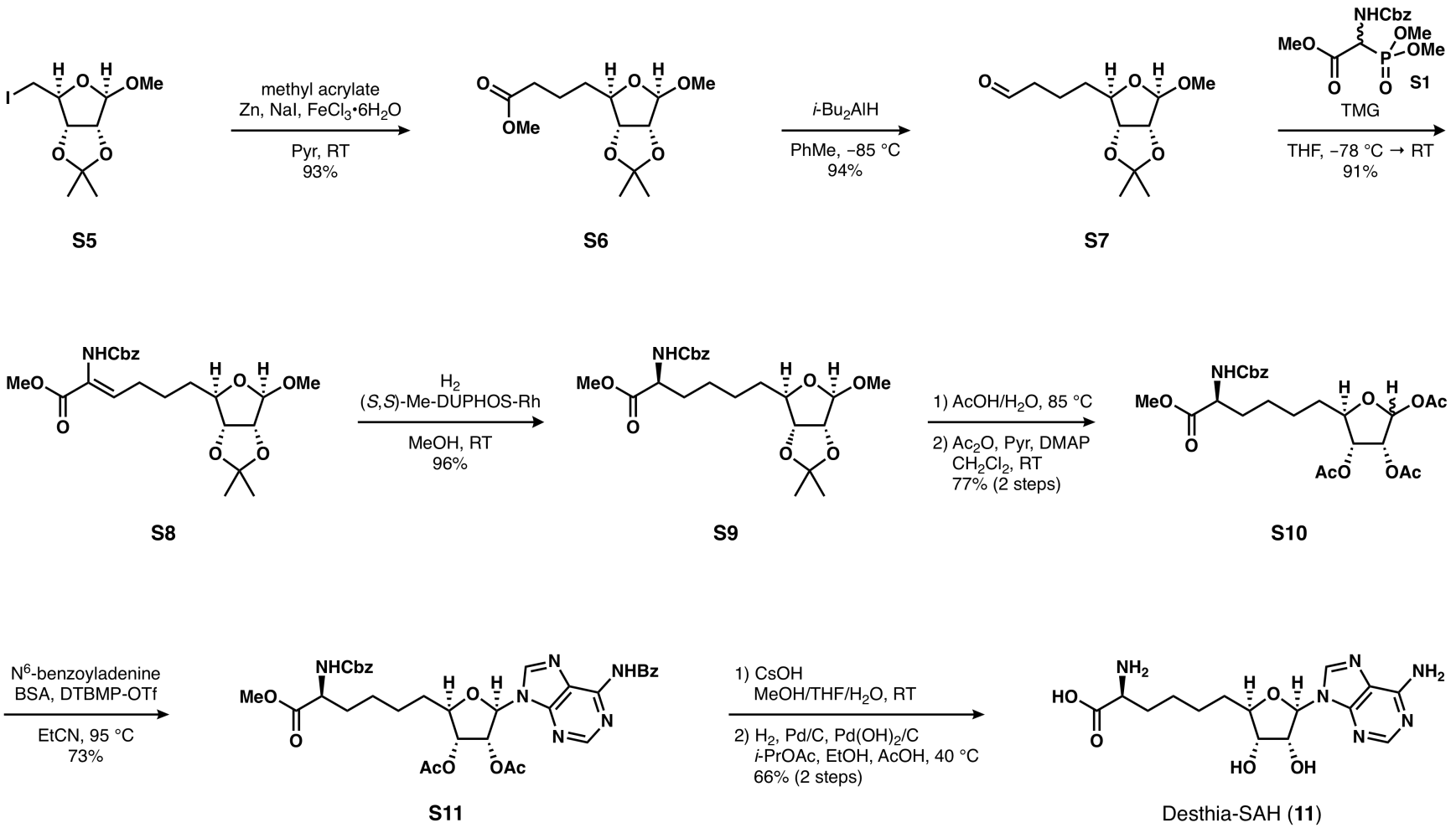
methyl acrylate
Zn, NaI, FeCl3•6H2O
Pyr, RT
93%
i-Bu2AlH
PhMe, −85 °C
94%
TMG
THF, −78 °C → RT
91%
S1
S5
S6
S7
H2
(S,S)-Me-DUPHOS-Rh
MeOH, RT
96%
1) AcOH/H2O, 85 °C
2) Ac2O, Pyr, DMAP
CH2Cl2, RT
77% (2 steps)
S8
S9
S10
N6-benzoyladenine
BSA, DTBMP-OTf
EtCN, 95 °C
73%
1) CsOH
MeOH/THF/H2O, RT
2) H2, Pd/C, Pd(OH)2/C
i-PrOAc, EtOH, AcOH, 40 °C
66% (2 steps)
S11
Desthia-SAH (11)

Scheme S4

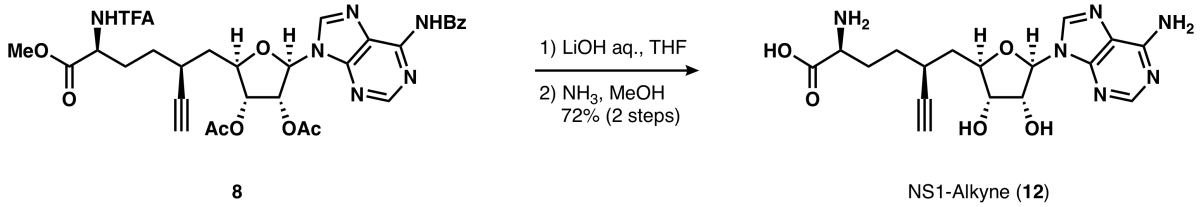

Scheme S5

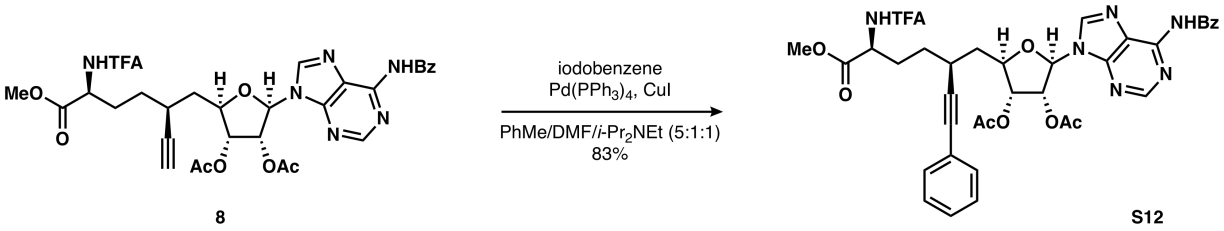

Scheme S6

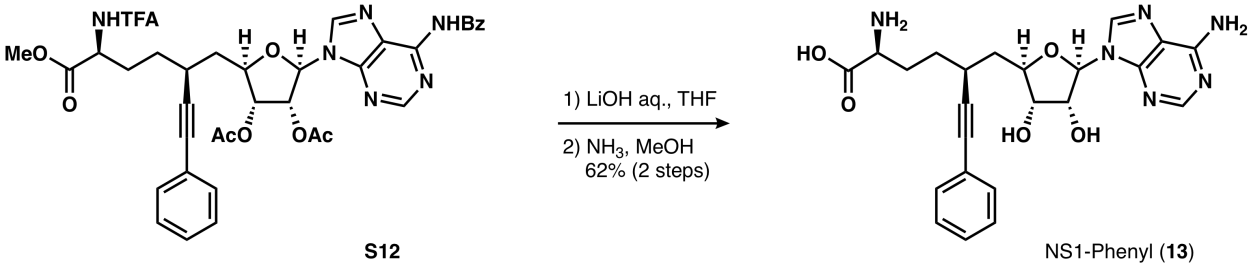

Scheme S7

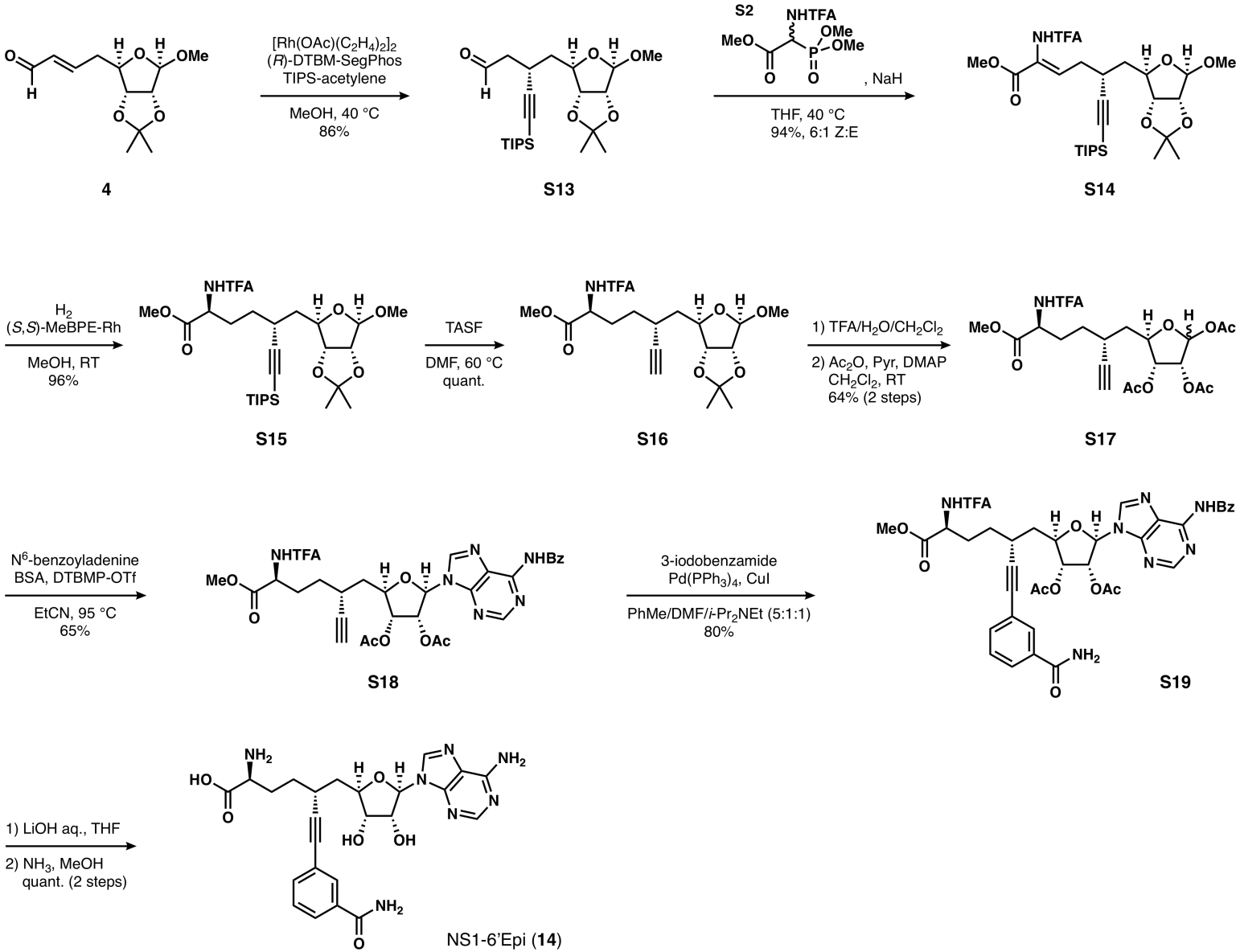
[Rh(OAc)(C2H4)2]2
(R)-DTBM-SegPhos
TIPS-acetylene
MeOH, 40 °C
86%
S2
NHTFA
OMe
OMe
MeO
P
O
O
, NaH
THF, 40 °C
94%, 6:1 Z:E
H2
(S,S)-MeBPE-Rh
MeOH, RT
96%
TASF
DMF, 60 °C
quant.
1) TFA/H2O/CH2Cl2
2) Ac2O, Pyr, DMAP
CH2Cl2, RT
64% (2 steps)
N6-benzoyladenine
BSA, DTBMP-OTf
EtCN, 95 °C
65%
3-iodobenzamide
Pd(PPh3)4, CuI
PhMe/DMF/i-Pr2NEt (5:1:1)
80%
1) LiOH aq., THF
2) NH3, MeOH
quant. (2 steps)
4
S13
S14
S15
S16
S17
S18
S19
NS1-6'Epi (14)

Scheme S8

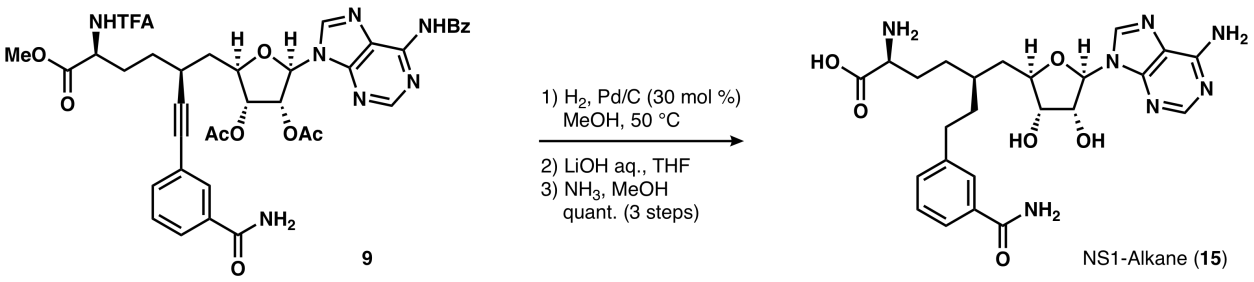

Scheme S9

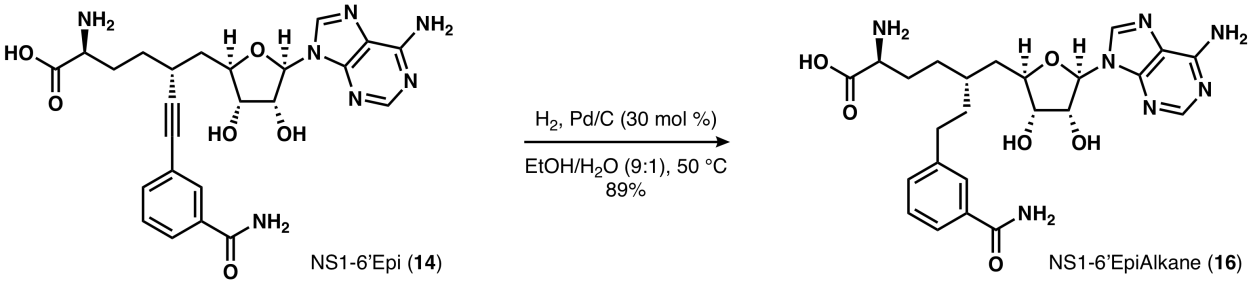

Scheme S10

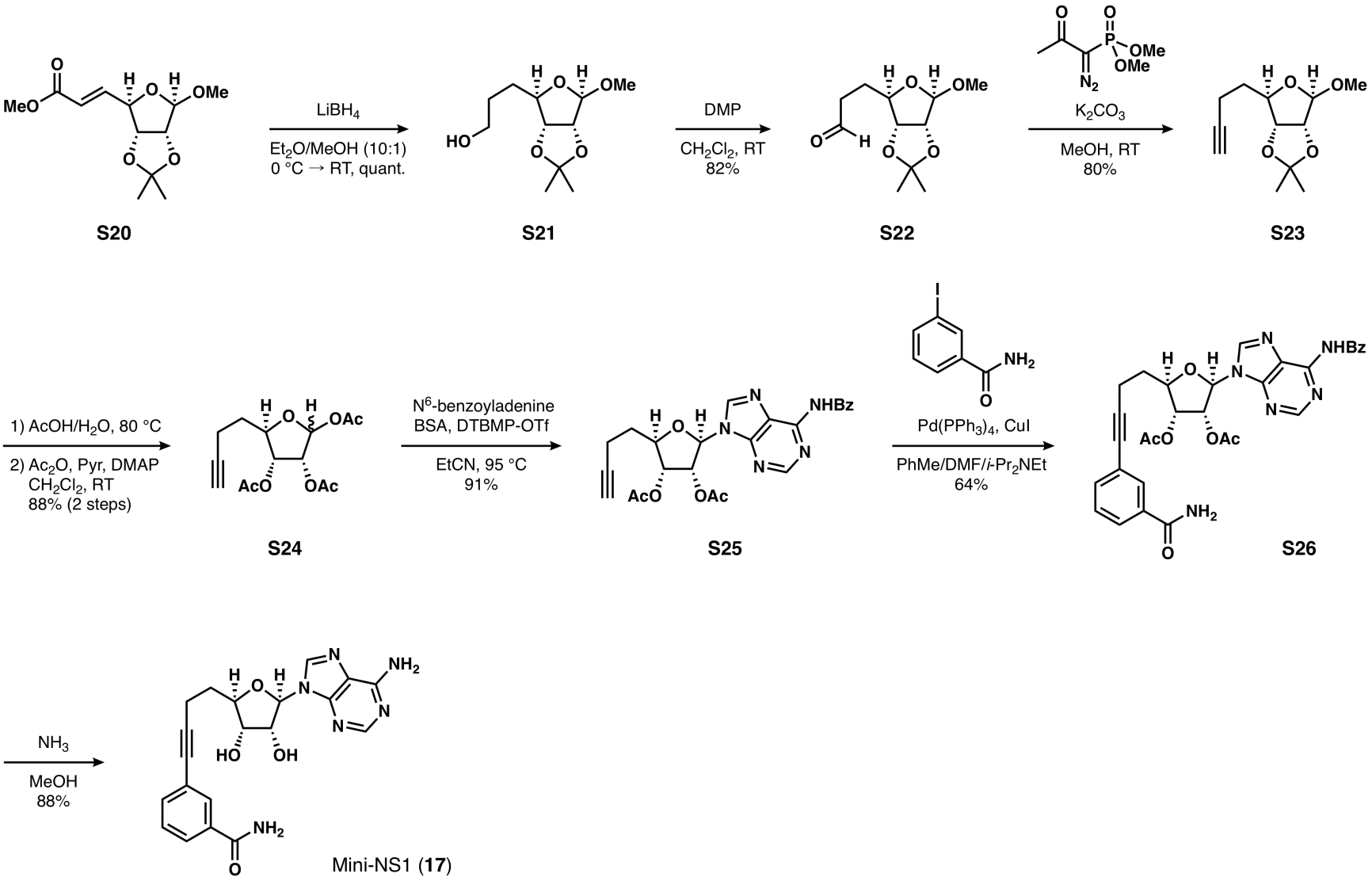
S20
LiBH4
Et2O/MeOH (10:1)
0 °C → RT, quant.
S21
DMP
CH2Cl2, RT
82%
S22
K2CO3
MeOH, RT
80%
S23
1) AcOH/H2O, 80 °C
2) Ac2O, Pyr, DMAP
CH2Cl2, RT
88% (2 steps)
S24
N6-benzoyladenine
BSA, DTBMP-OTf
EtCN, 95 °C
91%
S25
Pd(PPh3)4, CuI
PhMe/DMF/i-Pr2NEt
64%
S26
NH3
MeOH
88%
Mini-NS1 (17)

Scheme S11

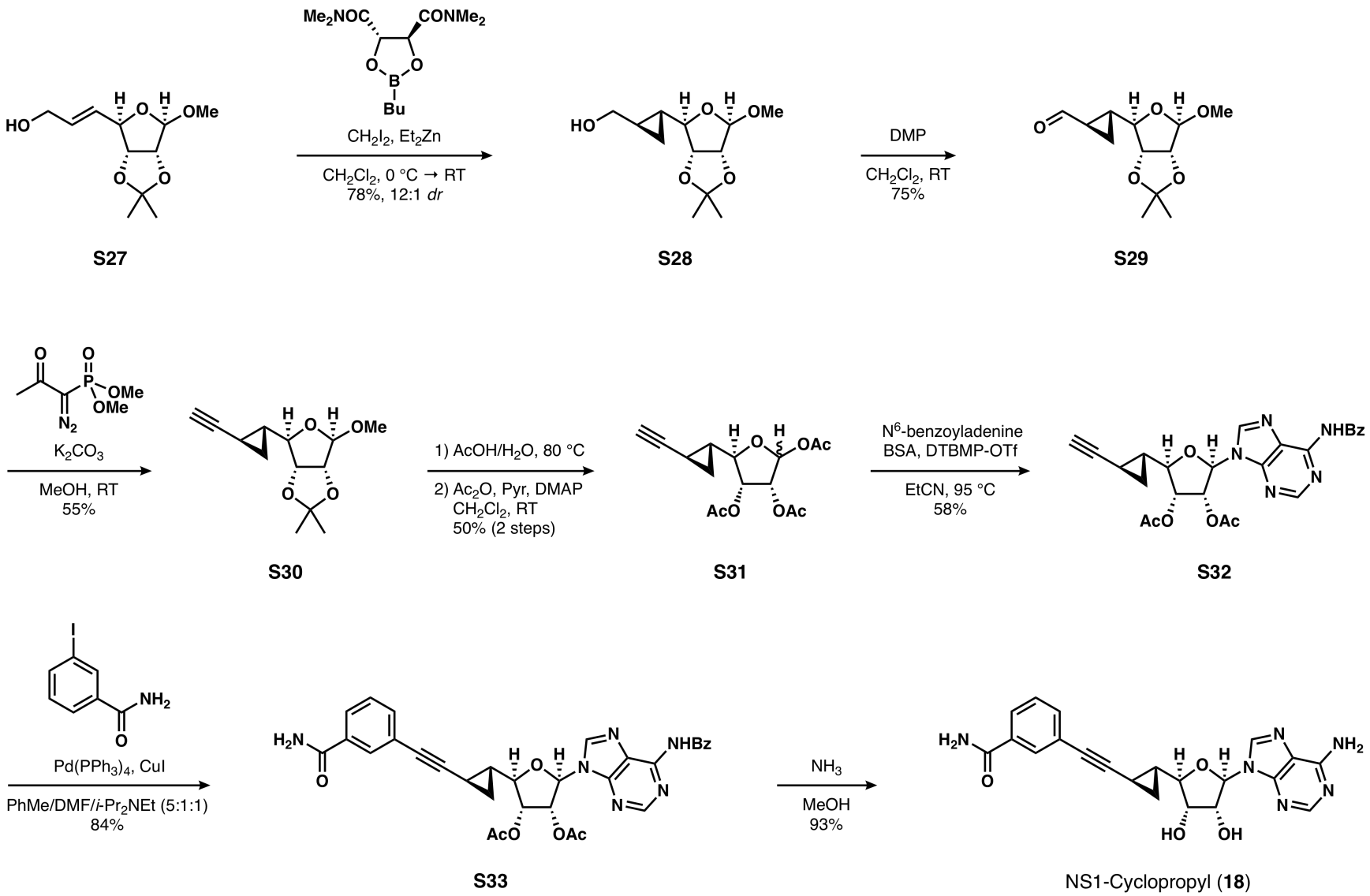
Me2NOC
CONMe2
Bu
CH2I2, Et2Zn
CH2Cl2, 0 °C → RT
78%, 12:1 dr
DMP
CH2Cl2, RT
75%
S27
S28
S29
K2CO3
MeOH, RT
55%
1) AcOH/H2O, 80 °C
2) Ac2O, Pyr, DMAP
CH2Cl2, RT
50% (2 steps)
N6-benzoyladenine
BSA, DTBMP-OTf
EtCN, 95 °C
58%
S30
S31
S32
Pd(PPh3)4, CuI
PhMe/DMF/i-Pr2NEt (5:1:1)
84%
NH3
MeOH
93%
S33
NS1-Cyclopropyl (18)

Scheme S12

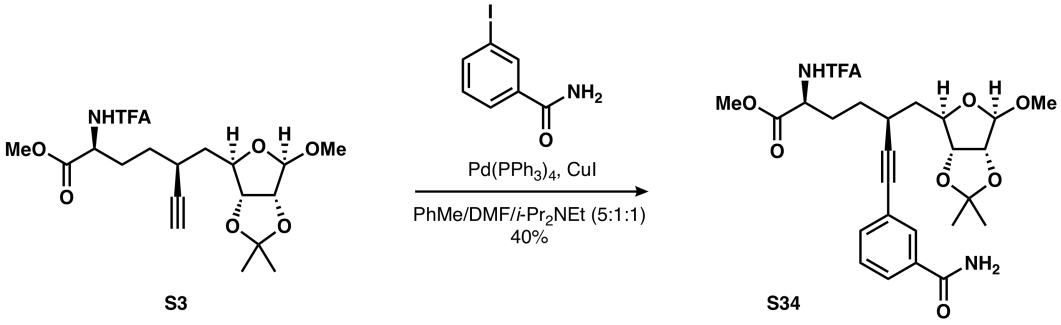

Scheme S13

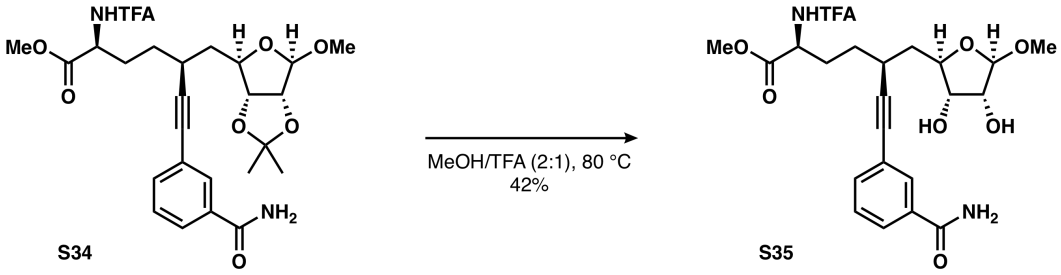

Scheme S14

Scheme S15

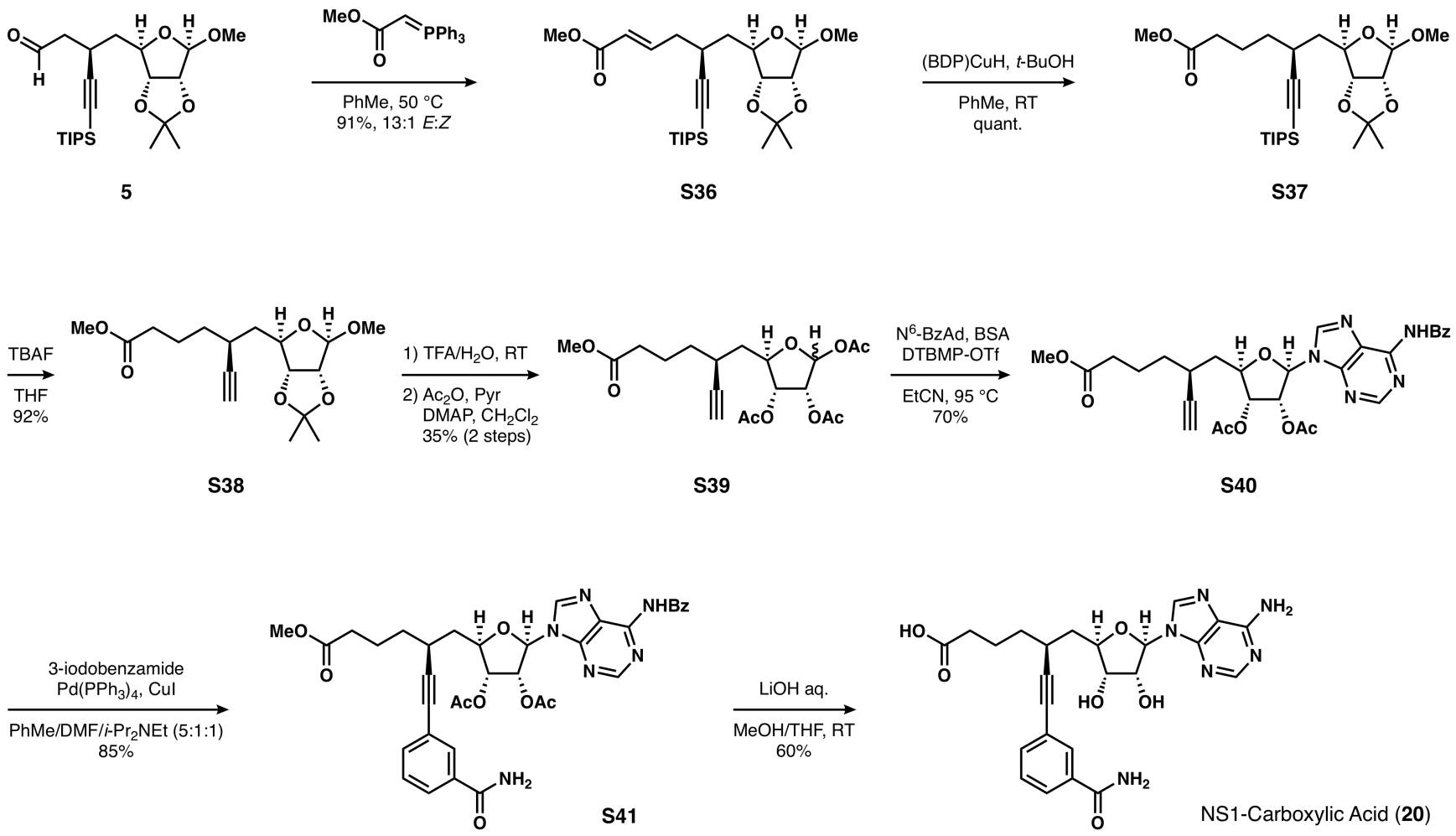
5
PhMe, 50 °C
91%, 13:1 E:Z
S36
(BDP)CuH, t-BuOH
PhMe, RT
quant.
S37
TBAF
THF
92%
S38
1) TFA/H2O, RT
2) Ac2O, Pyr
DMAP, CH2Cl2
35% (2 steps)
S39
N6-BzAd, BSA
DTBMP-OTf
EtCN, 95 °C
70%
S40
3-iodobenzamide
Pd(PPh3)4, CuI
PhMe/DMF/i-Pr2NEt (5:1:1)
85%
S41
LiOH aq.
MeOH/THF, RT
60%
NS1-Carboxylic Acid (20)

Scheme S16

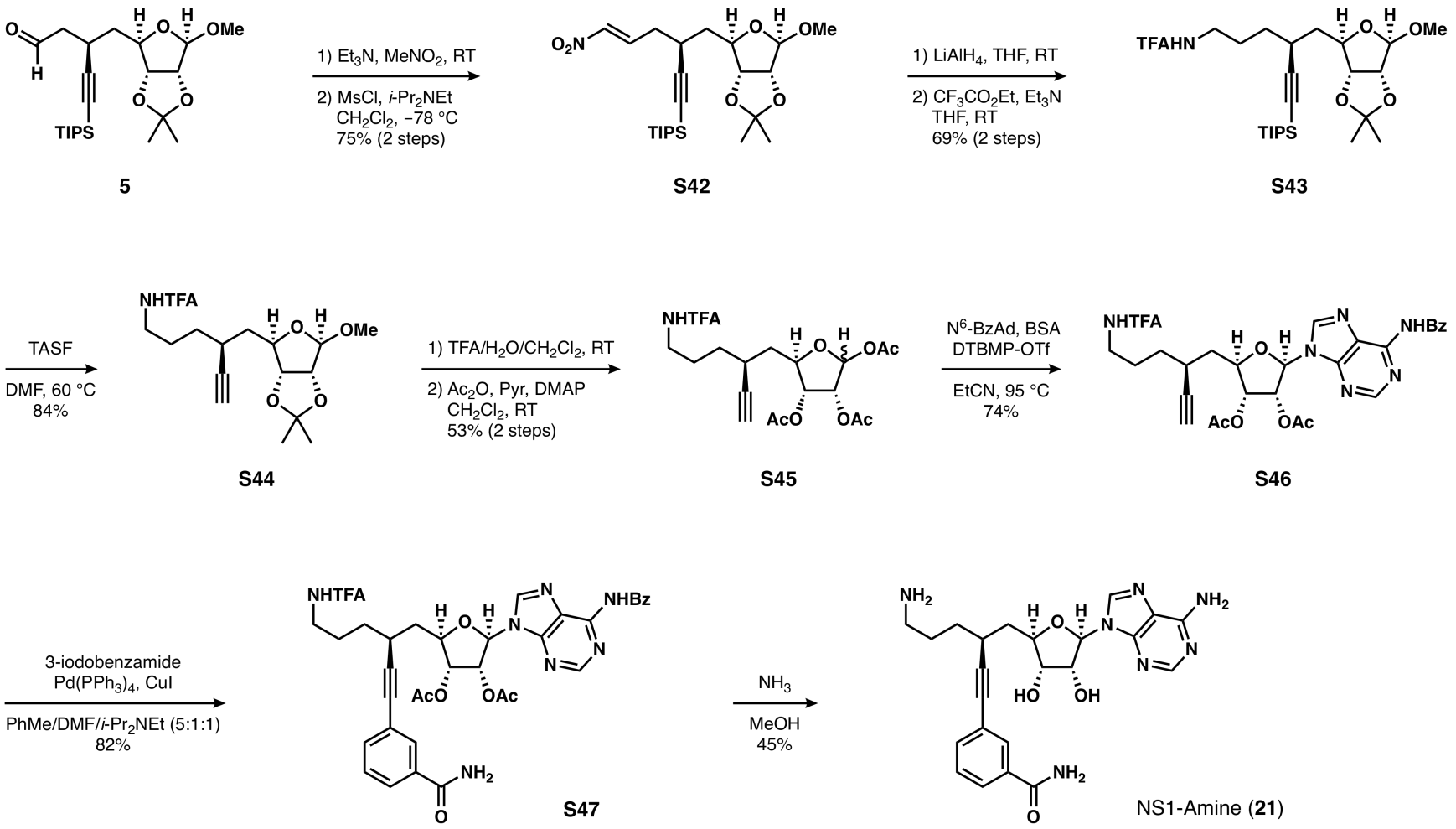
1) Et3N, MeNO2, RT
2) MsCl, i-Pr2NEt
CH2Cl2, −78 °C
75% (2 steps)
1) LiAlH4, THF, RT
2) CF3CO2Et, Et3N
THF, RT
69% (2 steps)
TASF
DMF, 60 °C
84%
1) TFA/H2O/CH2Cl2, RT
2) Ac2O, Pyr, DMAP
CH2Cl2, RT
53% (2 steps)
N6-BzAd, BSA
DTBMP-OTf
EtCN, 95 °C
74%
3-iodobenzamide
Pd(PPh3)4, CuI
PhMe/DMF/i-Pr2NEt (5:1:1)
82%
NH3
MeOH
45%
5
S42
S43
S44
S45
S46
S47
NS1-Amine (21)

Scheme S17

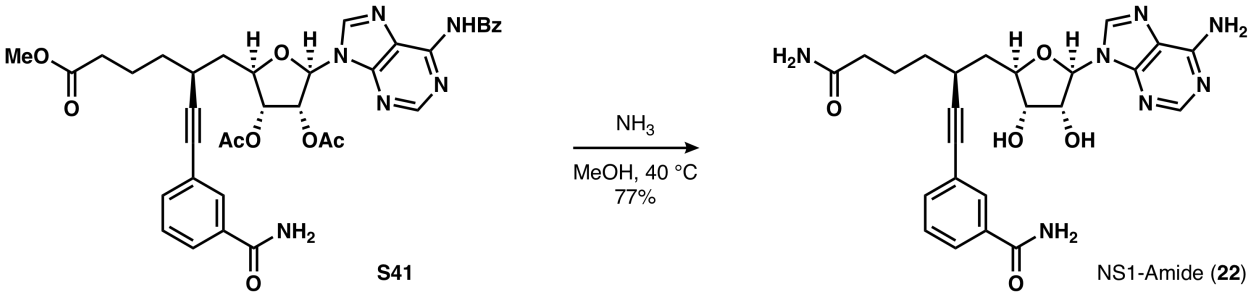
MeO
O
H
O
H
N
N
N
NHBz
AcO
OAc
NH2
O
S41
NH3
MeOH, 40 °C
77%
H2N
O
H
O
H
N
N
N
NH2
HO
OH
NH2
O
NS1-Amide (22)

Scheme S18

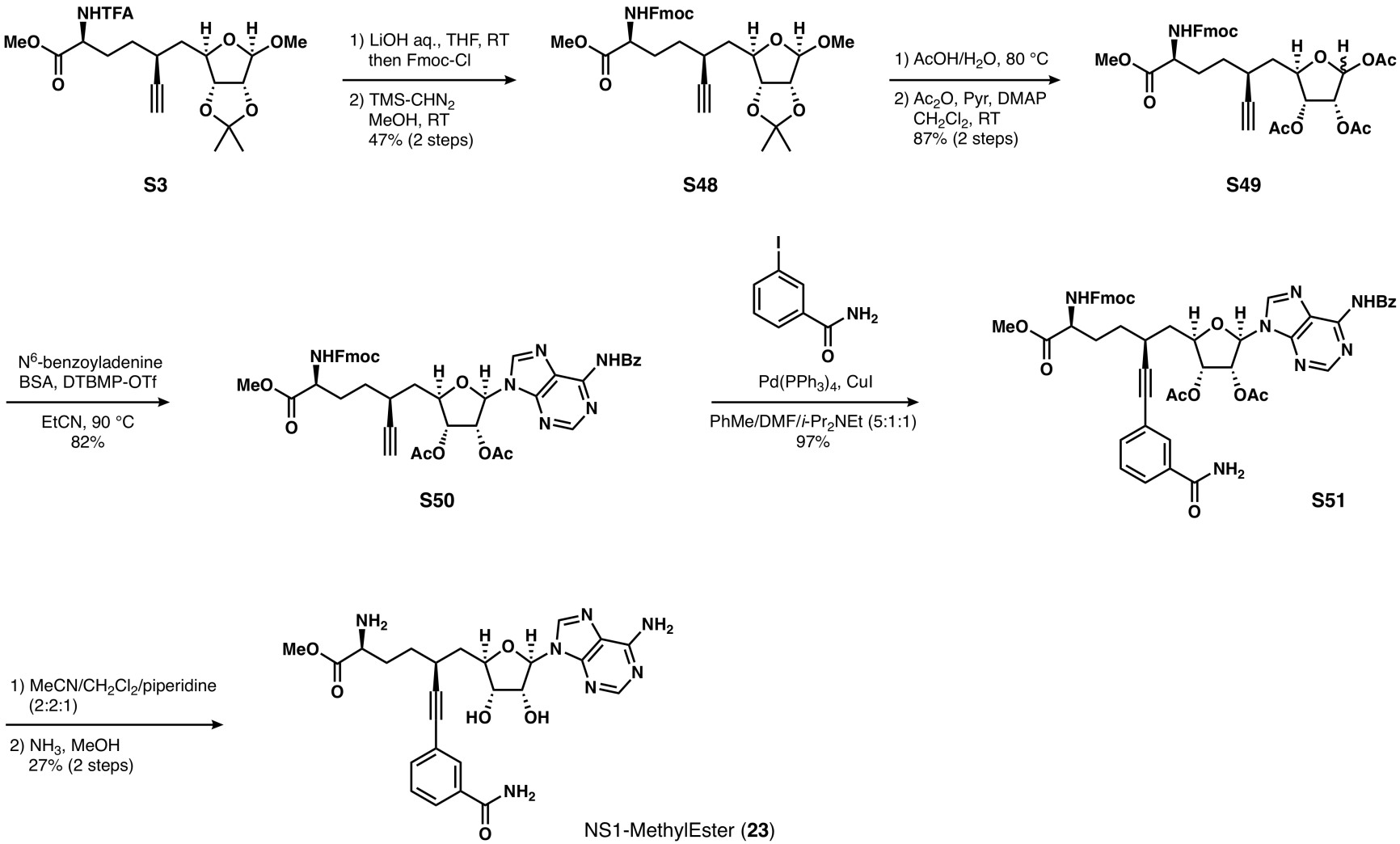
NHTFA
MeO
O
H
O
H
OMe
O
O
1) LiOH aq., THF, RT
then Fmoc-Cl
2) TMS-CHN2
MeOH, RT
47% (2 steps)
NHFmoc
1) AcOH/H2O, 80 °C
2) Ac2O, Pyr, DMAP
CH2Cl2, RT
87% (2 steps)
AcO
OAc
S3
S48
S49
N6-benzoyladenine
BSA, DTBMP-OTf
EtCN, 90 °C
82%
NHBz
N
I
NH2
Pd(PPh3)4, CuI
PhMe/DMF/i-Pr2NEt (5:1:1)
97%
S50
S51
1) MeCN/CH2Cl2/piperidine
(2:2:1)
2) NH3, MeOH
27% (2 steps)
HO
OH
NS1-MethylEster (23)

Scheme S19

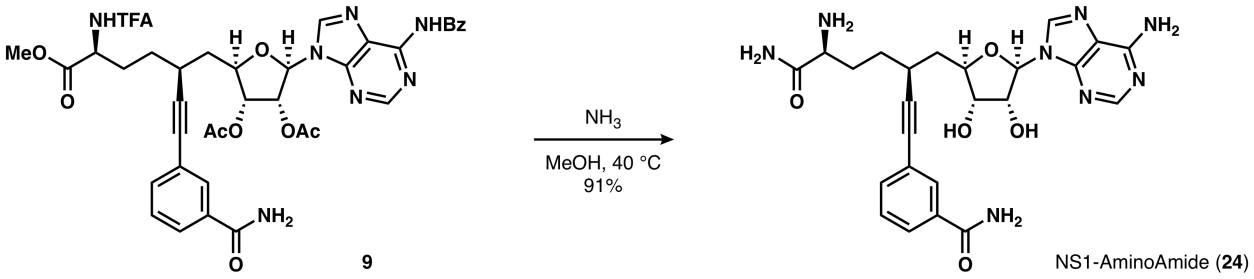
NHTFA
MeO
O
H
O
H
N
N
NHBz
N
N
AcO
OAc
NH2
O
9
NH3
MeOH, 40 °C
91%
NH2
H2N
O
H
O
H
N
N
NH2
N
N
HO
OH
NH2
O
NS1-AminoAmide (24)

Scheme S20

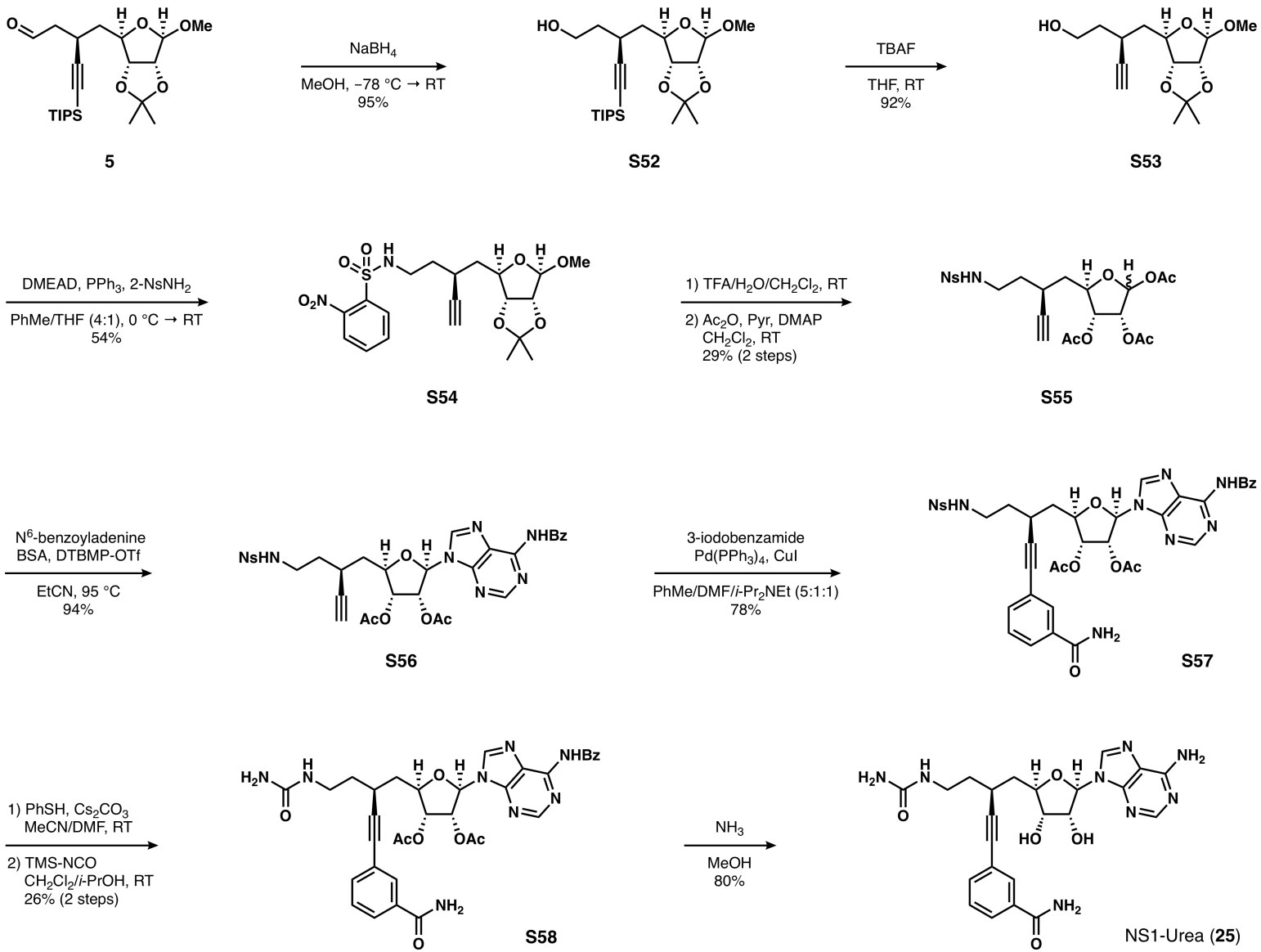
NaBH4
MeOH, −78 °C → RT
95%
TBAF
THF, RT
92%
DMEAD, PPh3, 2-NsNH2
PhMe/THF (4:1), 0 °C → RT
54%
1) TFA/H2O/CH2Cl2, RT
2) Ac2O, Pyr, DMAP
CH2Cl2, RT
29% (2 steps)
N6-benzoyladenine
BSA, DTBMP-OTf
EtCN, 95 °C
94%
3-iodobenzamide
Pd(PPh3)4, CuI
PhMe/DMF/i-Pr2NEt (5:1:1)
78%
1) PhSH, Cs2CO3
MeCN/DMF, RT
2) TMS-NCO
CH2Cl2/i-PrOH, RT
26% (2 steps)
NH3
MeOH
80%
5
S52
S53
S54
S55
S56
S57
S58
NS1-Urea (25)

Scheme S21

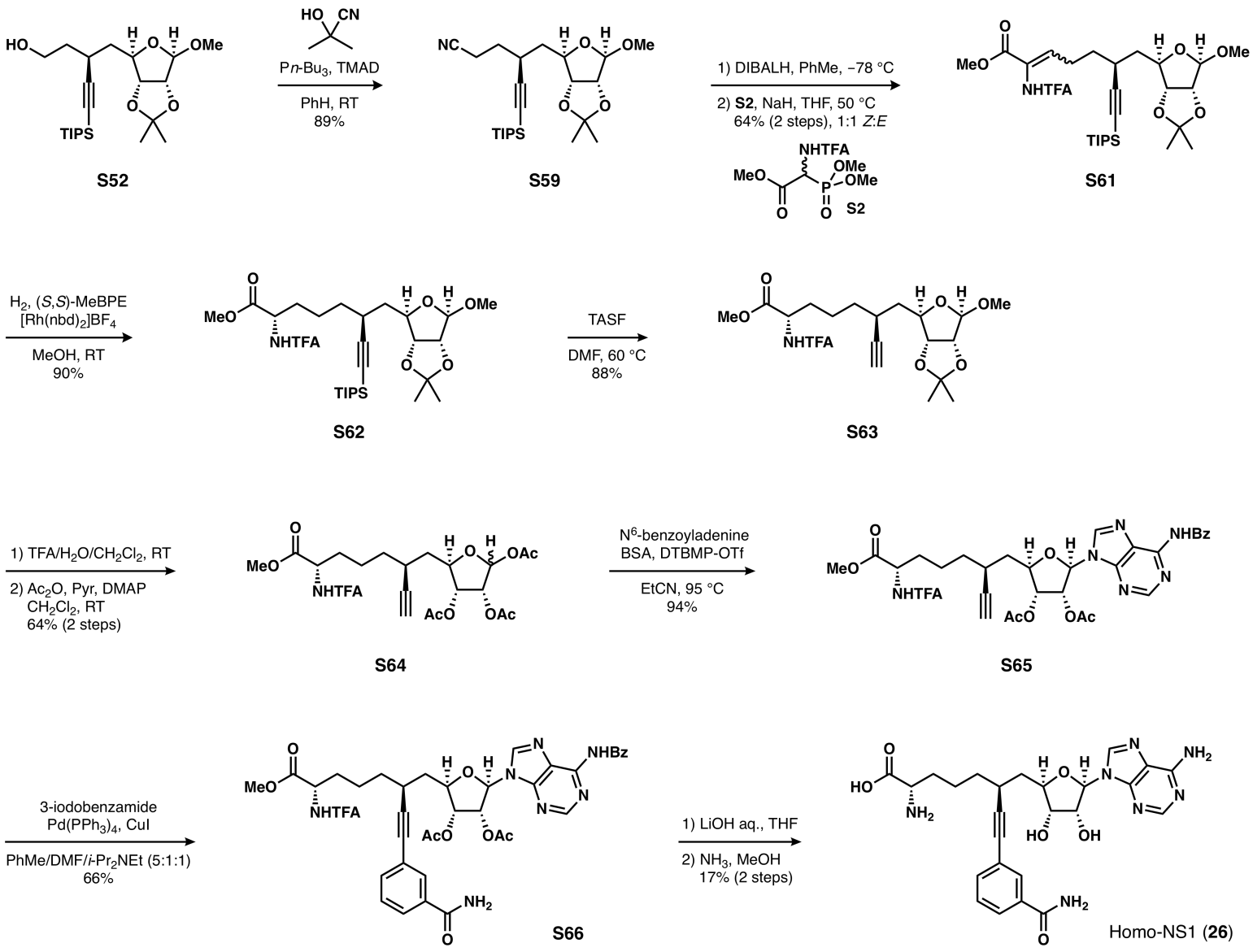
HO
TIPS
OMe
S52
HO CN
Pn-Bu$_3$, TMAD
PhH, RT
89%
NC
S59
1) DIBALH, PhMe, −78 °C
2) S2, NaH, THF, 50 °C
64% (2 steps), 1:1 Z:E
NHTFA
MeO
S2
S61
H$_2$, (S,S)-MeBPE
[Rh(nbd)$_2$]BF$_4$
MeOH, RT
90%
S62
TASF
DMF, 60 °C
88%
S63
1) TFA/H$_2$O/CH$_2$Cl$_2$, RT
2) Ac$_2$O, Pyr, DMAP
CH$_2$Cl$_2$, RT
64% (2 steps)
OAc
AcO
S64
N^6-benzoyladenine
BSA, DTBMP-OTf
EtCN, 95 °C
94%
NHBz
S65
3-iodobenzamide
Pd(PPh$_3$)$_4$, CuI
PhMe/DMF/i-Pr$_2$NEt (5:1:1)
66%
NH$_2$
S66
1) LiOH aq., THF
2) NH$_3$, MeOH
17% (2 steps)
Homo-NS1 (26)

Scheme S22

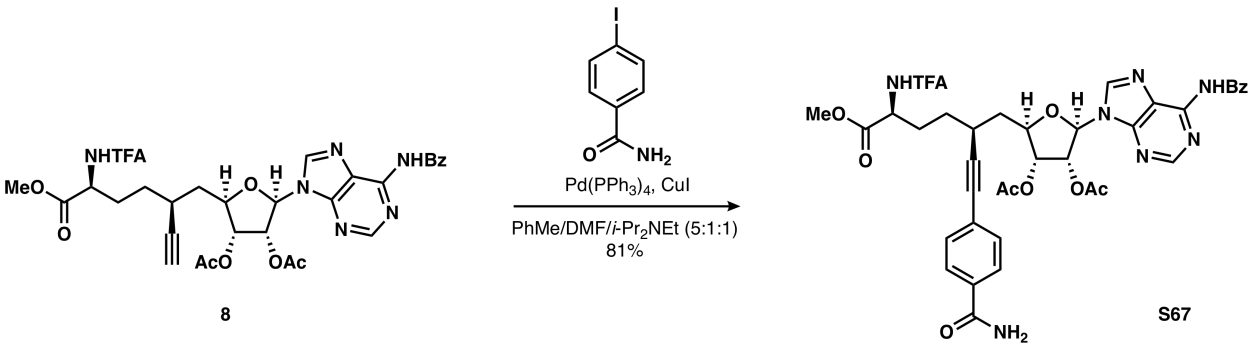

Scheme S23

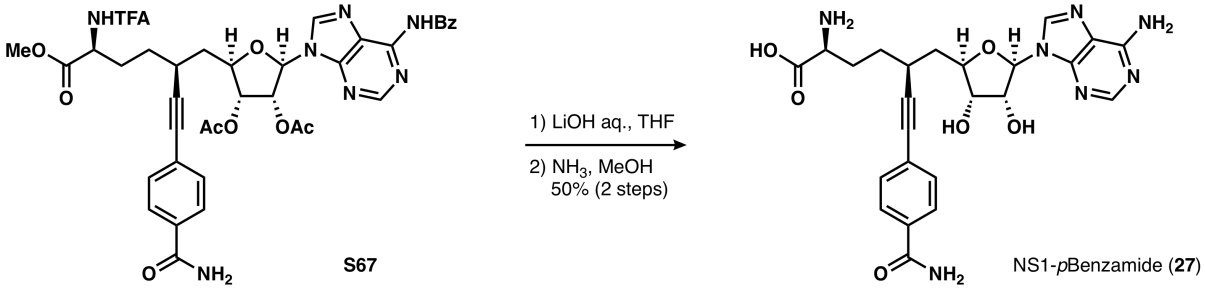

Scheme S24

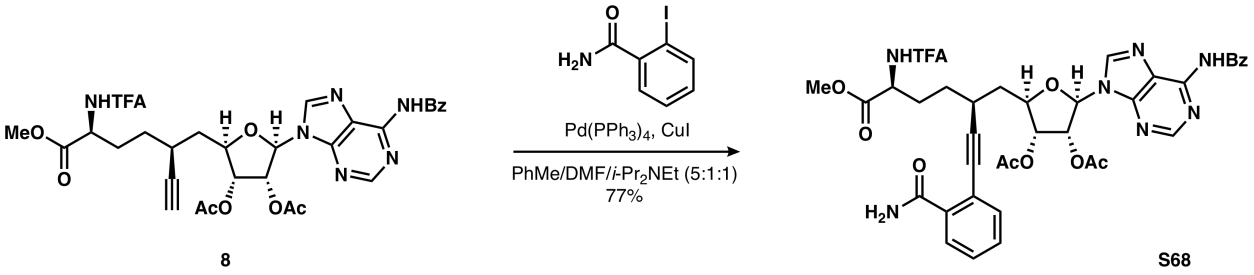

Scheme S25

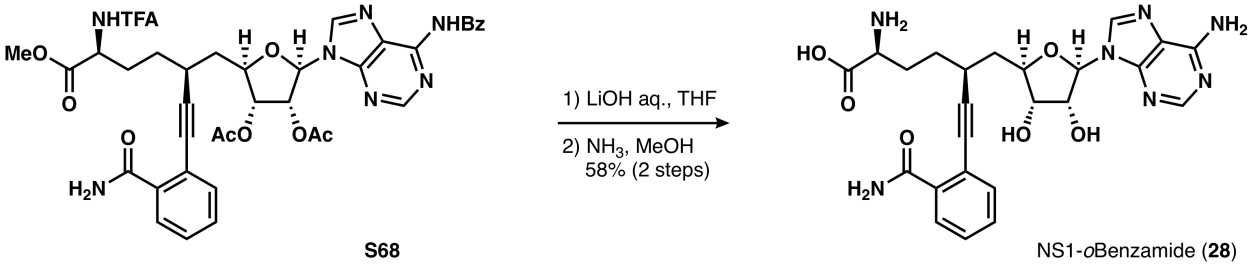

Scheme S26

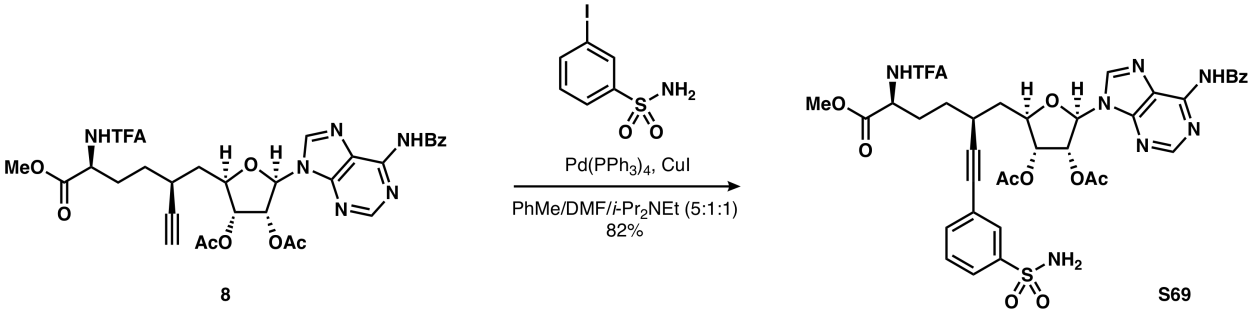

Scheme S27

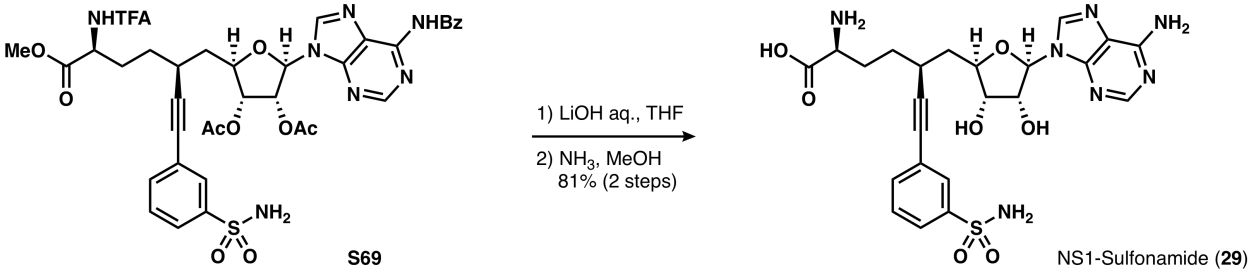

Scheme S28

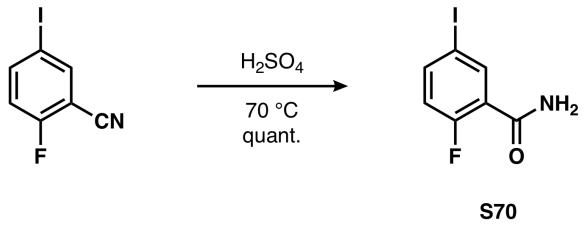

Scheme S29

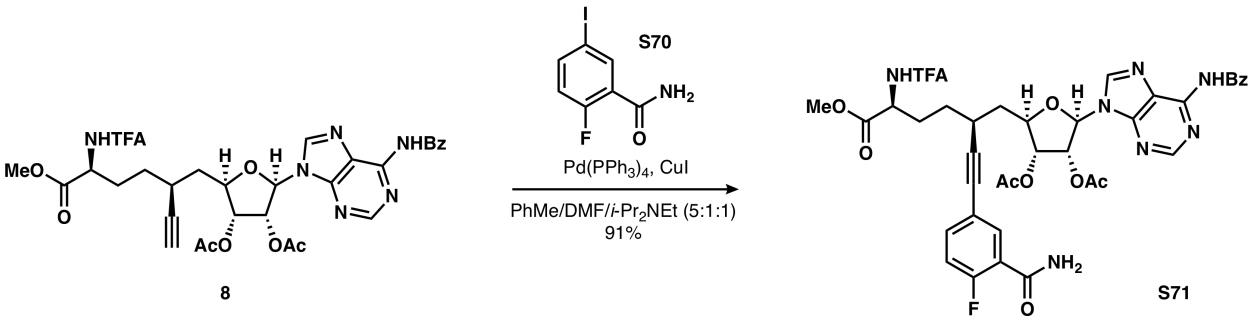

Scheme S30

Scheme S31

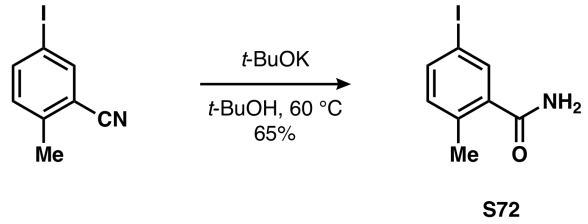

Scheme S32

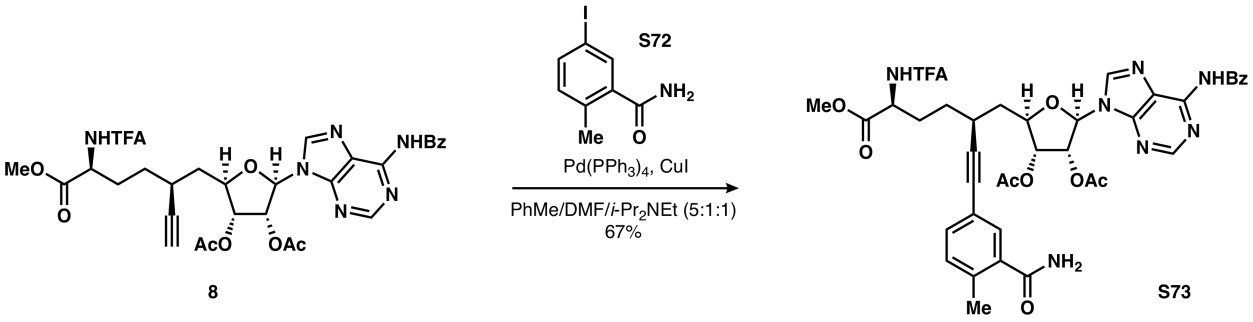

Scheme S33

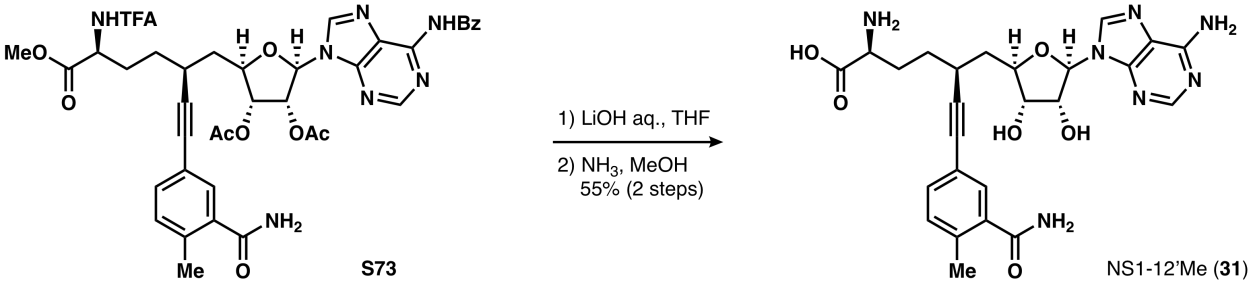

Scheme S34

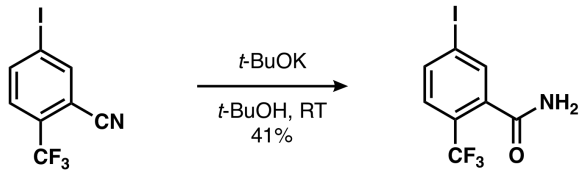

Scheme S35

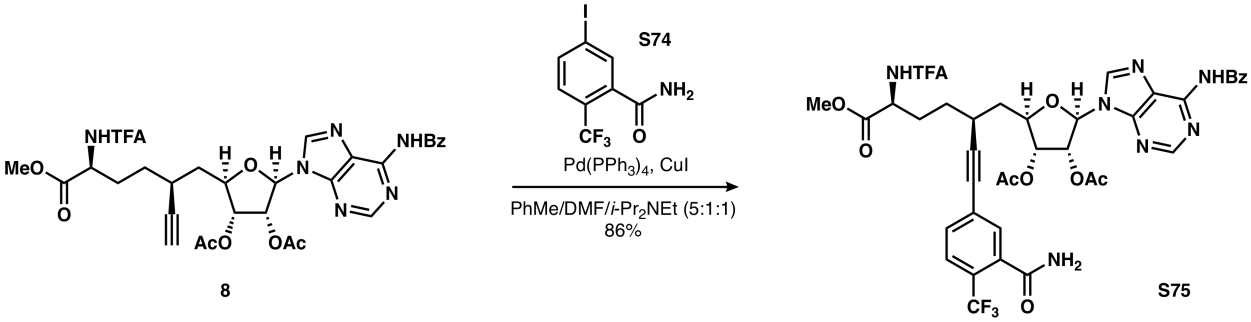

Scheme S36

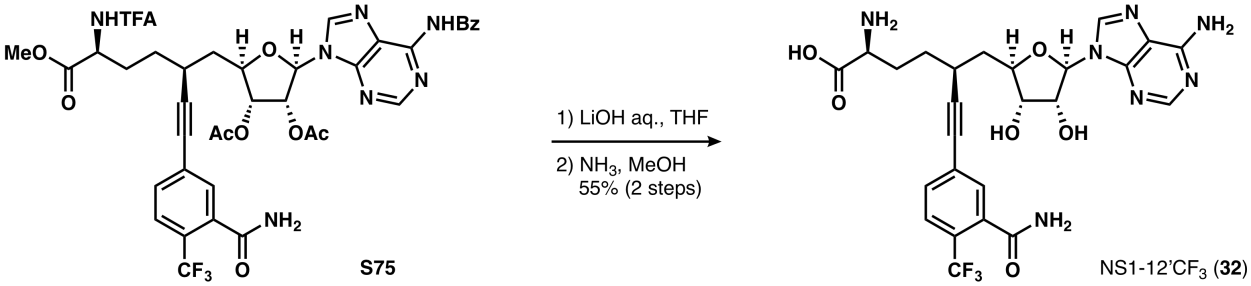

Scheme S37

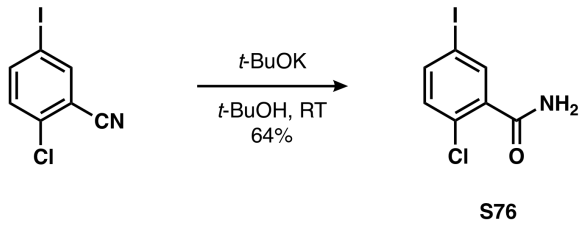

Scheme S38

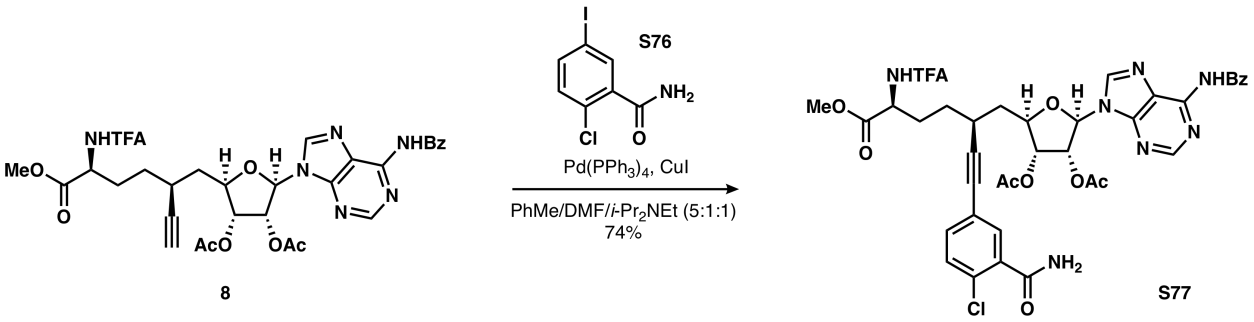

Scheme S39

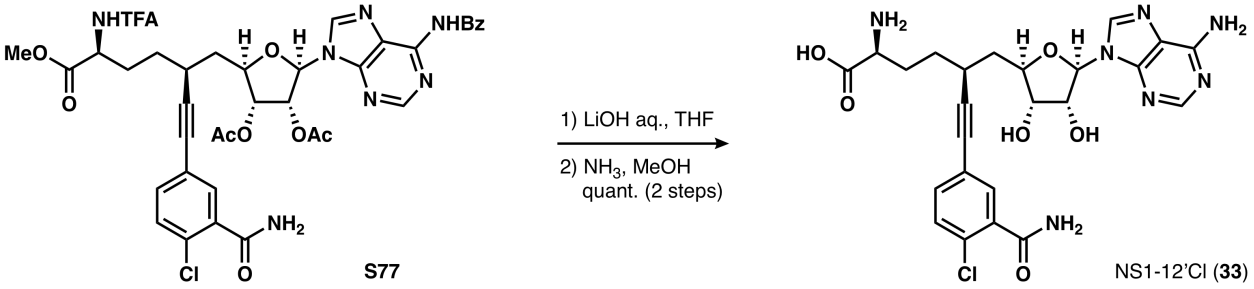

Scheme S40

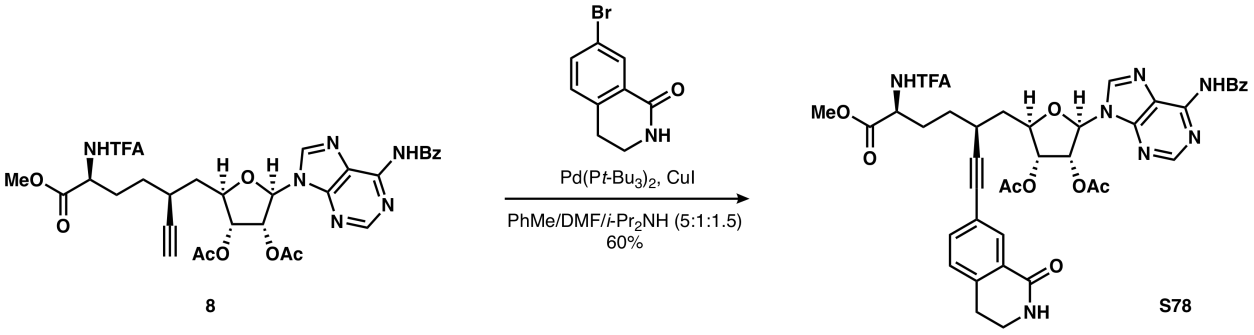

Scheme S41

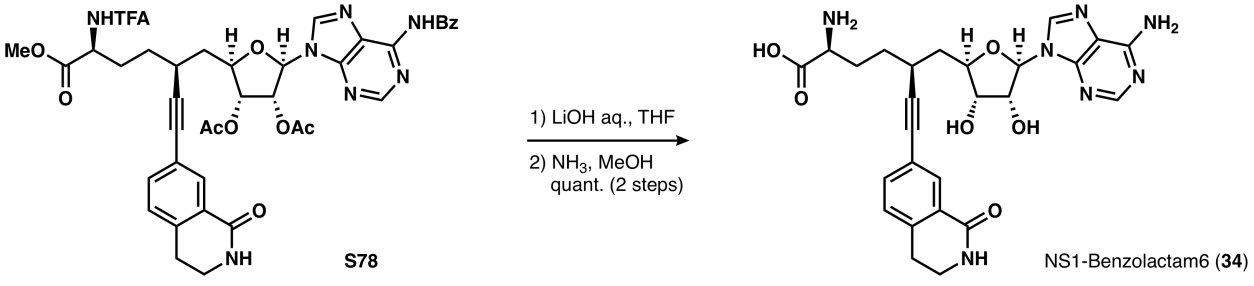

Scheme S42

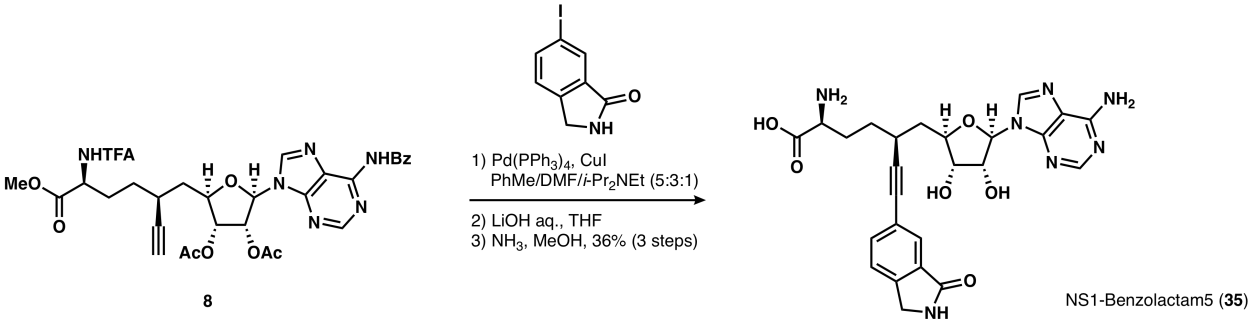

Scheme S43

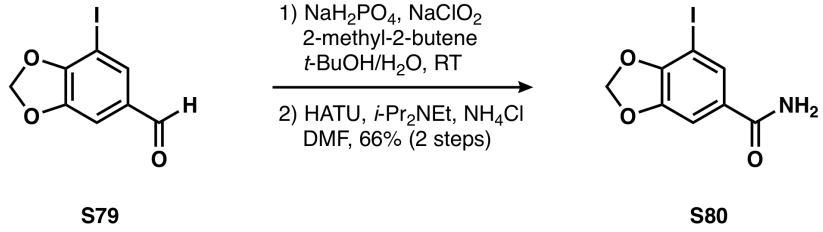

Scheme S44

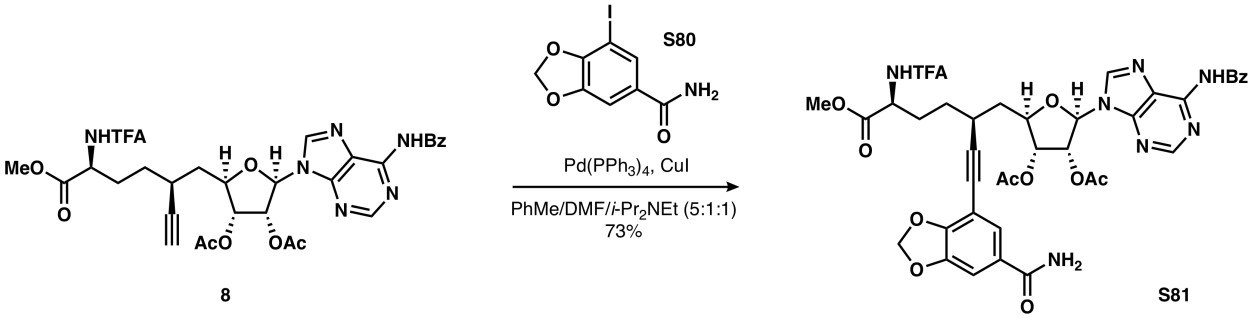

Scheme S45

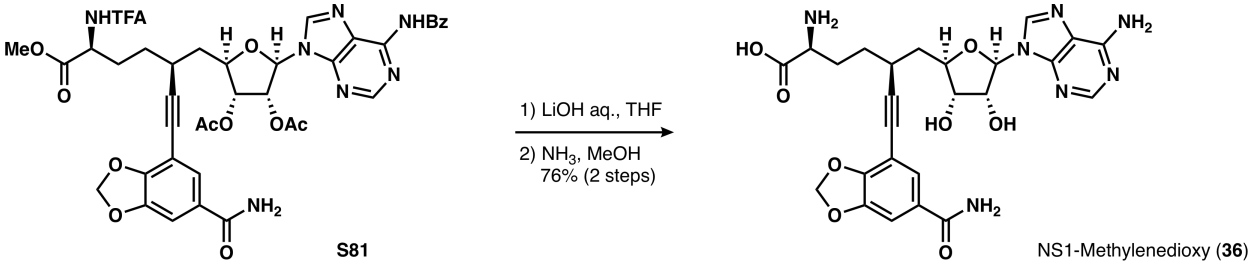

Scheme S46

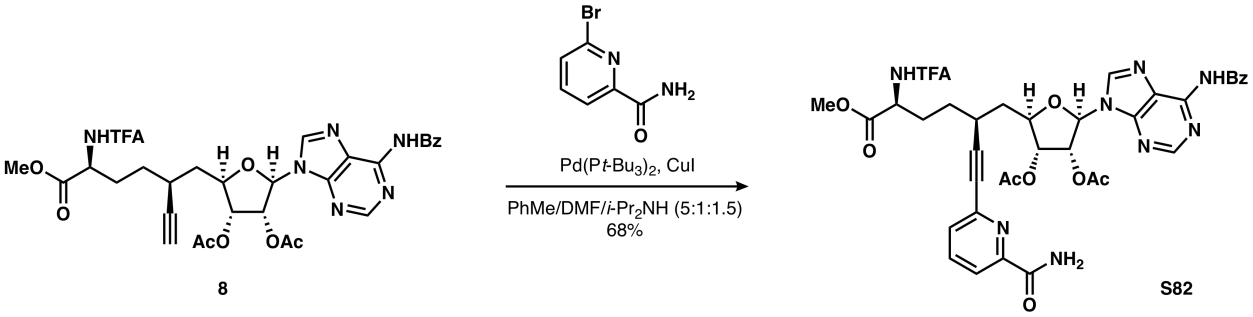

Scheme S47

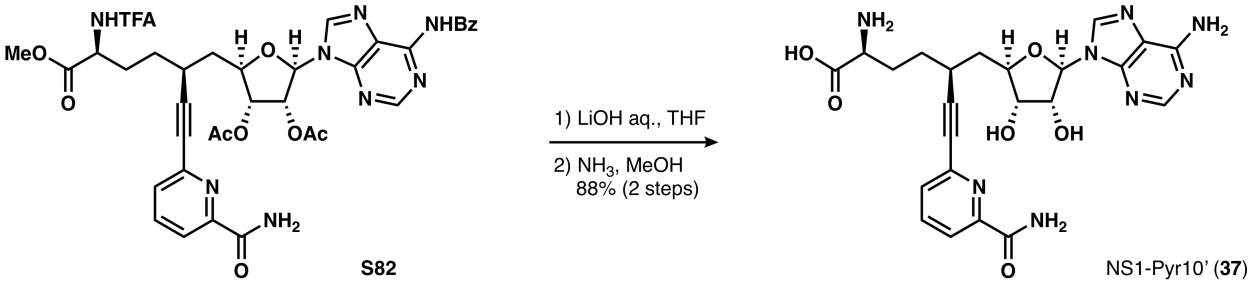

Scheme S48

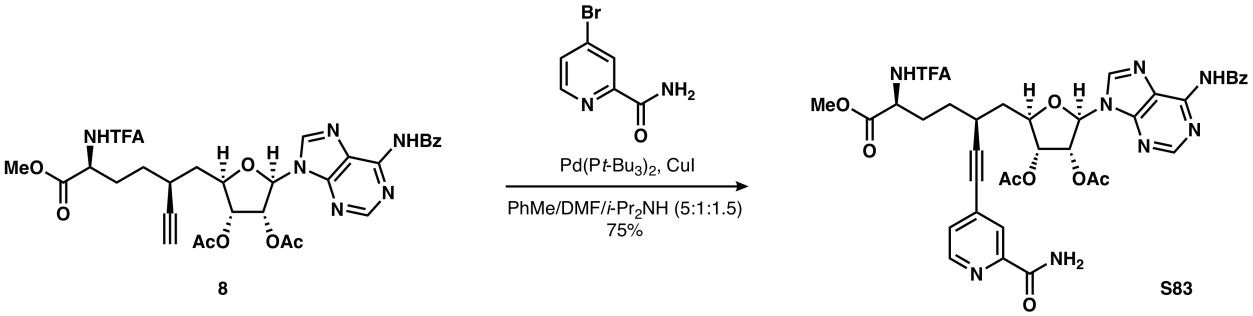

Scheme S49

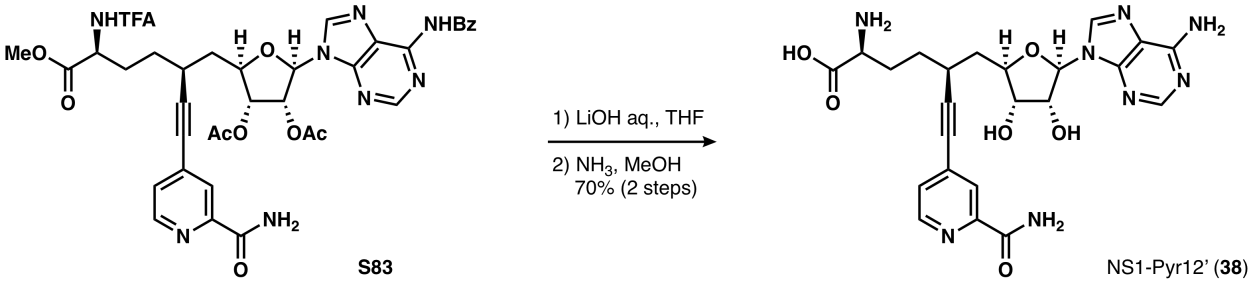

Scheme S50

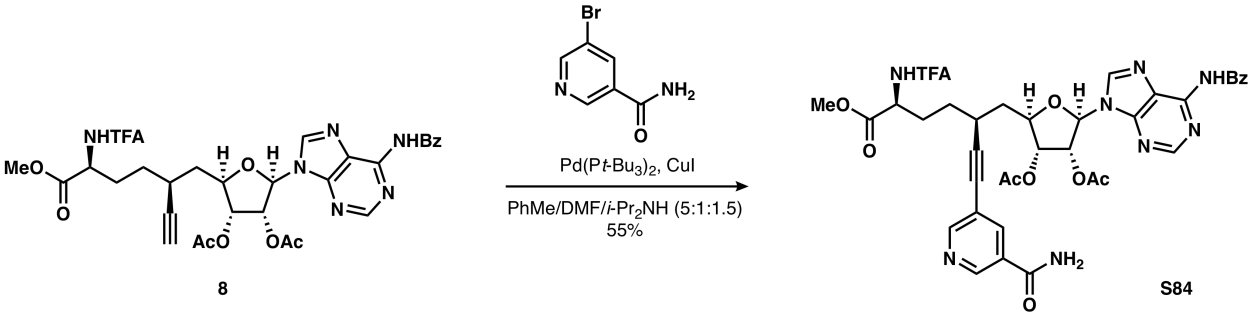

Scheme S51

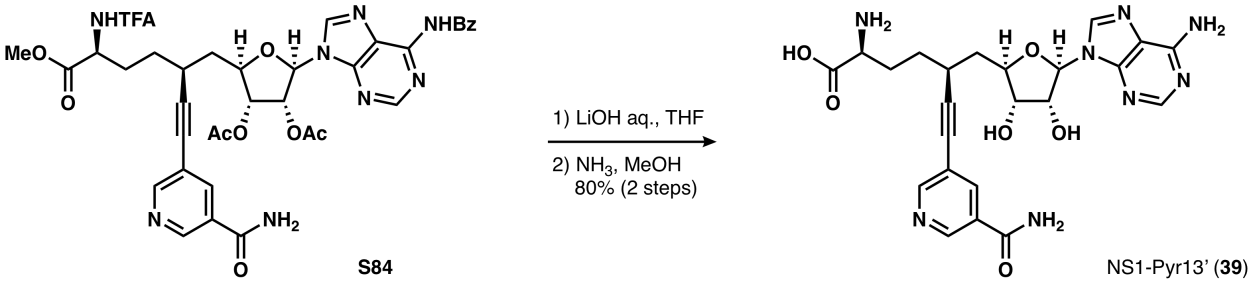

Scheme S52

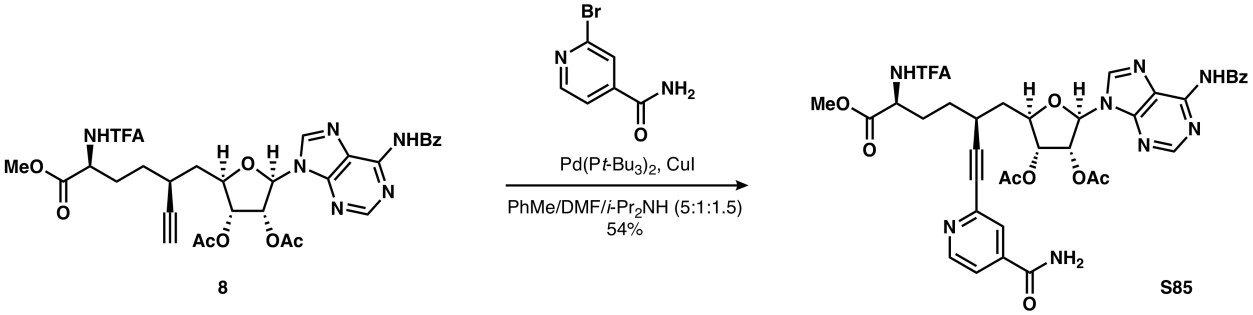

Scheme S53

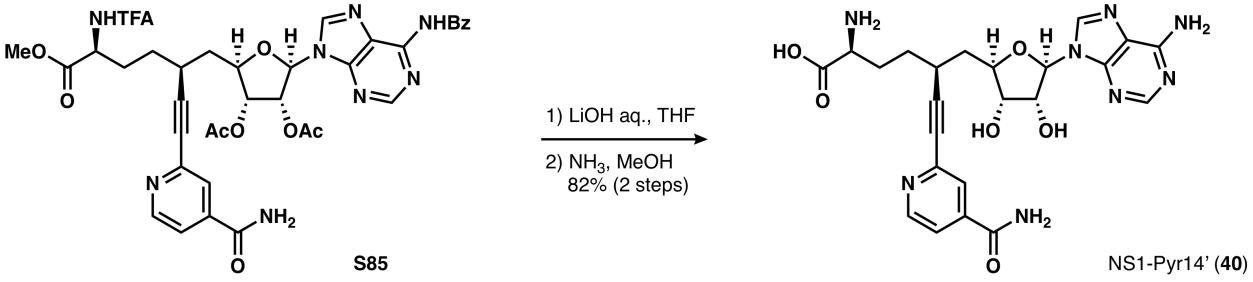

Scheme S54

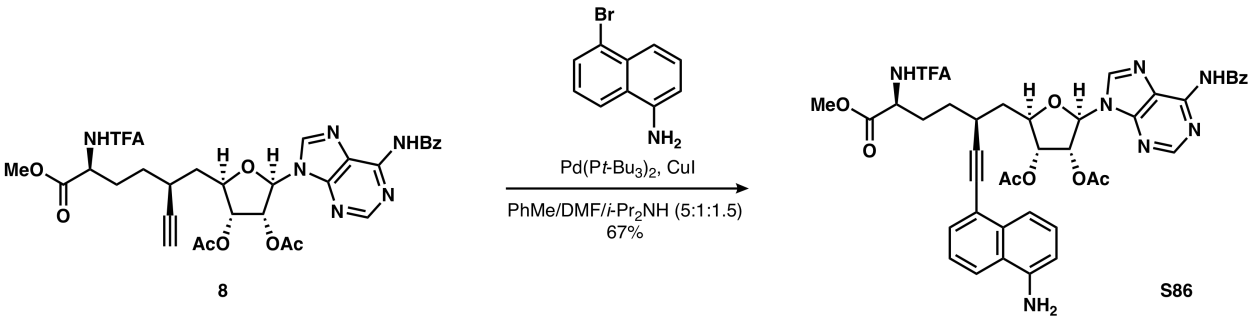

Scheme S55

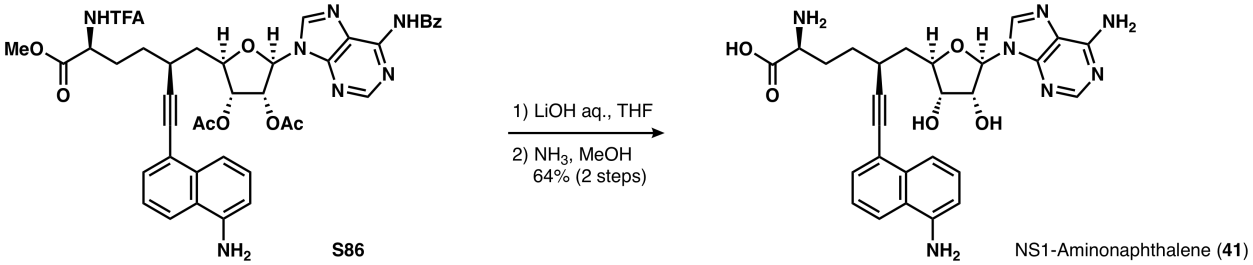

Scheme S56

5 Small-Molecule X-Ray Crystallography

A crystal mounted on a diffractometer was collected data at 100 K. The intensities of the reflections were collected by means of a Bruker APEX DUO CCD diffractometer ($Cu_{K\alpha}$ radiation, λ=1.54178 Å), and equipped with an Oxford Cryosystems nitrogen flow apparatus. The collection method involved 1.0° scans in ω at –30°, –55°, –80°, 30°, 55°, 80° and 115° in 2θ. Data integration down to 0.84 Å resolution was carried out using SAINT V8.37 A[2] with reflection spot size optimization. Absorption corrections were made with the program SADABS[2]. The structure was solved by the Intrinsic Phasing methods and refined by least-squares methods again F^2 using SHELXT-2014[3] and SHELXL-2014[4] with OLEX 2 interface[5]. Non-hydrogen atoms were refined anisotropically, and hydrogen atoms were allowed to ride on the respective atoms. Crystal data as well as details of data collection and refinement are summarized in Tables S11, S14, and S16, for compounds **10**, **S30**, and **S53**, respectively. Geometric parameters are shown in Tables S12, S15, S17 and hydrogen-bond parameters are listed in Tables S13 and S18. The Ortep plots were produced with SHELXL-2014, and the other images were produced with Accelrys DS Visualizer 2.0[6].

5.1 NS1 • TFA (10)

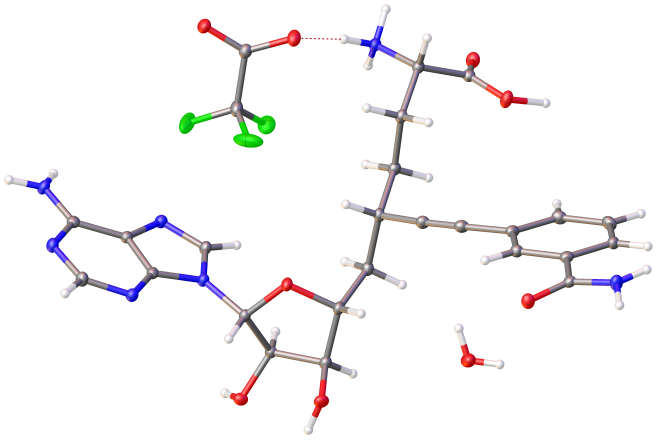

Table S11: Experimental Details

Crystal Data	
Chemical Formula	$C_{26}H_{30}F_3N_7O_9$
M_r	641.57
Crystal system, space group	Triclinic, $P1$
Temperature (K)	100
a, b, c (Å)	5.0591 (1), 10.9615 (2), 13.2000 (7)
α, β, γ (°)	103.0375 (11), 90.8460 (9), 90.3108 (10)

[2] Bruker AXS APEX3, Bruker AXS, Madison, Wisconsin, 2015.
[3] Sheldrick, G. M. *Acta Crystallogr., Sect. A* **2015**, *71*, 3–8.
[4] Sheldrick, G. M. *Acta Crystallogr., Sect. C* **2015**, *71*, 3–8.
[5] Dolomanov, O. V.; Bourhis, L. J.; Gildea, R. J.; Howard, J. A. K.; Puschmann, H. *J. Appl. Cryst.* **2009**, *42*, 339–341.
[6] Accelrys DS Visualizer v2.0.1, Accelrys Software Inc., 2007.

$V(\mathring{A}^3)$	713.03 (2)
Z	1
Radiation type	Cu $K\alpha$
μ (mm^{-1})	1.09
Crystal size (mm)	$0.18 \times 0.08 \times 0.06$
Data Collection	
Diffractometer	Bruker D8 goniometer with CCD area detector
Absorption correction	Multi-scan *SADABS*
T_{min}, T_{max}	0.738, 0.806
No. of measured, independent and observed $[I > 2\sigma(I)]$ reflections	17748, 4335, 4280
R_{int}	0.027
$(\sin\theta/\lambda)_{max}(\mathring{A}^{-1})$	0.596
Refinement	
$R[F^2 > 2\sigma(F^2)], wR(F^2), S$	0.027, 0.073, 1.02
No. of reflections	4335
No. of parameters	464
No. of restraints	9
H-atom treatment	H atom parameters constrained
$\Delta\rho_{max}, \Delta\rho_{min}(e\mathring{A}^{-3})$	0.53, -0.17
Absolute structure	Flack x determined using 1012 quotients [(I+)-(I-)]/[(I+)+(I-)][7]
Absolute structure parameter	-0.06 (8)

Computer programs: SAINT 8.37A (Bruker-AXS, 2015), SHELXT2014 (Sheldrick, 2015), SHELXL2014 (Sheldrick, 2015), Bruker SHELXTL (Sheldrick, 2015).

Table S12: Geometric parameters (Å, °)

O1–C6	1.417 (3)	C9–H9	1
O1–C9	1.466 (3)	C10–C11	1.537 (3)
O2–C7	1.409 (3)	C10–H10A	0.99
O2–H2	0.86 (4)	C10–H10B	0.99
O3–C8	1.421 (3)	C11–C16	1.474 (4)
O3–H3	0.88 (4)	C11–C12	1.549 (3)
O4–C15	1.220 (3)	C11–H11	1
O5–C15	1.301 (3)	C12–C13	1.524 (3)
O5–H5	1.14 (6)	C12–H12A	0.99
O6–C24	1.252 (3)	C12–H12B	0.99

[7] Parsons, S.; Flack, H. D.; Wagner, T. *Acta Crystallogr., Sect. B* **2013**, *69*, 249–259.

N1–C1	1.370 (3)	C13–C14	1.528 (3)
N1–C5	1.380 (3)	C13–H13A	0.99
N1–C6	1.462 (3)	C13–H13B	0.99
N2–C2	1.319 (3)	C14–C15	1.516 (3)
N2–C1	1.346 (3)	C14–H14	1
N3–C2	1.339 (3)	C16–C17	1.195 (4)
N3–C3	1.359 (3)	C17–C18	1.442 (4)
N4–C3	1.322 (3)	C18–C23	1.394 (3)
N4–H4A	0.92 (4)	C18–C19	1.401 (4)
N4–H4B	0.88 (4)	C19–C20	1.381 (4)
N5–C5	1.303 (3)	C19–H19	0.95
N5–C4	1.386 (3)	C20–C21	1.393 (4)
N6–C14	1.492 (3)	C20–H20	0.95
N6–H6A	0.93 (4)	C21–C22	1.402 (4)
N6–H6B	0.92 (4)	C21–H21	0.95
N6–H6C	0.97 (3)	C22–C23	1.389 (4)
N7–C24	1.319 (4)	C22–C24	1.499 (3)
N7–H7A	0.90 (4)	C23–H23	0.95
N7–H7B	0.88 (4)	O11–C31	1.232 (3)
C1–C4	1.391 (3)	O12–C31	1.253 (3)
C2–H2A	0.95	C31–C32A	1.540 (3)
C3–C4	1.417 (3)	C31–C32	1.540 (3)
C5–H5A	0.95	C32–F1	1.335 (9)
C6–C7	1.531 (3)	C32–F2	1.338 (9)
C6–H6	1	C32–F3	1.374 (6)
C7–C8	1.516 (4)	C32A–F3A	1.283 (12)
C7–H7	1	C32A–F1A	1.311 (18)
C8–C9	1.527 (3)	C32A–F2A	1.378 (18)
C8–H8	1	O1W–H1WA	0.85 (6)
C9–C10	1.522 (3)	O1W–H1WB	0.79 (5)
C6–O1–C9	109.24 (17)	C16–C11–C12	109.25 (19)
C7–O2–H2	104 (2)	C10–C11–C12	113.13 (19)
C8–O3–H3	103 (3)	C16–C11–H11	108
C15–O5–H5	112 (3)	C10–C11–H11	108
C1–N1–C5	105.4 (2)	C12–C11–H11	108
C1–N1–C6	126.1 (2)	C13–C12–C11	110.10 (19)
C5–N1–C6	128.5 (2)	C13–C12–H12A	109.6
C2–N2–C1	111.4 (2)	C11–C12–H12A	109.6
C2–N3–C3	120.7 (2)	C13–C12–H12B	109.6
C3–N4–H4A	120 (2)	C11–C12–H12B	109.6

C3–N4–H4B	123 (2)	H12A–C12–H12B	108.2
H4A–N4–H4B	116 (3)	C12–C13–C14	116.8 (2)
C5–N5–C4	104.1 (2)	C12–C13–H13A	108.1
C14–N6–H6A	109 (2)	C14–C13–H13A	108.1
C14–N6–H6B	114 (2)	C12–C13–H13B	108.1
H6A–N6–H6B	111 (3)	C14–C13–H13B	108.1
C14–N6–H6C	108.9 (19)	H13A–C13–H13B	107.3
H6A–N6–H6C	106 (3)	N6–C14–C15	109.3 (2)
H6B–N6–H6C	108 (3)	N6–C14–C13	113.8 (2)
C24–N7–H7A	117 (2)	C15–C14–C13	113.6 (2)
C24–N7–H7B	125 (2)	N6–C14–H14	106.5
H7A–N7–H7B	116 (3)	C15–C14–H14	106.5
N2–C1–N1	127.3 (2)	C13–C14–H14	106.5
N2–C1–C4	126.6 (2)	O4–C15–O5	125.5 (2)
N1–C1–C4	106.1 (2)	O4–C15–C14	122.5 (2)
N2–C2–N3	128.2 (2)	O5–C15–C14	112.0 (2)
N2–C2–H2A	115.9	C17–C16–C11	173.0 (3)
N3–C2–H2A	115.9	C16–C17–C18	172.7 (3)
N4–C3–N3	119.1 (2)	C23–C18–C19	119.1 (2)
N4–C3–C4	125.3 (2)	C23–C18–C17	122.6 (2)
N3–C3–C4	115.6 (2)	C19–C18–C17	118.3 (2)
N5–C4–C1	110.4 (2)	C20–C19–C18	120.6 (2)
N5–C4–C3	132.1 (2)	C20–C19–H19	119.7
C1–C4–C3	117.5 (2)	C18–C19–H19	119.7
N5–C5–N1	114.1 (2)	C19–C20–C21	120.2 (2)
N5–C5–H5A	122.9	C19–C20–H20	119.9
N1–C5–H5A	122.9	C21–C20–H20	119.9
O1–C6–N1	109.56 (19)	C20–C21–C22	119.8 (2)
O1–C6–C7	106.44 (19)	C20–C21–H21	120.1
N1–C6–C7	113.56 (19)	C22–C21–H21	120.1
O1–C6–H6	109.1	C23–C22–C21	119.6 (2)
N1–C6–H6	109.1	C23–C22–C24	118.8 (2)
C7–C6–H6	109.1	C21–C22–C24	121.5 (2)
O2–C7–C8	113.55 (19)	C22–C23–C18	120.7 (2)
O2–C7–C6	112.21 (19)	C22–C23–H23	119.7
C8–C7–C6	101.34 (19)	C18–C23–H23	119.7
O2–C7–H7	109.8	O6–C24–N7	121.6 (2)
C8–C7–H7	109.8	O6–C24–C22	120.0 (2)
C6–C7–H7	109.8	N7–C24–C22	118.4 (2)
O3–C8–C7	110.95 (19)	O11–C31–O12	130.5 (2)
O3–C8–C9	108.27 (19)	O11–C31–C32A	115.1 (2)

C7–C8–C9	101.94 (18)	O12–C31–C32A	114.3 (2)
O3–C8–H8	111.7	O11–C31–C32	115.1 (2)
C7–C8–H8	111.7	O12–C31–C32	114.3 (2)
C9–C8–H8	111.7	F1–C32–F2	104.1 (11)
O1–C9–C10	107.96 (18)	F1–C32–F3	105.6 (7)
O1–C9–C8	105.45 (18)	F2–C32–F3	110.3 (7)
C10–C9–C8	115.4 (2)	F1–C32–C31	112.2 (9)
O1–C9–H9	109.3	F2–C32–C31	113.1 (7)
C10–C9–H9	109.3	F3–C32–C31	111.1 (3)
C8–C9–H9	109.3	F3A–C32A–F1A	112.6 (16)
C9–C10–C11	111.14 (19)	F3A–C32A–F2A	96.4 (15)
C9–C10–H10A	109.4	F1A–C32A–F2A	108 (2)
C11–C10–H10A	109.4	F3A–C32A–C31	115.7 (6)
C9–C10–H10B	109.4	F1A–C32A–C31	118 (2)
C11–C10–H10B	109.4	F2A–C32A–C31	103.0 (14)
H10A–C10–H10B	108	H1WA–O1W–H1WB	113 (5)
C16–C11–C10	110.3 (2)		
C2–N2–C1–N1	179.2 (2)	O3–C8–C9–C10	154.9 (2)
C2–N2–C1–C4	0.9 (3)	C7–C8–C9–C10	-88.1 (2)
C5–N1–C1–N2	-178.1 (2)	O1–C9–C10–C11	62.3 (2)
C6–N1–C1–N2	3.3 (4)	C8–C9–C10–C11	179.94 (19)
C5–N1–C1–C4	0.5 (2)	C9–C10–C11–C16	72.6 (2)
C6–N1–C1–C4	-178.1 (2)	C9–C10–C11–C12	-164.7 (2)
C1–N2–C2–N3	-0.5 (4)	C16–C11–C12–C13	-60.6 (3)
C3–N3–C2–N2	-0.9 (4)	C10–C11–C12–C13	176.03 (19)
C2–N3–C3–N4	-177.5 (2)	C11–C12–C13–C14	177.8 (2)
C2–N3–C3–C4	1.7 (3)	C12–C13–C14–N6	72.3 (3)
C5–N5–C4–C1	0.6 (3)	C12–C13–C14–C15	-53.6 (3)
C5–N5–C4–C3	178.2 (2)	N6–C14–C15–O4	7.7 (3)
N2–C1–C4–N5	177.9 (2)	C13–C14–C15–O4	136.0 (2)
N1–C1–C4–N5	-0.7 (2)	N6–C14–C15–O5	-174.33 (19)
N2–C1–C4–C3	-0.1 (3)	C13–C14–C15–O5	-46.0 (3)
N1–C1–C4–C3	-178.70 (19)	C23–C18–C19–C20	0.1 (4)
N4–C3–C4–N5	0.5 (4)	C17–C18–C19–C20	-177.7 (2)
N3–C3–C4–N5	-178.6 (2)	C18–C19–C20–C21	-0.2 (4)
N4–C3–C4–C1	177.9 (2)	C19–C20–C21–C22	0.5 (3)
N3–C3–C4–C1	-1.2 (3)	C20–C21–C22–C23	-0.6 (3)
C4–N5–C5–N1	-0.3 (3)	C20–C21–C22–C24	175.8 (2)
C1–N1–C5–N5	-0.2 (3)	C21–C22–C23–C18	0.4 (3)
C6–N1–C5–N5	178.5 (2)	C24–C22–C23–C18	-176.1 (2)

C9–O1–C6–N1	-138.04 (18)	C19–C18–C23–C22	-0.2 (3)
C9–O1–C6–C7	-14.9 (2)	C17–C18–C23–C22	177.5 (2)
C1–N1–C6–O1	-110.1 (2)	C23–C22–C24–O6	7.0 (3)
C5–N1–C6–O1	71.5 (3)	C21–C22–C24–O6	-169.5 (2)
C1–N1–C6–C7	131.0 (2)	C23–C22–C24–N7	-173.9 (2)
C5–N1–C6–C7	-47.3 (3)	C21–C22–C24–N7	9.7 (3)
O1–C6–C7–O2	155.32 (19)	O11–C31–C32–F1	148.7 (9)
N1–C6–C7–O2	-84.1 (2)	O12–C31–C32–F1	-33.4 (9)
O1–C6–C7–C8	33.9 (2)	O11–C31–C32–F2	-93.9 (9)
N1–C6–C7–C8	154.47 (19)	O12–C31–C32–F2	84.0 (9)
O2–C7–C8–O3	-44.0 (3)	O11–C31–C32–F3	30.7 (6)
C6–C7–C8–O3	76.6 (2)	O12–C31–C32–F3	-151.4 (5)
O2–C7–C8–C9	-159.06 (19)	O11–C31–C32A–F3A	1.0 (9)
C6–C7–C8–C9	-38.5 (2)	O12–C31–C32A–F3A	178.9 (9)
C6–O1–C9–C10	113.7 (2)	O11–C31–C32A–F1A	139 (2)
C6–O1–C9–C8	-10.2 (2)	O12–C31–C32A–F1A	-43 (2)
O3–C8–C9–O1	-86.1 (2)	O11–C31–C32A–F2A	-102.8 (17)
C7–C8–C9–O1	30.9 (2)	O12–C31–C32A–F2A	75.1 (17)

Table S13: Hydrogen-bond parameters

D – H ⋯ A	D – H (Å)	H ⋯ A (Å)	D ⋯ A (Å)	D – H ⋯ A (°)
O2–H2 · · · N2^{i}	0.86 (4)	1.92 (4)	2.757 (3)	163 (3)
O3–H3 · · · O11^{ii}	0.88 (4)	1.94 (4)	2.784 (2)	162 (4)
O3–H3 · · · O2	0.88 (4)	2.38 (4)	2.766 (3)	107 (3)
O5–H5 · · · N3^{iii}	1.14 (6)	1.41 (6)	2.542 (3)	172 (5)
N4–H4A · · · O4^{iv}	0.92 (4)	2.19 (4)	3.070 (3)	159 (3)
N4–H4B · · · O6^{v}	0.88 (4)	2.01 (4)	2.876 (3)	166 (3)
N6–H6B · · · O12^{i}	0.92 (4)	1.95 (4)	2.861 (3)	174 (3)
N6–H6A · · · O12	0.93 (4)	2.11 (4)	2.991 (3)	158 (3)
N6–H6A · · · O3^{vi}	0.93 (4)	2.64 (3)	2.948 (3)	100 (2)
N6–H6C · · · O1W^{vi}	0.97 (3)	1.91 (3)	2.830 (3)	156 (3)
N7–H7B · · · O11^{vii}	0.88 (4)	2.18 (4)	3.005 (3)	157 (3)
N7–H7A · · · N5^{viii}	0.90 (4)	2.10 (4)	2.975 (3)	165 (3)
O1W–H1WB · · · O6i	0.79 (5)	2.09 (5)	2.870 (3)	173 (5)
N4–H4A · · · O6^{ix}	0.92 (4)	2.85 (4)	3.310 (3)	112 (3)
O1W–H1WB · · · O4^{x}	0.79 (5)	2.79 (5)	3.052 (3)	102 (4)

Symmetry code(s): (i) x-1, y, z; (ii) x-1, y+1, z; (iii) x-1, y, z+1; (iv) x+1, y, z-1; (v) x-1, y-1, z-1; (vi) x, y-1, z; (vii) x, y+1, z+1; (viii) x+1, y+1, z+1; (ix) x, y-1, z-1; (x) x, y+1, z.

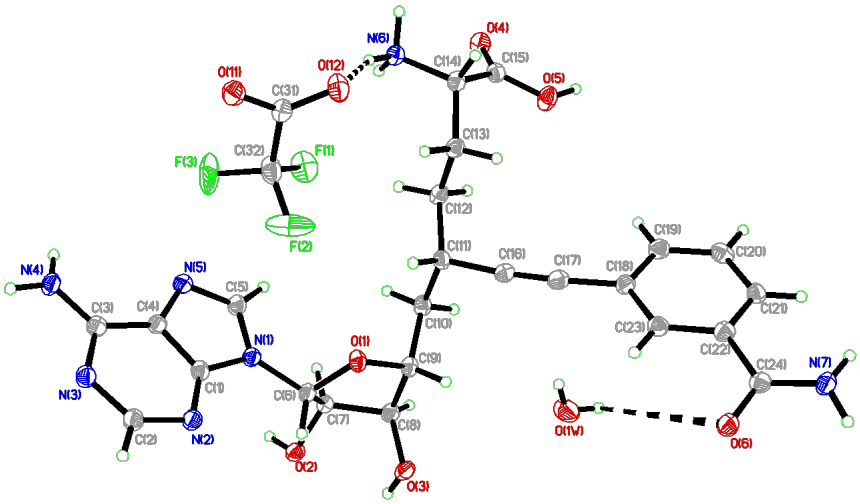

Figure S10: Perspective views showing 50% probability displacement.

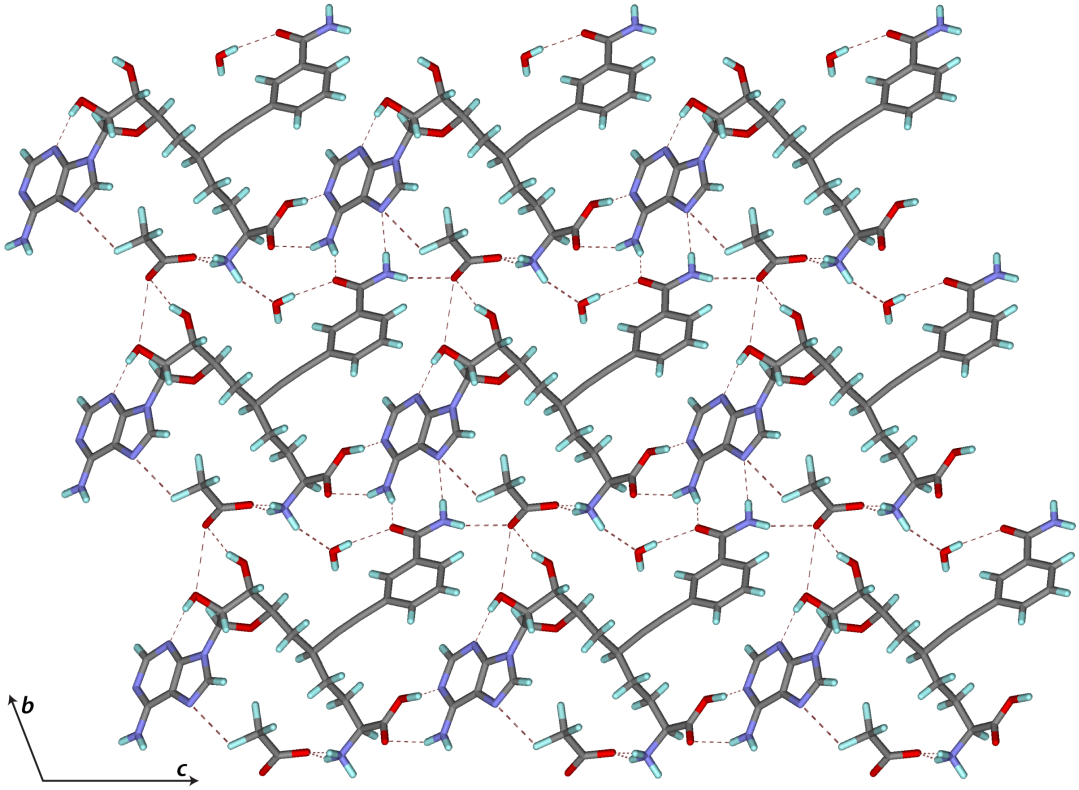

Figure S11: Three-dimensional supramolecular architecture viewed along the *a*-axis direction.

5.2 NS1-Cyclopropyl: Cyclopropyl Alkyne S30

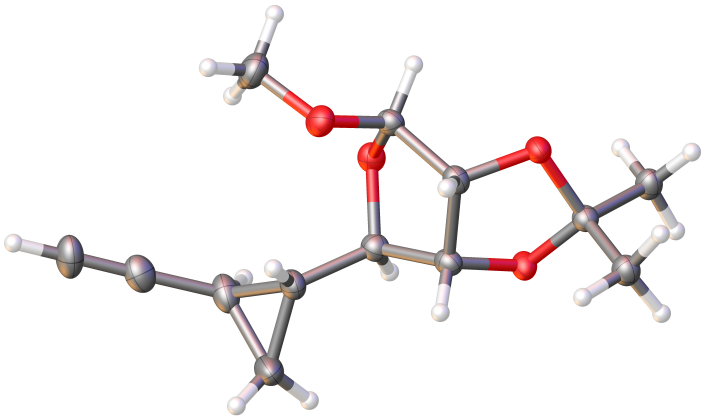

Table S14: Experimental Details

Crystal Data	
Chemical Formula	$C_{13}H_{18}O_4$
M_r	238.27
Crystal system, space group	Monoclinic, $F2_1$
Temperature (K)	100
a, b, c (Å)	5.7618 (1), 19.4824 (4), 11.8204 (2)
β (°)	90.0232 (11)
V(Å^3)	1326.88 (4)
Z	4
Radiation type	Cu $K\alpha$
μ (mm^{-1})	0.72
Crystal size (mm)	0.14 × 0.10 × 0.06
Data Collection	
Diffractometer	Bruker D8 goniometer with CCD area detector
Absorption correction	Multi-scan *SADABS*
$T_{\min}, T_{\max}$	0.797, 0.864
No. of measured, independent and observed $[I > 2\sigma(I)]$ reflections	26548, 4269, 4245
R_{int}	0.032
$(\sin\theta/\lambda)_{\max}$(Å^{-1})	0.596
Refinement	
$R[F^2 > 2\sigma(F^2)], wR(F^2), S$	0.026, 0.064, 1.06
No. of reflections	4269
No. of parameters	314

No. of restraints	1
H atom parameters constrained	
$\Delta\rho_{\max}, \Delta\rho_{\min}(e\mathring{A}^{-3})$	0.11, -0.15
Absolute structure	Flack x determined using 1834 quotients [(I+)-(I-)]/[(I+)+(I-)][8]
Absolute structure parameter	-0.02 (9)

Computer programs: SAINT 8.37A (Bruker-AXS, 2015), SHELXT2014 (Sheldrick, 2015), SHELXL2014 (Sheldrick, 2015), Bruker SHELXTL (Sheldrick, 2015).

Table S15: Geometric parameters (Å, °)

O1–C2	1.426 (3)	O5–C21	1.421 (3)
O1–C1	1.438 (3)	O5–C25	1.428 (3)
O2–C3	1.410 (3)	O6–C23	1.408 (3)
O2–C4	1.439 (3)	O6–C24	1.442 (3)
O3–C1	1.428 (3)	O7–C22	1.428 (3)
O3–C5	1.429 (3)	O7–C21	1.434 (4)
O4–C3	1.415 (3)	O8–C23	1.413 (3)
O4–C8	1.433 (4)	O8–C28	1.434 (4)
C1–C7	1.512 (4)	C21–C26	1.505 (4)
C1–C6	1.516 (4)	C21–C27	1.508 (4)
C2–C3	1.529 (4)	C22–C23	1.521 (4)
C2–C5	1.550 (4)	C22–C25	1.540 (4)
C2–H2	1	C22–H22	1
C3–H3	1	C23–H23	1
C4–C9	1.509 (4)	C24–C29	1.510 (4)
C4–C5	1.528 (4)	C24–C25	1.520 (4)
C4–H4	1	C24–H24	1
C5–H5	1	C25–H25	1
C6–H6A	0.98	C26–H26A	0.98
C6–H6B	0.98	C26–H26B	0.98
C6–H6C	0.98	C26–H26C	0.98
C7–H7A	0.98	C27–H27A	0.98
C7–H7B	0.98	C27–H27B	0.98
C7–H7C	0.98	C27–H27C	0.98
C8–H8A	0.98	C28–H28A	0.98
C8–H8B	0.98	C28–H28B	0.98
C8–H8C	0.98	C28–H28C	0.98
C9–C10	1.492 (4)	C29–C30	1.500 (4)
C9–C11	1.514 (4)	C29–C31	1.517 (4)
C9–H9	1	C29–H29	1

[8] Parsons, S.; Flack, H. D.; Wagner, T. *Acta Crystallogr., Sect. B* **2013**, *69*, 249–259.

C10–C11	1.519 (5)	C30–C31	1.520 (4)
C10–H10A	0.99	C30–H30A	0.99
C10–H10B	0.99	C30–H30B	0.99
C11–C12	1.441 (5)	C31–C32	1.439 (4)
C11–H11	1	C31–H31	1
C12–C13	1.182 (5)	C32–C33	1.181 (4)
C13–H13	0.95	C33–H33	0.95
C2–O1–C1	107.74 (19)	C21–O5–C25	107.6 (2)
C3–O2–C4	107.8 (2)	C23–O6–C24	107.9 (2)
C1–O3–C5	107.19 (19)	C22–O7–C21	107.4 (2)
C3–O4–C8	112.1 (2)	C23–O8–C28	112.1 (2)
O3–C1–O1	103.8 (2)	O5–C21–O7	104.4 (2)
O3–C1–C7	108.9 (2)	O5–C21–C26	108.6 (2)
O1–C1–C7	109.1 (2)	O7–C21–C26	109.0 (2)
O3–C1–C6	111.3 (2)	O5–C21–C27	110.7 (2)
O1–C1–C6	111.1 (2)	O7–C21–C27	111.2 (3)
C7–C1–C6	112.2 (2)	C26–C21–C27	112.6 (2)
O1–C2–C3	110.1 (2)	O7–C22–C23	109.2 (2)
O1–C2–C5	104.7 (2)	O7–C22–C25	104.9 (2)
C3–C2–C5	103.9 (2)	C23–C22–C25	104.3 (2)
O1–C2–H2	112.5	O7–C22–H22	112.6
C3–C2–H2	112.5	C23–C22–H22	112.6
C5–C2–H2	112.5	C25–C22–H22	112.6
O2–C3–O4	111.9 (2)	O6–C23–O8	111.8 (2)
O2–C3–C2	106.2 (2)	O6–C23–C22	105.5 (2)
O4–C3–C2	107.4 (2)	O8–C23–C22	107.3 (2)
O2–C3–H3	110.4	O6–C23–H23	110.7
O4–C3–H3	110.4	O8–C23–H23	110.7
C2–C3–H3	110.4	C22–C23–H23	110.7
O2–C4–C9	112.7 (2)	O6–C24–C29	112.5 (2)
O2–C4–C5	104.2 (2)	O6–C24–C25	104.1 (2)
C9–C4–C5	114.6 (2)	C29–C24–C25	114.5 (2)
O2–C4–H4	108.4	O6–C24–H24	108.5
C9–C4–H4	108.4	C29–C24–H24	108.5
C5–C4–H4	108.4	C25–C24–H24	108.5
O3–C5–C4	108.9 (2)	O5–C25–C24	108.5 (2)
O3–C5–C2	103.72 (19)	O5–C25–C22	104.1 (2)
C4–C5–C2	104.5 (2)	C24–C25–C22	104.8 (2)
O3–C5–H5	113	O5–C25–H25	112.9
C4–C5–H5	113	C24–C25–H25	112.9

C2–C5–H5	113	C22–C25–H25	112.9
C1–C6–H6A	109.5	C21–C26–H26A	109.5
C1–C6–H6B	109.5	C21–C26–H26B	109.5
H6A–C6–H6B	109.5	H26A–C26–H26B	109.5
C1–C6–H6C	109.5	C21–C26–H26C	109.5
H6A–C6–H6C	109.5	H26A–C26–H26C	109.5
H6B–C6–H6C	109.5	H26B–C26–H26C	109.5
C1–C7–H7A	109.5	C21–C27–H27A	109.5
C1–C7–H7B	109.5	C21–C27–H27B	109.5
H7A–C7–H7B	109.5	H27A–C27–H27B	109.5
C1–C7–H7C	109.5	C21–C27–H27C	109.5
H7A–C7–H7C	109.5	H27A–C27–H27C	109.5
H7B–C7–H7C	109.5	H27B–C27–H27C	109.5
O4–C8–H8A	109.5	O8–C28–H28A	109.5
O4–C8–H8B	109.5	O8–C28–H28B	109.5
H8A–C8–H8B	109.5	H28A–C28–H28B	109.5
O4–C8–H8C	109.5	O8–C28–H28C	109.5
H8A–C8–H8C	109.5	H28A–C28–H28C	109.5
H8B–C8–H8C	109.5	H28B–C28–H28C	109.5
C10–C9–C4	119.2 (3)	C30–C29–C24	118.2 (2)
C10–C9–C11	60.7 (2)	C30–C29–C31	60.49 (19)
C4–C9–C11	116.3 (3)	C24–C29–C31	115.2 (2)
C10–C9–H9	116.3	C30–C29–H29	117
C4–C9–H9	116.3	C24–C29–H29	117
C11–C9–H9	116.3	C31–C29–H29	117
C9–C10–C11	60.4 (2)	C29–C30–C31	60.32 (19)
C9–C10–H10A	117.7	C29–C30–H30A	117.7
C11–C10–H10A	117.7	C31–C30–H30A	117.7
C9–C10–H10B	117.7	C29–C30–H30B	117.7
C11–C10–H10B	117.7	C31–C30–H30B	117.7
H10A–C10–H10B	114.9	H30A–C30–H30B	114.9
C12–C11–C9	119.9 (3)	C32–C31–C29	120.3 (3)
C12–C11–C10	121.5 (3)	C32–C31–C30	119.9 (3)
C9–C11–C10	58.9 (2)	C29–C31–C30	59.20 (19)
C12–C11–H11	115	C32–C31–H31	115.3
C9–C11–H11	115	C29–C31–H31	115.3
C10–C11–H11	115	C30–C31–H31	115.3
C13–C12–C11	179.2 (4)	C33–C32–C31	179.2 (4)
C12–C13–H13	180	C32–C33–H33	180
C5–O3–C1–O1	-36.5 (3)	C25–O5–C21–O7	-34.3 (3)

C5–O3–C1–C7	-152.6 (2)	C25–O5–C21–C26	-150.4 (2)
C5–O3–C1–C6	83.1 (3)	C25–O5–C21–C27	85.5 (3)
C2–O1–C1–O3	32.7 (3)	C22–O7–C21–O5	32.5 (3)
C2–O1–C1–C7	148.7 (2)	C22–O7–C21–C26	148.4 (2)
C2–O1–C1–C6	-87.1 (3)	C22–O7–C21–C27	-86.9 (3)
C1–O1–C2–C3	-127.7 (2)	C21–O7–C22–C23	-129.6 (2)
C1–O1–C2–C5	-16.6 (3)	C21–O7–C22–C25	-18.4 (3)
C4–O2–C3–O4	-81.8 (2)	C24–O6–C23–O8	-80.3 (2)
C4–O2–C3–C2	35.1 (3)	C24–O6–C23–C22	36.1 (3)
C8–O4–C3–O2	-61.9 (3)	C28–O8–C23–O6	-60.8 (3)
C8–O4–C3–C2	-178.2 (2)	C28–O8–C23–C22	-176.1 (2)
O1–C2–C3–O2	93.6 (2)	O7–C22–C23–O6	91.4 (2)
C5–C2–C3–O2	-18.1 (3)	C25–C22–C23–O6	-20.3 (3)
O1–C2–C3–O4	-146.4 (2)	O7–C22–C23–O8	-149.2 (2)
C5–C2–C3–O4	101.9 (2)	C25–C22–C23–O8	99.1 (2)
C3–O2–C4–C9	87.5 (3)	C23–O6–C24–C29	87.8 (3)
C3–O2–C4–C5	-37.3 (3)	C23–O6–C24–C25	-36.7 (3)
C1–O3–C5–C4	136.6 (2)	C21–O5–C25–C24	133.7 (2)
C1–O3–C5–C2	25.7 (3)	C21–O5–C25–C22	22.4 (3)
O2–C4–C5–O3	-86.3 (2)	O6–C24–C25–O5	-88.8 (2)
C9–C4–C5–O3	150.1 (2)	C29–C24–C25–O5	148.0 (2)
O2–C4–C5–C2	24.0 (3)	O6–C24–C25–C22	22.0 (3)
C9–C4–C5–C2	-99.6 (3)	C29–C24–C25–C22	-101.2 (2)
O1–C2–C5–O3	-5.4 (3)	O7–C22–C25–O5	-2.3 (3)
C3–C2–C5–O3	110.1 (2)	C23–C22–C25–O5	112.5 (2)
O1–C2–C5–C4	-119.4 (2)	O7–C22–C25–C24	-116.2 (2)
C3–C2–C5–C4	-3.9 (3)	C23–C22–C25–C24	-1.4 (3)
O2–C4–C9–C10	147.8 (3)	O6–C24–C29–C30	143.8 (3)
C5–C4–C9–C10	-93.2 (3)	C25–C24–C29–C30	-97.7 (3)
O2–C4–C9–C11	78.2 (3)	O6–C24–C29–C31	75.2 (3)
C5–C4–C9–C11	-162.8 (3)	C25–C24–C29–C31	-166.2 (2)
C4–C9–C10–C11	-105.6 (3)	C24–C29–C30–C31	-104.6 (3)
C10–C9–C11–C12	110.9 (4)	C30–C29–C31–C32	108.9 (3)
C4–C9–C11–C12	-138.8 (3)	C24–C29–C31–C32	-141.6 (3)
C4–C9–C11–C10	110.3 (3)	C24–C29–C31–C30	109.5 (3)
C9–C10–C11–C12	-108.3 (3)	C29–C30–C31–C32	-109.5 (3)

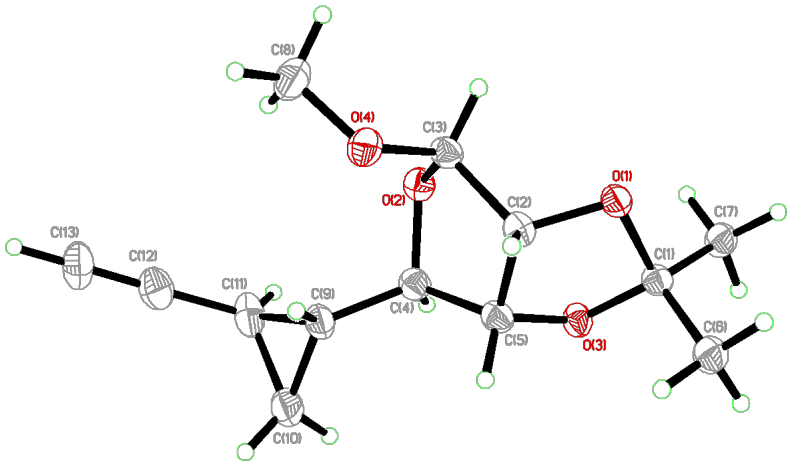

Figure S12: Perspective views showing 50% probability displacement.

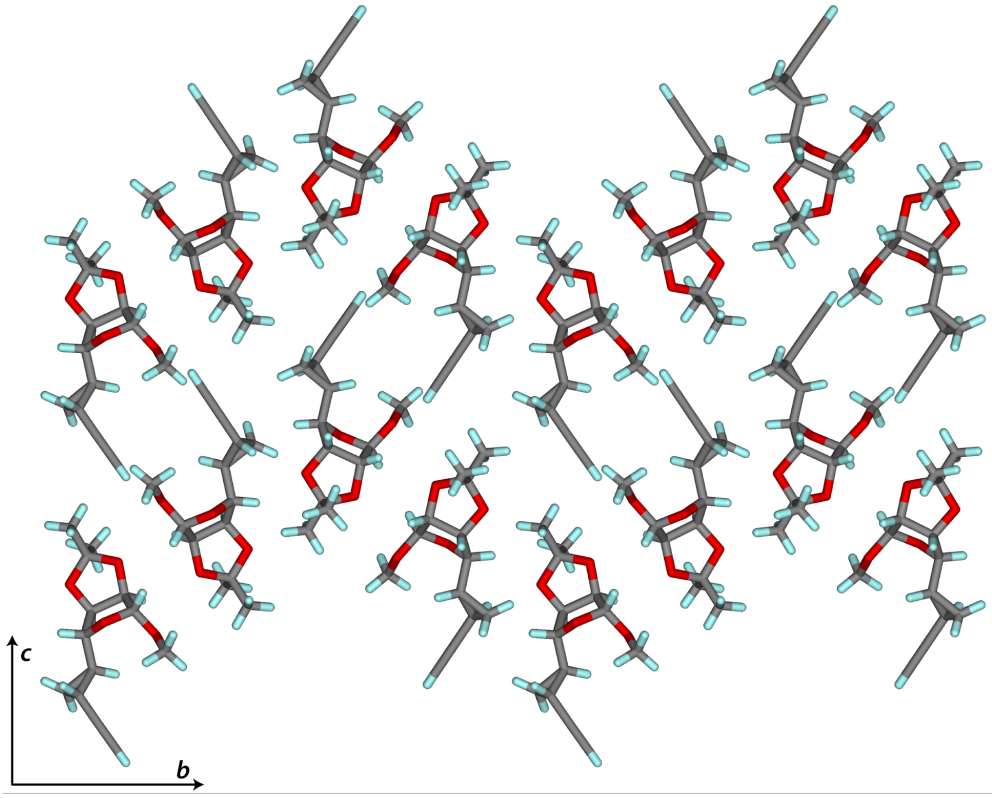

Figure S13: Three-dimensional supramolecular architecture viewed along the *a*-axis direction.

5.3 NS1-Urea: Alkynyl Alcohol S53

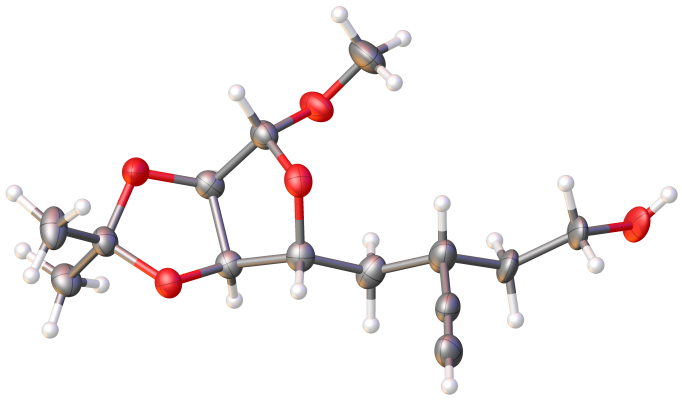

Table S16: Experimental Details

Crystal Data	
Chemical Formula	$C_{14}H_{22}O_5$
M_r	270.31
Crystal system, space group	Orthorhombic, $P2_12_12_1$
Temperature (K)	100
a, b, c (Å)	5.7488 (1), 9.3963 (2), 27.2172 (7)
V(Å^3)	1470.20 (6)
Z	4
Radiation type	Cu $K\alpha$
μ (mm^{-1})	0.76
Crystal size (mm)	$0.18 \times 0.12 \times 0.10$
Data Collection	
Diffractometer	Bruker D8 goniometer with CCD area detector
Absorption correction	Multi-scan *SADABS*
$T_{\min}, T_{\max}$	0.796, 0.864
No. of measured, independent and observed $[I > 2\sigma(I)]$ reflections	31333, 2577, 2531
R_{int}	0.035
$(\sin\theta/\lambda)_{\max}$(Å^{-1})	0.596
Refinement	
$R[F^2 > 2\sigma(F^2)], wR(F^2), S$	0.040, 0.107, 1.09
No. of reflections	2577
No. of parameters	206
No. of restraints	252

H-atom treatment	H atom parameters constrained
$\Delta\rho_{\max}, \Delta\rho_{\min}(e\mathring{A}^{-3})$	0.43, -0.23
Absolute structure	Flack x determined using 1012 quotients [(I+)-(I-)]/[(I+)+(I-)][9]
Absolute structure parameter	0.10 (4)

Computer programs: APEX3 v2016.9-0 (Bruker-AXS, 2016), SAINT 8.37A (Bruker-AXS, 2015), SHELXT2014 (Sheldrick, 2015), SHELXL2014 (Sheldrick, 2015), Bruker SHELXTL (Sheldrick, 2015).

Table S17: Geometric parameters (Å, °)

O1–C1	1.419 (3)	C8A–H8AA	0.99
O1–C5	1.438 (3)	C8A–H8AB	0.99
O2–C1	1.410 (3)	C9A–O5A	1.480 (9)
O2–C10	1.416 (4)	C9A–H9AA	0.99
O3–C2	1.424 (3)	C9A–H9AB	0.99
O3–C3	1.425 (3)	O5A–H5AA	0.84
O4–C3	1.428 (3)	C7B–C13	1.460 (4)
O4–C4	1.430 (3)	C7B–C8B	1.449 (15)
C1–C2	1.528 (4)	C7B–H7B	1
C1–H1	1	C8B–C9B	1.510 (19)
C2–C4	1.536 (3)	C8B–H8BA	0.99
C2–H2	1	C8B–H8BB	0.99
C3–C11	1.510 (4)	C9B–O5B	1.491 (11)
C3–C12	1.512 (4)	C9B–H9BA	0.99
C4–C5	1.527 (3)	C9B–H9BB	0.99
C4–H4	1	O5B–H5B	0.84
C5–C6	1.523 (3)	C7C–C13	1.460 (4)
C5–H5	1	C7C–C8C	1.606 (17)
C6–C7C	1.539 (4)	C7C–H7C	1
C6–C7	1.539 (4)	C8C–C9C	1.465 (18)
C6–C7A	1.539 (4)	C8C–H8CA	0.99
C6–C7B	1.539 (4)	C8C–H8CB	0.99
C6–H6A	0.99	C9C–O5C	1.497 (11)
C6–H6B	0.99	C9C–H9CA	0.99
C7–C13	1.460 (4)	C9C–H9CB	0.99
C7–C8	1.587 (11)	O5C–H5C	0.84
C7–H7	1	C10–H10A	0.98
C8–C9	1.505 (11)	C10–H10B	0.98
C8–H8A	0.99	C10–H10C	0.98
C8–H8B	0.99	C11–H11A	0.98
C9–O5	1.458 (8)	C11–H11B	0.98

[9] Parsons, S.; Flack, H. D.; Wagner, T. *Acta Crystallogr., Sect. B* **2013**, *69*, 249–259.

C9–H9A	0.99	C11–H11C	0.98
C9–H9B	0.99	C12–H12A	0.98
O5–H5A	0.84	C12–H12B	0.98
C7A–C13	1.460 (4)	C12–H12C	0.98
C7A–C8A	1.596 (13)	C13–C14	1.185 (4)
C7A–H7AA	1	C14–H14	0.95
C8A–C9A	1.567 (14)		
C1–O1–C5	109.19 (19)	C9A–C8A–H8AB	110
C1–O2–C10	111.5 (2)	C7A–C8A–H8AB	110
C2–O3–C3	108.15 (19)	H8AA–C8A–H8AB	108.4
C3–O4–C4	107.27 (18)	O5A–C9A–C8A	104.6 (10)
O2–C1–O1	112.0 (2)	O5A–C9A–H9AA	110.8
O2–C1–C2	108.0 (2)	C8A–C9A–H9AA	110.8
O1–C1–C2	106.3 (2)	O5A–C9A–H9AB	110.8
O2–C1–H1	110.2	C8A–C9A–H9AB	110.8
O1–C1–H1	110.2	H9AA–C9A–H9AB	108.9
C2–C1–H1	110.2	C9A–O5A–H5AA	109.5
O3–C2–C1	109.7 (2)	C13–C7B–C8B	123.8 (9)
O3–C2–C4	105.43 (19)	C13–C7B–C6	109.8 (2)
C1–C2–C4	104.7 (2)	C8B–C7B–C6	120.8 (10)
O3–C2–H2	112.2	C13–C7B–H7B	97.9
C1–C2–H2	112.2	C8B–C7B–H7B	97.9
C4–C2–H2	112.2	C6–C7B–H7B	97.9
O3–C3–O4	103.81 (19)	C7B–C8B–C9B	101.5 (13)
O3–C3–C11	108.9 (2)	C7B–C8B–H8BA	111.5
O4–C3–C11	109.1 (2)	C9B–C8B–H8BA	111.5
O3–C3–C12	110.8 (2)	C7B–C8B–H8BB	111.5
O4–C3–C12	111.1 (2)	C9B–C8B–H8BB	111.5
C11–C3–C12	112.8 (2)	H8BA–C8B–H8BB	109.3
O4–C4–C5	109.61 (19)	O5B–C9B–C8B	98.8 (13)
O4–C4–C2	102.89 (19)	O5B–C9B–H9BA	112
C5–C4–C2	105.0 (2)	C8B–C9B–H9BA	112
O4–C4–H4	112.9	O5B–C9B–H9BB	112
C5–C4–H4	112.9	C8B–C9B–H9BB	112
C2–C4–H4	112.9	H9BA–C9B–H9BB	109.7
O1–C5–C6	111.8 (2)	C9B–O5B–H5B	109.5
O1–C5–C4	104.0 (2)	C13–C7C–C6	109.8 (2)
C6–C5–C4	113.4 (2)	C13–C7C–C8C	103.7 (13)
O1–C5–H5	109.2	C6–C7C–C8C	124.7 (11)
C6–C5–H5	109.2	C13–C7C–H7C	105.8

C4–C5–H5	109.2	C6–C7C–H7C	105.8
C5–C6–C7C	112.5 (2)	C8C–C7C–H7C	105.8
C5–C6–C7	112.5 (2)	C9C–C8C–C7C	133 (2)
C5–C6–C7A	112.5 (2)	C9C–C8C–H8CA	103.8
C5–C6–C7B	112.5 (2)	C7C–C8C–H8CA	103.8
C5–C6–H6A	109.1	C9C–C8C–H8CB	103.8
C7–C6–H6A	109.1	C7C–C8C–H8CB	103.8
C5–C6–H6B	109.1	H8CA–C8C–H8CB	105.4
C7–C6–H6B	109.1	C8C–C9C–O5C	159 (3)
H6A–C6–H6B	107.8	C8C–C9C–H9CA	96.5
C13–C7–C6	109.8 (2)	O5C–C9C–H9CA	96.5
C13–C7–C8	113.5 (6)	C8C–C9C–H9CB	96.5
C6–C7–C8	104.0 (5)	O5C–C9C–H9CB	96.5
C13–C7–H7	109.8	H9CA–C9C–H9CB	103.4
C6–C7–H7	109.8	C9C–O5C–H5C	109.5
C8–C7–H7	109.8	O2–C10–H10A	109.5
C9–C8–C7	107.9 (8)	O2–C10–H10B	109.5
C9–C8–H8A	110.1	H10A–C10–H10B	109.5
C7–C8–H8A	110.1	O2–C10–H10C	109.5
C9–C8–H8B	110.1	H10A–C10–H10C	109.5
C7–C8–H8B	110.1	H10B–C10–H10C	109.5
H8A–C8–H8B	108.4	C3–C11–H11A	109.5
O5–C9–C8	112.2 (8)	C3–C11–H11B	109.5
O5–C9–H9A	109.2	H11A–C11–H11B	109.5
C8–C9–H9A	109.2	C3–C11–H11C	109.5
O5–C9–H9B	109.2	H11A–C11–H11C	109.5
C8–C9–H9B	109.2	H11B–C11–H11C	109.5
H9A–C9–H9B	107.9	C3–C12–H12A	109.5
C9–O5–H5A	109.5	C3–C12–H12B	109.5
C13–C7A–C6	109.8 (2)	H12A–C12–H12B	109.5
C13–C7A–C8A	112.1 (9)	C3–C12–H12C	109.5
C6–C7A–C8A	115.2 (6)	H12A–C12–H12C	109.5
C13–C7A–H7AA	106.4	H12B–C12–H12C	109.5
C6–C7A–H7AA	106.4	C14–C13–C7	176.6 (3)
C8A–C7A–H7AA	106.4	C14–C13–C7A	176.6 (3)
C9A–C8A–C7A	108.3 (10)	C14–C13–C7B	176.6 (3)
C9A–C8A–H8AA	110	C14–C13–C7C	176.6 (3)
C7A–C8A–H8AA	110	C13–C14–H14	180
C10–O2–C1–O1	-66.2 (3)	O1–C5–C6–C7C	57.3 (3)
C10–O2–C1–C2	177.1 (2)	C4–C5–C6–C7C	174.5 (2)

C5–O1–C1–O2	-88.6 (2)	O1–C5–C6–C7	57.3 (3)
C5–O1–C1–C2	29.2 (2)	C4–C5–C6–C7	174.5 (2)
C3–O3–C2–C1	-124.8 (2)	O1–C5–C6–C7A	57.3 (3)
C3–O3–C2–C4	-12.5 (3)	C4–C5–C6–C7A	174.5 (2)
O2–C1–C2–O3	-138.6 (2)	O1–C5–C6–C7B	57.3 (3)
O1–C1–C2–O3	101.1 (2)	C4–C5–C6–C7B	174.5 (2)
O2–C1–C2–C4	108.7 (2)	C5–C6–C7–C13	64.9 (3)
O1–C1–C2–C4	-11.6 (2)	C5–C6–C7–C8	-173.3 (6)
C2–O3–C3–O4	29.9 (3)	C13–C7–C8–C9	-75.3 (10)
C2–O3–C3–C11	146.0 (2)	C6–C7–C8–C9	165.5 (8)
C2–O3–C3–C12	-89.5 (3)	C7–C8–C9–O5	-167.4 (9)
C4–O4–C3–O3	-36.6 (2)	C5–C6–C7A–C13	64.9 (3)
C4–O4–C3–C11	-152.5 (2)	C5–C6–C7A–C8A	-167.3 (11)
C4–O4–C3–C12	82.6 (2)	C13–C7A–C8A–C9A	-62.2 (17)
C3–O4–C4–C5	139.4 (2)	C6–C7A–C8A–C9A	171.2 (12)
C3–O4–C4–C2	28.2 (2)	C7A–C8A–C9A–O5A	-172.7 (13)
O3–C2–C4–O4	-9.4 (2)	C5–C6–C7B–C13	64.9 (3)
C1–C2–C4–O4	106.3 (2)	C5–C6–C7B–C8B	-140.7 (10)
O3–C2–C4–C5	-124.1 (2)	C13–C7B–C8B–C9B	80.0 (17)
C1–C2–C4–C5	-8.4 (2)	C6–C7B–C8B–C9B	-70.7 (17)
C1–O1–C5–C6	88.4 (2)	C7B–C8B–C9B–O5B	-178.6 (14)
C1–O1–C5–C4	-34.3 (2)	C5–C6–C7C–C13	64.9 (3)
O4–C4–C5–O1	-84.7 (2)	C5–C6–C7C–C8C	-171.4 (18)
C2–C4–C5–O1	25.2 (2)	C13–C7C–C8C–C9C	-69 (4)
O4–C4–C5–C6	153.6 (2)	C6–C7C–C8C–C9C	165 (3)
C2–C4–C5–C6	-96.5 (2)	C7C–C8C–C9C–O5C	162 (7)

Table S18: Hydrogen-bond parameters

D – H ··· A	D – H (Å)	H ··· A (Å)	D ··· A (Å)	D – H ··· A (°)
O5 – H5A ··· O5^{i}	0.84	2.33	3.132 (5)	159.9

Symmetry code(s): (i) x-1/2, -y+3/2, -z+1.

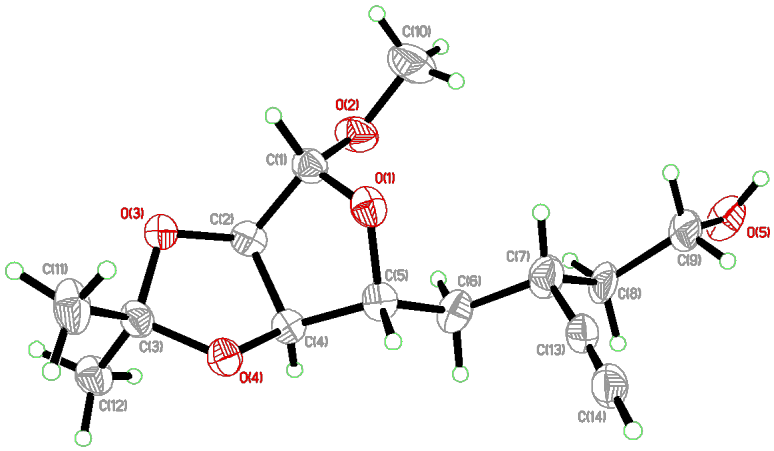

Figure S14: Perspective views showing 50% probability displacement.

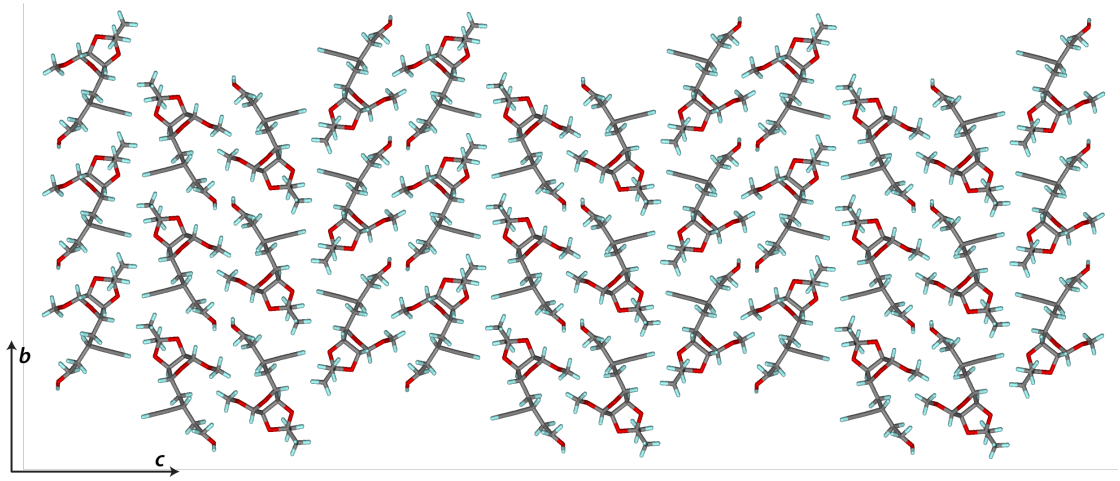

Figure S15: Three-dimensional supramolecular architecture viewed along the *a*-axis direction.

6 *Methods*: Molecular Docking, Biochemical Assays, Bioinformatic Analyses, and Protein Crystallography

6.1 Molecular Docking with Schrödinger Glide

General Considerations

The molecular docking workflow presented below was performed in Schrödinger Maestro Version 11.8.012, MMshare Version 4.4.012, Release 2018-4, Platform Windows-x64. A detailed tutorial (Structure-Based Virtual Screening Using Glide Workshop Tutorial, 2018-4) published by Schrödinger can be found at `https://www.schrodinger.com/training/tutorials`.

Protein Preparation

Glide docking began with the Protein Preparation Wizard. The PDB entry 3ROD[10] (NAM and SAH bound to NNMT) was imported into the workspace. Preprocessing parameters in the *Import and Process* tab were set as presented in Figure S16. The imported structure was preprocessed. Parameters in the *Review and Modify* tab were set as presented in Figure S17. All chains, waters, and hets not belonging to chain C were deleted. Parameters in the *Refine* tab were set as presented in Figure S18. H-bond assignment was optimized, waters were removed, and restrained minimization was performed.

Receptor Grid Generation

Receptor grid generation was performed according to the parameters outlined in Figure S19. No other tabs (*Site*, *Constraints*, *Rotatable Groups*, *Excluded Volumes*) were edited. Nicotinamide (NCA, NAM) was deleted from the workspace prior to choosing the workspace ligand SAH for grid generation.

Ligand Preparation

NS1 was drawn in ChemDraw and saved as an MDL Molfile (.mol). The .mol file was opened in the LigPrep wizard and was prepared using the parameters outlined in Figure S20.

Glide Docking

The Ligand Docking panel was opened and the output file from LigPrep was loaded with the parameters shown in Figure S21 and Figure S22. Docking calculations were run locally and NS1 was determined to have a Glide Score of –15.991. A table of output values is presented below in Table S19. An image of the NS1

[10] Peng, Y.; Sartini, D.; Pozzi, V.; Wilk, D.; Emanuelli, M.; Yee, V. C. *Biochemistry* **2011**, *50*, 7800–7808.

output pose is presented in Figure S23. Reference ligand S-adenosylmethionine (SAM) was docked using this same protocol, having a Glide score of –12.741. An image of the SAM output pose is presented in Figure S24.

Table S19: Docking output values from the Maestro docking table.

parameter	**NS1**	**SAM**
glide rotatable bonds	12	9
docking score	-15.991	-12.741
glide ligand efficiency	-0.432	-0.472
glide ligand efficiency sa	-1.44	-1.416
glide ligand efficiency ln	-3.468	-2.966
glide gscore	-15.991	-12.741
glide lipo	-4.095	-2.187
glide hbond	-1.584	-0.986
glide metal	0	0
glide rewards	-3.069	-3.744
glide evdw	-72.943	-49.357
glide ecoul	-30.436	-29.203
glide erotb	0.631	0.737
glide esite	-0.227	-0.093
glide emodel	-213.421	-157.523
glide energy	-103.378	-78.56
glide einternal	9.997	8.134

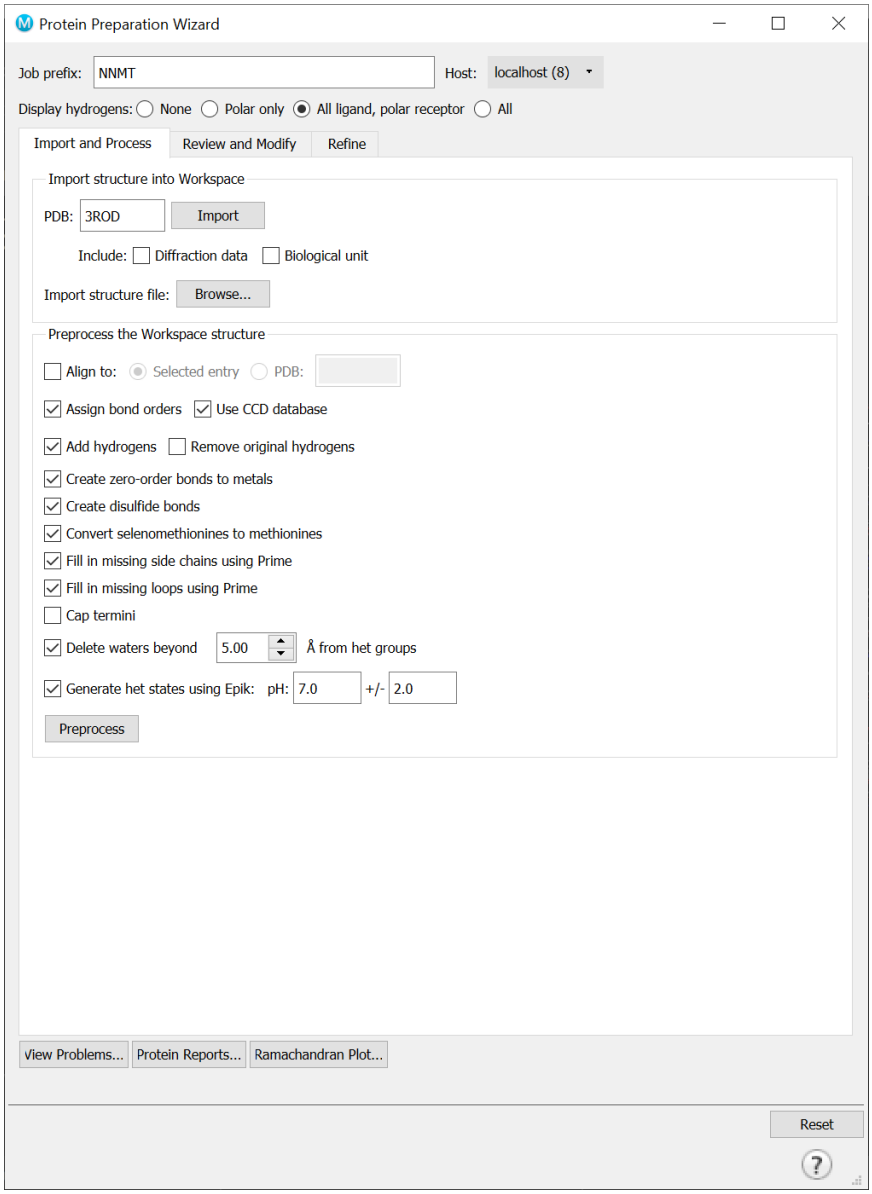

Figure S16: *Import and Process* parameters in the Protein Preparation Wizard.

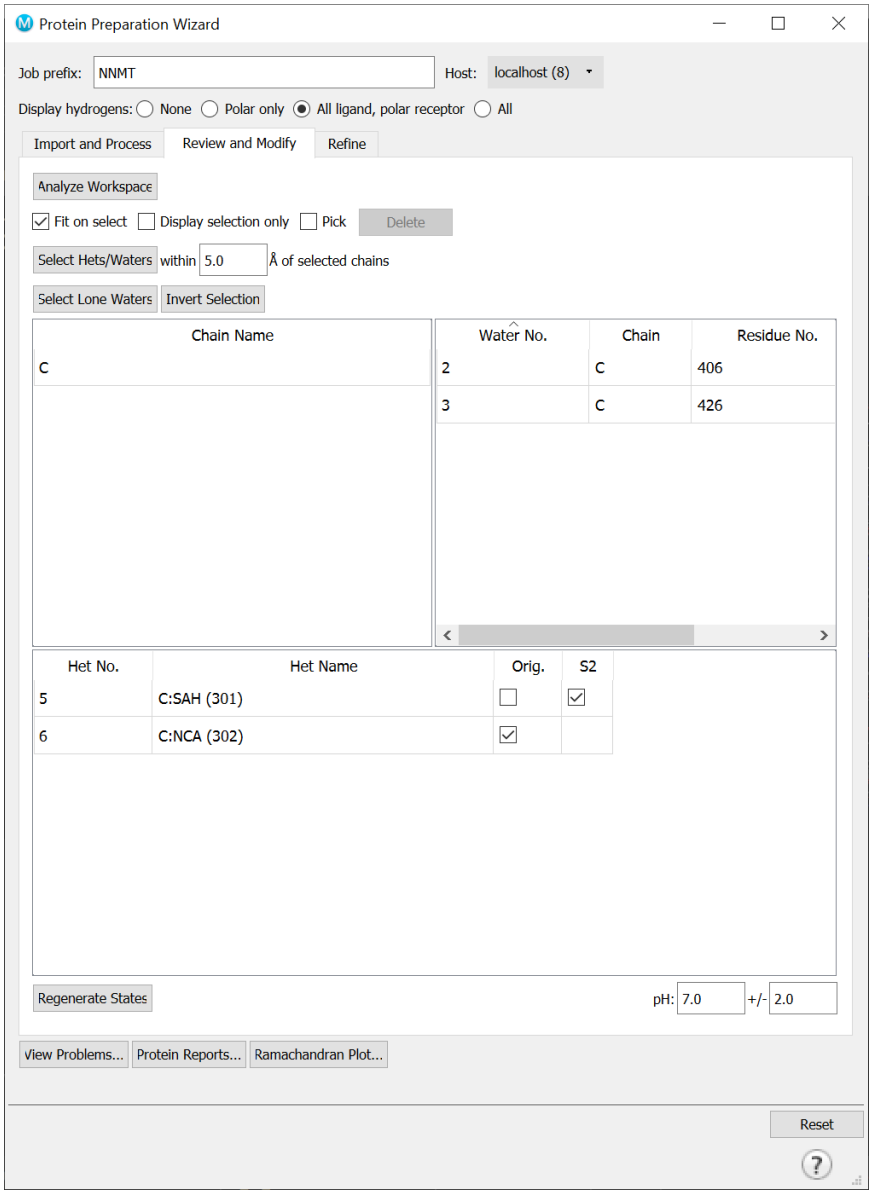

Figure S17: *Review and Modify* parameters in the Protein Preparation Wizard.

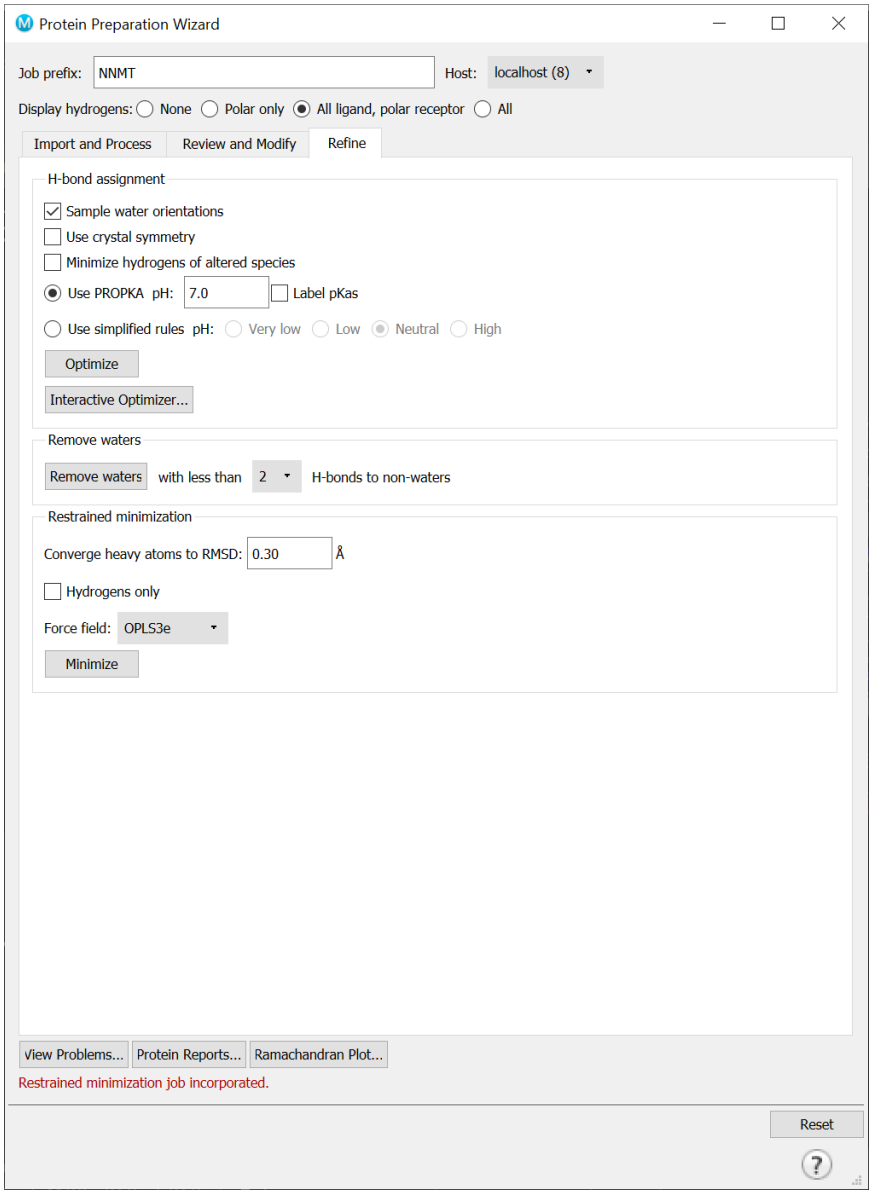

Figure S18: *Refine* parameters in the Protein Preparation Wizard.

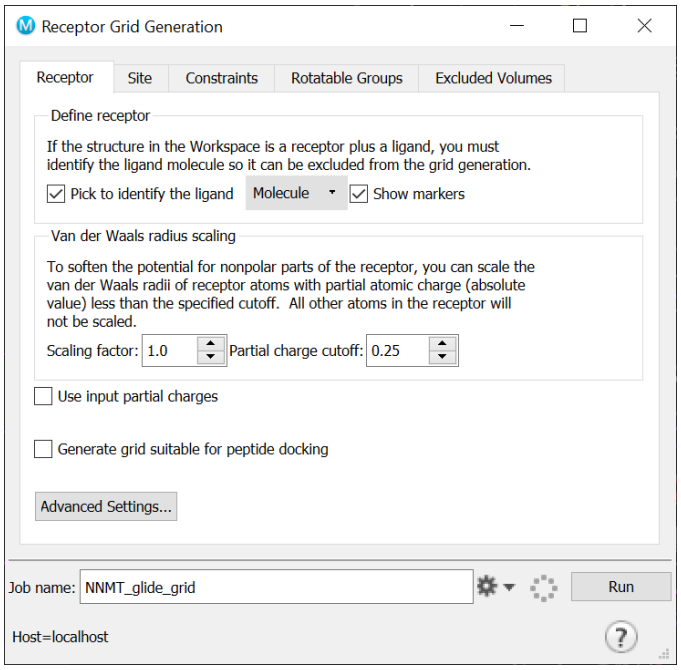

Figure S19: Parameters set in the Receptor Grid Generation.

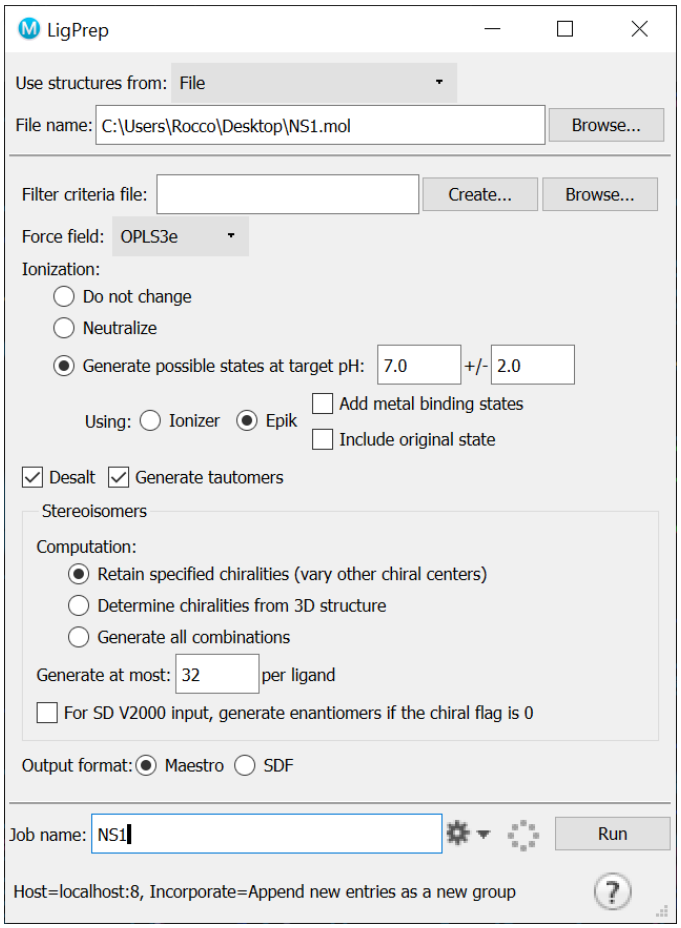

Figure S20: Parameters set during ligand preparation in LigPrep.

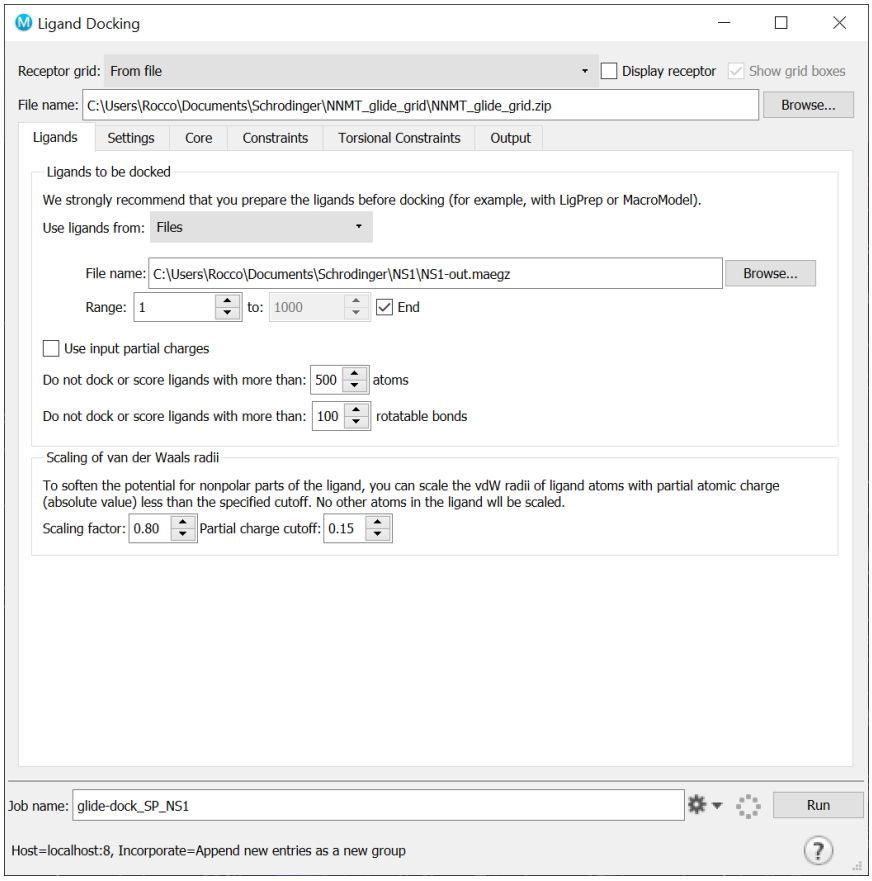

Figure S21: Parameters set in Ligand Docking (Ligands tab).

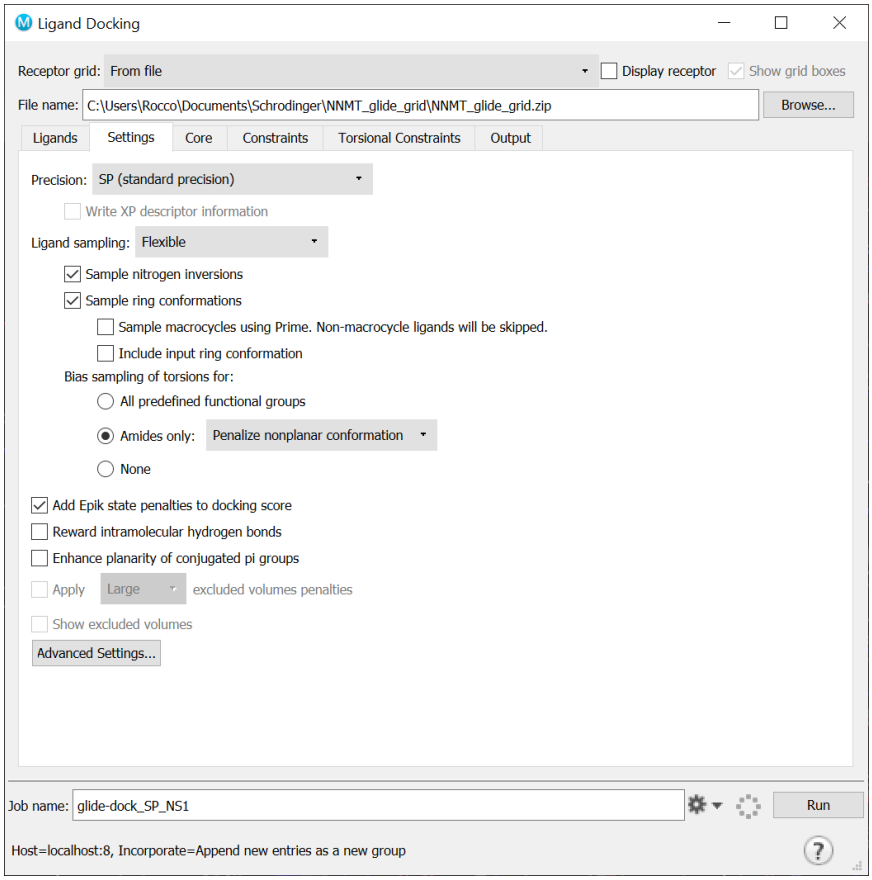

Figure S22: Parameters set in Ligand Docking (Settings tab).

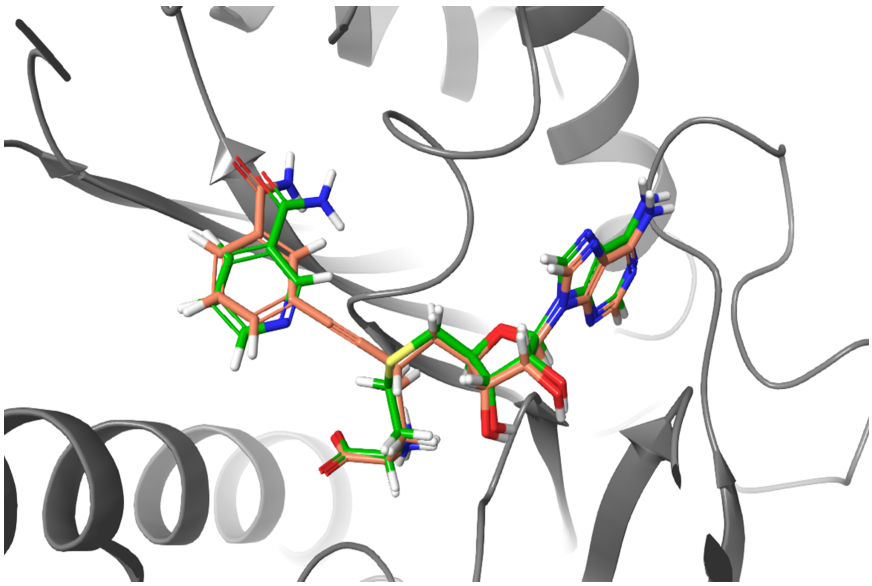

Figure S23: Output image of docked NS1 (orange), taken directly from the Maestro workspace, overlaid with substrates SAH and NAM (green).

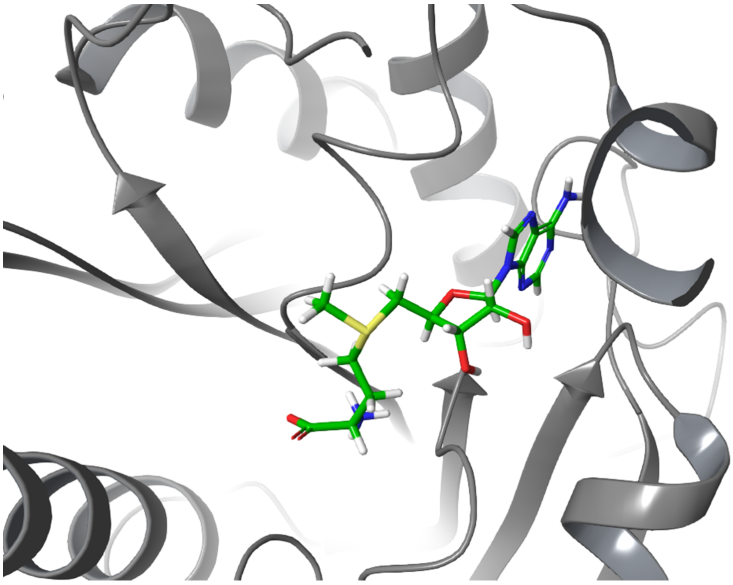

Figure S24: Output image of docked reference ligand SAM, taken directly from the Maestro workspace.

6.2 NNMT Inhibition Assay

6.2.1 wt-hNNMT Preparation

Cloning

The tm-hNNMT plasmid obtained from Addgene (40734; `http://n2t.net/addgene:40734`; RRID:Addgene _40734) and used in protein crystallography experiments was supplied as a K100A:E101A:E103A mutant. In order to study the wild-type enzyme, we performed site-directed mutagenesis using Agilent's QuikChange Lightning Kit (P/N 210515) to generate a wt-hNNMT plasmid. The following primers were used:

forward: 5'-ggaccagtcaaaggcctctggctctttcttcagccacttctcc-3'

reverse: 5'-ggagaagtggctgaagaaagagccagaggcctttgactggtcc-3'

The wt-hNNMT protein sequence is as follows:

MGSSHHHHHHSSGLVPRGSMESGFTSKDTYLSHFNPRDYLEKYYKFGSRHSAESQILKHLLKNLFKIFCLDGVKGDLLI
DIGSGPTIYQLLSACESFKEIVVTDYSDQNLQELEKWLKKEPEAFDWSPVVTYVCDLEGNRVKGPEKEEKLRQAVKQVL
KCDVTQSQPLGAVPLPPADCVLSTLCLDAACPDLPTYCRALRNLGSLLKPGGFLVIMDALKSSYYMIGEQKFSSLPLGR
EAVEAAVKEAGYTIEWFEVISQSYSSTMANNEGLFSLVARKLSRPL

Protein Expression and Purification

The plasmid containing N-terminally His_6-tagged wt-hNNMT (generated via cloning above) was transformed into NiCo21(DE3) Competent E. coli (New England BioLabs Catalog # C2529H) according to the manufacturer's protocol. Bacteria were subsequently grown up in 1L LB (containing 50 µg/mL kanamycin sulfate and supplemented with 0.5 mM $MgCl_2$ and 0.5 mM $CaCl_2$) at 37 °C, induced with IPTG (1 mM) when they reached an OD_{600} of ∼0.8, and incubated overnight at 37 °C.

The following day the cell pellet was harvested by centrifugation and then suspended in 25 mL lysis buffer (*50 mL prepared*: 20 mM Tris-HCl pH 8.0, 0.5 M NaCl, 40 mM imidazole, 1 mM DTT, 20% glycerol, and 1 tablet of Roche cOmplete™ EDTA-containing protease inhibitor cocktail in 50 mL V_{tot}). To the pellet/lysis buffer containing tube were added 10 mg lysozyme and 1 mL DNase and the contents were vortexed briefly to suspend the cells. The cell suspension was incubated on ice for 30 minutes and then sonicated on ice for 7 minutes (total sonication time) employing a duty cycle of 10/50 sec on/off at 20% power. The crude lysate was clarified by centrifugation and $MgCl_2$ was added to a final concentration of 2 mM (to chelate EDTA and prevent interference Ni-NTA affinity chromatography).

The clarified lysate was purified by automated affinity chromatography using a GE Healthcare ÄKTA chromatography system and a 5 mL GE FF HisTrap Crude Ni-NTA affinity chromatography column. The column was equilibrated with buffer A (40 mM imidazole, 500 mM NaCl, 20 mM Tris-HCl pH 8.0, 1.0 mM DTT, 10% glycerol) and the clarified lysate was loaded via sample application pump. The column was washed with 30 CV (column volumes) buffer A and then a gradient of 0 → 100 % buffer B (500 mM imidazole, 500 mM NaCl, 20 mM Tris-HCl pH 8.0, 1.0 mM DTT, 10% glycerol) was delivered over 20 CV. Eluted fractions corresponding to UV detector peaks were checked by SDS-PAGE analysis and showed clean elution of a single protein at the appropriate MW. Fractions were combined, concentrated, and desalted into storage buffer (20 mM Tris-HCl pH 8.0, 50 mM NaCl, 1 mM DTT, 5% glycerol) via GE HiTrap Desalting column. Fractions were combined, concentrated to 11.4 mg/mL, flash-frozen in liquid nitrogen and stored at –80 °C for future use.

6.2.2 Detailed NNMT Inhibition Assay Protocol

Molecular biology grade water and Tris-HCl buffer (pH 8.0 ± 0.1, 1 M) were obtained from Corning (Manassas, VA). DL-dithiothreitol (DTT, for molecular biology, ≥ 98% (HPLC)) and quinoline (reagent grade, 98%) were purchased from Sigma-Aldrich (St. Louis, MO). DTT was used as received, while quinoline was distilled under reduced pressure before use and stored in the dark. *S*-adenosyl-L-methionine was obtained from New England BioLabs (Ipswich, MA) as a 32 mM solution in 0.005 M H_2SO_4 and 10% EtOH and used

as received (NEB catalog #: B9003S).

The protocol described below was adapted from those outlined in Neelakantan et al.[11] Enzymatic reactions were performed at room temperature in 96-well plates (costar® black, flat bottom, non-treated, polystyrene, 14.3 mm height). To minimize potential small differences in initial reaction concentrations due to pipetting errors, a master stock consisting of 5 mM Tris-HCl (pH 8.0), 1 mM DTT and 109 µM quinoline was prepared by adding to a 50 mL falcon tube water (50 mL), Tris-HCl pH 8.0 ± 0.1 buffer (1 M, 250.0 μL), DTT (7.7 mg, 50 μmol) and a solution of quinoline in water (20 mM, 272.5 μL). This 50 mL stock was then split into 4 mL stocks.

Using ten PCR tubes of a twelve 0.2 mL tube strip, a dilution series of inhibitor concentrations was prepared. With a multichannel pipette, 10 µL of each of these solutions of inhibitor in water were transferred to the first ten PCR tubes of another twelve 0.2 mL tube strip. The two remaining tubes were charged with 10 µL of water (controls). To each of these tubes was then added 10 µL of a 250 μM solution of SAM in water (prepared by mixing 15.6 µL of a freshly thawed 32 mM SAM solution in 2 mL of water). The reactions were initiated by adding to each tube 230 μL of a 109 nM solution of NNMT in master stock (prepared by adding 1.2 μL of a 362 μM freshly thawed NNMT aliquot in 4 mL of master stock), bringing the final composition of each reaction to 4.6 mM Tris-HCl (pH 8.0), 0.92 mM DTT, 100 μM quinoline, 10 μM SAM and 100 nM NNMT.

Immediately after initiation, the progress of each reaction was monitored using a SpectraMax® i3x multimode microplate reader and data were collected approximately every 27 seconds for 5.5 minutes (13 reads, 100 flashes/read, 1.00 mm read height). The production of 1-MQ in each well was monitored by recording fluorescence emission intensities at 400 nm (excitation wavelength at 310 nm) with the detector bandwidths set up at 9 nm for the excitation and at 15 nm for the emission.

6.3 Sequence Similarity Analysis

To generate a data set for sequence similarity analysis, the UniProtKB[12,13] was queried with the following conditions: ec:2.1.1.– ipr029063 AND reviewed:yes AND organism: "Homo sapiens (Human) [9606]" AND proteome:up000005640. These conditions searched the UniProt database for human (organism: "Homo sapiens (Human) [9606]") methyltransferases (ec:2.1.1.–, *transferases*, *transferring one-carbon groups*, *methyltransferases*) that were Swiss-Prot reviewed (reviewed:yes) belonging to the InterPro Homologous Superfamily of SAM-dependent MTases (ipr029063) in the human proteome (proteome:up000005640).

This query returned 113 UniProt IDs which were submitted to the Enzyme Function Initiative Enzyme

[11] Neelakantan, H.; Vance, V.; Wang, H.-Y. L.; McHardy, S. F.; Watowich, S. J. *Biochemistry* **2017**, *56*, 824–832.
[12] `https://www.uniprot.org/`
[13] UniProt *Nucleic Acids Res.* **2018**, *47*, D506–D515.

Similarity Tool[14,15,16] (EFI-EST, settings: *Computation Type*: Option D, *E-Value*: 5, *Fraction*: 1). A sequence similarity network (SSN) was generated using an *alignment score for output* value of 18. The SSN was processed in Cytoscape v3.7.1. Specifically, node labels were set to *Gene Name* and edges were colored via continuous mapping based on *%ID*. The node labels found in Figure S2 correlate to UniProt IDs and Protein Names in Table S3.

6.4 DALI Structural Similarity Analysis

The DALI server[17] (`http://ekhidna2.biocenter.helsinki.fi/dali/`) was queried using PDB search and entering identifier 3ROD (Chain A). The DALI structural alignment server returned 1792 hits with a DALI Z-score >2. Chain identifiers were removed from the DALI output (leaving a list of only PDB codes) and the list was then uploaded to the UniProt Retrieve/ID Mapping utility (`https://www.uniprot.org/uploadlists/`). 871 out of 914 PDB identifiers were successfully mapped to 453 UniProtKB IDs, with the remaining 43 (unmatched) set aside for manual curation. Of the remaining 43 unmatched PDB IDs, none corresponded to human proteins, so they were not included in further analysis.

The list of 453 UniProtKB IDs was filtered to show only methyltransferase enzymes from Homo Sapiens (query with operators: ec:2.1.1.– AND organism:"Homo sapiens (Human) [9606]") leaving 34 UniProtKB IDs remaining (Class EC 2.1.1.– represents enzymes from the methyltransferase family). In many cases multiple PDB IDs mapped to a single UniProtKB ID. These redundancies in the data set were removed by selecting the PDB ID (and chain) with the highest Dali Z-score for further analysis. The authors noted that the PDB code for a known human small-molecule methyltransferase (guanidinoacetate N-methyltransferase, GAMT, with structure 3orh available in the PDB) was missing, so 3orh (chain A) was manually added to the list. The list of PDB codes (and chain identifiers) was uploaded to the DALI server and an *all-against-all* query was submitted. The *all-against-all* output was used to generate the dendrogram presented in Figure S3 and the heatmap presented in Figure S4.

6.5 Protein Crystallography

The tm-hNNMT plasmid obtained from Addgene (40734) and used in protein crystallography experiments was supplied as a K100A:E101A:E103A mutant (see Section 6.2.1. These mutations reduce the entropy of surface residues and facilitate crystallization.

[14] `https://efi.igb.illinois.edu/efi-est/`
[15] Gerlt, J. A.; Bouvier, J. T.; Davidson, D. B.; Imker, H. J.; Sadkhin, B.; Slater, D. R.; Whalen, K. L. *Biochim. Biophys. Acta, Proteins Proteomics* **2015**, *1854*, 1019–1037.
[16] Zallot, R.; Oberg, N. O.; Gerlt, J. A. *Curr. Opin. Chem. Biol.* **2018**, *47*, 77–85.
[17] Holm, L.; Laakso, L. M. *Nucleic Acids Res.* **2016**, *44*, W351–W355.

The tm-hNNMT protein sequence is as follows:

MGSSHHHHHHSSGLVPRGSMESGFTSKDTYLSHFNPRDYLEKYYKFGSRHSAESQILKHLLKNLFKIFCLDGVKGDLLI
DIGSGPTIYQLLSACESFKEIVVTDYSDQNLQELEKWLKAAPAAFDWSPVVTYVCDLEGNRVKGPEKEEKLRQAVKQVL
KCDVTQSQPLGAVPLPPADCVLSTLCLDAACPDLPTYCRALRNLGSLLKPGGFLVIMDALKSSYYMIGEQKFSSLPLGR
EAVEAAVKEAGYTIEWFEVISQSYSSTMANNEGLFSLVARKLSRPL

6.5.1 tm-hNNMT Preparation

The pET-28a plasmid containing N-terminally His_6-tagged tm-hNNMT (Addgene) was transformed into BL21(DE3) cells, which were subsequently grown in terrific broth at 37 °C. The cultures were induced with 1 mM IPTG when they reached an OD_{600} of ∼1.1 and incubated overnight at 25 °C. Cell pellets were harvested by centrifugation and solubilized in lysis buffer (50 mM Tris-HCl pH 8.0, 0.5 M NaCl, 5 mM imidazole, 2 mM β-mercaptoethanol, 5% glycerol) supplemented with 1 mM PMSF and 1 µg/mL lysozyme. Solubilized cell pellets were centrifuged and the supernatant was loaded onto Ni-NTA Agarose resin (Qiagen), washed with wash buffer (50 mM Tris-HCl pH 8.0, 0.5 M NaCl, 25 mM imidazole, 5% glycerol), and the tm-hNNMT protein was eluted with 50 mM Tris-HCl pH 8.0, 0.5 M NaCl, 250 mM imidazole, and 5% glycerol. Eluted fractions were concentrated and buffer exchanged using a PD-10 desalting column (GE) into NNMT storage buffer (20 mM Tris-HCl pH 8.0, 50 mM NaCl, 1 mM DTT). The final purified protein was concentrated to 18 mg/mL, flash-frozen in liquid nitrogen and stored at –80 °C for future use.

6.5.2 Crystallization and Data Collection

The purified tm-hNNMT was diluted by adding NNMT storage buffer and NS1 formulated in water to final concentrations of 10 mg/mL protein and 1 mM NS1. Co-crystals of tm-hNNMT and NS1 were obtained by sitting drop vapor diffusion at 20 °C with a protein:precipitant volume ratio of 1:1 in 2 µL total volume drops. Crystals appeared after about one week in a precipitant condition containing 100 mM HEPES pH 6.8 and 2 M ammonium sulfate and were harvested about six weeks after setting the drops. Crystals were cryoprotected by briefly soaking in artificial mother liquor to which 16-20% glycerol had been added before flash-freezing in liquid nitrogen. Diffraction data were collected at Beamline ID-24C of the Northeastern Collaborative Access Team (NE-CAT) at the Advanced Photon Source in Argonne, Illinois.

6.5.3 Data Processing and Refinement

The crystals grew in clusters, and our diffraction data had multiple lattices. Images were indexed and integrated with the Diffraction Integration for Advanced Light Sources (DIALS)[18] package using the multi-lattice search functionality within *dials.index*[19]. We searched for three lattices, providing initial unit cell parameters from the published NNMT structure 3ROD[20]. We chose the lattice accounting for the largest number of indexed spots for integration. Data were scaled and merged using the CCP4 suite programs POINTLESS and AIMLESS[21,22,23]. The NS1-bound NNMT structure was determined by molecular replacement with a previous NNMT structure (PDB ID 3ROD; chain A with all ligands removed)[50] as a search model in PHASER as implemented in PHENIX[24]. Subsequent model building and refinement were done in Coot[25] and PHENIX[54]. The asymmetric unit contains four protein chains (A-D) each bound to an NS1 inhibitor molecule. For all analyses and figures, chain A was used. Figures were prepared using PyMOL (Schrödinger)[26]. The diffraction images are available at the SBGrid Data Bank. The structure factors and refined coordinates are deposited in the Protein Data Bank (PDB ID **6ORR**).

6.6 INMT Selectivity Study

6.6.1 wt-hINMT Preparation

The pET-28a plasmid containing N-terminally His_6-tagged hINMT (Addgene 25475; `http://n2t.net/addgene:25475`; RRID:Addgene_25475) was transformed into Agilent BL21-CodonPlus (DE3)-RIL Competent Cells (Agilent P/N: 230245) according to the manufacturer's protocol. Bacteria were subsequently grown up in terrific broth (containing 50 µg per mL kanamycin sulfate and 50 µg per mL chloramphenicol) at 37 °C, induced with IPTG (1 mM) when they reached an OD_{600} of ∼0.8, and incubated overnight at 32 °C.

The following day cell pellets were harvested by centrifugation. Five grams of cell pellet was then suspended in lysis buffer (15 mL, 20 mM Tris-HCl pH 8, 0.5 M NaCl, 40 mM imidazole, 1 mM DTT, 10% glycerol) supplemented with 1 tablet Roche cOmplete EDTA-free protease inhibitor cocktail, 10 mg lysozyme, and 1 mL DNase. The cell suspension was incubated on ice for 30 min and then sonicated on ice for 7 minutes

[18] Winter, G. et al. *Acta Crystallogr., Sect. D* **2018**, *74*, 85–97.
[19] Gildea, R. J.; Waterman, D. G.; Parkhurst, J. M.; Axford, D.; Sutton, G.; Stuart, D. I.; Sauter, N. K.; Evans, G.; Winter, G. *Acta Crystallogr., Sect. D* **2014**, *70*, 2652–2666.
[20] Peng, Y.; Sartini, D.; Pozzi, V.; Wilk, D.; Emanuelli, M.; Yee, V. C. *Biochemistry* **2011**, *50*, 7800–7808.
[21] Winn, M. D. et al. *Acta Crystallogr., Sect. D* **2011**, *67*, 235–242.
[22] Evans, P. R. *Acta Crystallogr., Sect. D* **2011**, *67*, 282–292.
[23] Evans, P. R.; Murshudov, G. N. *Acta Crystallogr., Sect. D* **2013**, *69*, 1204–1214.
[24] Adams, P. D. et al. *Acta Crystallogr., Sect. D* **2010**, *66*, 213–221.
[25] Emsley, P.; Lohkamp, B.; Scott, W. G.; Cowtan, K. *Acta Crystallogr., Sect. D* **2010**, *66*, 486–501.
[26] Schrödinger, LLC The PyMOL Molecular Graphics System, Version 1.8., 2015.

(total sonication time) employing a duty cycle of 10/50 on/off at 20% power. The crude lysate was clarified by centrifugation and manually loaded onto a 5 mL GE FF HisTrap Crude Ni-NTA affinity chromatography column via syringe. The column was washed with 20 mL lysis buffer and then protein was eluted with 10 mL of elution buffer (20 mM Tris-HCl pH 8, 0.5 M NaCl, 400 mM imidazole, 1 mM DTT, 10% glycerol) while collecting 1.2 mL fractions. Eluted fractions were checked for the presence of protein via Bradford assay. Those containing purified INMT as evidenced by SDS-PAGE analysis were combined, concentrated, and desalted into storage buffer (20 mM Tris-HCl pH 8.0, 50 mM NaCl, 1 mM DTT, 5% glycerol) via GE HiTrap Desalting column. Fractions were combined, concentrated to 13.5 mg/mL, flash-frozen in liquid nitrogen and stored at –80 °C for future use.

The hINMT protein sequence is as follows:

```
MGSSHHHHHHSSGLVPRGSMKGGFTGGDEYQKHFLPRDYLATYYSFDGSPSPEAEMLKFNLECLHKTFGPGGLQGDTLI
DIGSGPTIYQVLAACDSFQDITLSDFTDRNREELEKWLKKEPGAYDWTPAVKFACELEGNSGRWEEKEEKLRAAVKRVL
KCDVHLGNPLAPAVLPLADCVLTLLAMECACCSLDAYRAALCNLASLLKPGGHLVTTVTLRLPSYMVGKREFSCVALEK
GEVEQAVLDAGFDIEQLLHSPQSYSVTNAANNGVCCIVARKKPGP
```

6.6.2 INMT Inhibition Assay

A luminescence-based indolethylamine N-methyltransferase (INMT) assay was developed based on the Promega MTase-Glo™ Methyltransferase Assay (catalog #: V7601). The Promega MTase-Glo ™ assay is a coupled luminescence-based assay that converts S-adenosylhomocysteine (SAH) to ADP which is then converted to light.[27] Full instructions and protocols outlining assay development and validation can be found in Promega application note #AN297 and technical manual TM453 (Revised 4/17).

INMT is capable of methylating a variety of tryptamine, harmine, and phenethylamine derivatives at variable rates, but the typical substrate is tryptamine. INMT is also known as thioether S-methyltransferase (TEMT) and is known to methylate a variety of thioethers and related compounds. From the UniProt[28] entry O95050[29] (INMT_HUMAN):

> Functions as thioether S-methyltransferase and is active with a variety of thioethers and the corresponding selenium and tellurium compounds, including 3-methylthiopropionaldehyde, dimethyl selenide, dimethyl telluride, 2-methylthioethylamine, 2-methylthioethanol, methyl-n-propyl sulfide and diethyl sulfide. Plays an important role in the detoxification of selenium compounds (By

[27] Hsiao, K.; Zegzouti, H.; Goueli, S. A. *Epigenomics* **2016**, *8*, 321–339.
[28] UniProt *Nucleic Acids Res.* **2018**, *47*, D506–D515.
[29] `https://www.uniprot.org/uniprot/O95050`

similarity). Catalyzes the N-methylation of tryptamine and structurally related compounds.

Our first goal was to choose substrate concentrations that were physiologically relevant (close to INMT substrate $K_m^{app.}$ values) and would also generate luminescence signal with adequate signal/noise ratio to study INMT inhibition. A literature search[30,31] revealed the apparent K_m of tryptamine to be ca. 0.3-2.9 mM, so we pursued INMT assay development using 1.0-2.0 mM tryptamine. A SAM concentration of 20-30 µM was employed in our experiments, again close to literature reported apparent K_m values of SAM.

Assay validation according to protocols outlined in the Promega technical manual led us to the final conditions for the hINMT IC_{50} assay: [hINMT]=150 nM, [tryptamine]=2 mM, [SAM]=30 µM, and reaction time=20 min. A detailed IC_{50} assay protocol is reported below.

Reagents and Materials:

- SpectraMax i3x Multi-Mode Microplate Reader (Molecular Devices)
- MTase-Glo™Methyltransferase Assay (Promega V7601)
- assay plate, 384 well, with lid (Corning 3570)
- PCR strip tubes, with caps (Axygen Scientific, PCR-0208-A, PCR-02CP-A)
- disposable pipetting reservoir (polystyrene, 25 mL, VWR 89094-662)
- molecular biology grade water (Corning 46-000-CM)
- 0.5 M EDTA, pH 8.0 (Boston BioProducts BM-150)
- 5M NaCl (Cell Signaling Technologies 7010S)
- 1M $MgCl_2$ (invitrogen AM9530G)
- albumin standard (2.0 mg/mL BSA in 0.9% NaCl solution containing NaN_3); (Thermo Scientific 23209)
- ethyl alcohol, 200 proof for molecular biology (Millipore Sigma E7023)
- DL-dithiothreitol BioUltra, for molecular biology (Millipore Sigma 43815)
- tryptamine (Millipore Sigma 193747)
- trifluoroacetic acid (VWR BDH15311.100)

[30] Thompson M.A., W. R.; Thompson M. A., W. R. *J. Biol. Chem.* **1998**, *273*, 34502–10.
[31] Chu, U. B.; Vorperian, S. K.; Satyshur, K.; Eickstaedt, K.; Cozzi, N. V.; Mavlyutov, T.; Hajipour, A. R.; Ruoho, A. E. *Biochemistry* **2014**, *53*, 2956–2965.

Protocol (NS1 IC_{50} curve):

Reactions were performed in PCR strip tubes (with caps), and only transferred to a 384-well plate for final luminescence reading. Only every other well in a given row on the 384-well plate was used (the intermediate wells were left empty). The methyltransferase reaction mixture (including hINMT, tryptamine, SAM, and NS1) had a total volume of 20 µL. The experiment reported in Figure S5 was performed in duplicate.

To begin, 12 PCR tubes were aligned in an empty pipette tip box to allow for multichannel pipetting. From left to right, tubes 1–9 were experimental wells (NS1 at varying concentrations), 10 and 11 were positive controls (no NS1), and tube 12 was a negative control (no SAM).

1. 5 µL of 4× NS1 (prepared from a serial dilution to achieve the desired concentrations) was added to tubes 1–9, and 5 µL 1× reaction buffer added to tubes 10–12.
2. 5 µL of 4× SAM was added to tubes 1–11, and 5 µL 1× reaction buffer added to tube 12.
3. A master mix containing 2× hINMT and 2× tryptamine was prepared in a Falcon tube and poured into a multichannel pipette reagent reservoir.
4. Using a multichannel pipette, 10 µL of this master mix solution was transferred to all 12 tubes to initiate the INMT reaction.
5. The reactions were capped and incubated at RT for 20 min.
6. Reactions were quenched with 5 µL of 0.5% TFA and incubated for 5 min at RT to stop the methyltransferase reaction.
7. 5 µL of prepared 6× MTase-Glo™ Reagent was added and the reactions were capped and incubated for 30 min at RT.
8. 30 µL of MTase-Glo™ Detection Solution was added to the reactions and they were mixed by pipetting up-and-down.
9. 50 µL of each reaction was immediately transferred to a 384-well plate using a 12-channel (multichannel) pipette. Tubes 1–12 map to a 384-well plate as shown in Table S20 below.
10. The plate was centrifuged at 300 RPM for 2 min and immediately moved to the SpectraMax i3x Multi-Mode Microplate Reader.
11. Luminescence was read 5 min after transfer of the reaction mixtures from PCR tubes to the 384-well plate.

Table S20: Example 384-well plate layout showing final contents of each well. Row A shown here for illustrative purposes.

	1	**3**	**5**	**7**	**9**	**11**	**13**	**15**	**17**	**19**	**21**	**23**
A	35.0000 µM NS1	14.0000 µM NS1	5.6000 µM NS1	2.2400 µM NS1	0.8960 M NS1	0.3584 µM NS1	0.1434 µM NS1	0.0573 µM NS1	0.0229 µM NS1	+ control (no NS1)	+ control (no NS1)	− control (no SAM)

Data analysis: Luminescence data were analyzed in Microsoft Excel and GraphPad Prism v8.0.2. To begin, background signal (value from A23) was subtracted from all wells. Positive control wells A19 and A21 (containing no inhibitor) were then averaged to provide a value representing signal derived from uninhibited hINMT reactions. Luminescence counts from wells containing inhibitor (A1–A17) were then each divided by the control value to generate values representing % enzyme activity (relative to control). A plot of log(NS1) vs. % hINMT activity was then fitted via nonlinear regression in Prism using the model log(inhibitor) vs. response–Variable slope (four parameters) to generate the IC_{50} value.